

Identification and characterization of novel α L β 2 inhibitors and their differentiation from known inhibitors

Inauguraldissertation

zur

Erlangung der Würde eines Doktors der Philosophie
vorgelegt der
Philosophisch-Naturwissenschaftlichen Fakultät
der Universität Basel

von

Riccardo Mancuso

aus Italien

Basel, 2017

Originaldokument gespeichert auf dem Dokumentenserver der Universität Basel edoc.unibas.ch



Dieses Werk ist unter dem Vertrag „Creative Commons Namensnennung - Keine kommerzielle
Nutzung – Keine Bearbeitung 3.0 Schweiz“ (CC BY-NC-ND 3.0 CH) lizenziert.

Die vollständige Lizenz kann unter <https://creativecommons.org/licenses/by-nc-nd/3.0/ch>
eingesehen werden.

Genehmigt von der Philosophisch-Naturwissenschaftlichen Fakultät auf Antrag von

Prof. Dr. med. Stephan Krähenbühl

PD Dr. Gabriele Weitz-Schmidt

Prof. Dr. Jörg Huwyler

Basel, 15.11.2016

Prof. Dr. Jörg Schibler

To my parents

Acknowledgement

Firstly, I would like to express my sincere gratitude to Prof. Dr. Stephan Krähenbühl for giving me the opportunity to enrol as a PhD student. Without his support and precious advice, it wouldn't have been possible to conduct this research.

Many thanks to Prof. Dr. Marianne Hürzeler Müller, Martin, Jonas, and the other members of her group, for synthesizing all the compounds I tested and worked on.

Thanks to Prof. Dr. Daniel Gygax for giving me the opportunity to start working at FHNW in this project.

Thank you to Dr. Karl Welzenbach. I really enjoyed the short time spent in his lab and I am grateful for his comments and advice about the project.

I would like to thank my thesis committee members: Prof. Dr. Alex Odermatt for accepting to be the chairman and for all the interesting discussions during the Prodoc's retreats, and Prof. Dr. Jörg Huwyler, who besides all his activities and duties managed to supervise my thesis as co-referee.

My biggest thanks go to Dr. Gabriele Weitz-Schmidt. Her motivation, knowledge and guidance helped me during the entire period of researching and writing this thesis. She creates a perfect environment at the interface of academics and industry level. I could not have imagined having a better advisor and mentor for my PhD study.

“Choose a job you love, and you will never have to work a day in your life.”

Confucius

Big thanks go to each member of the Clinical Pharmacology & Toxicology department. Thank you for helping me enjoy each day, even a Monday morning!

Thank you to Andrea, Anna, Annalisa for the funny in-code conversations, Bea, Benji and his creative nicknames, Carole the best (...and only) master student I ever had, Cécile, Deborah for all the rubber band wars, Evelyne, Fabio, Franziska, Gerda for bringing joy and Zumba to the lab, Jamal, Karolina “Karotina” for the thought provoking challenging conversations, for her nice feedback and for slaying in life, Mijliencko, Patrizia, who introduced me to the lab and for all the fun we had as workplace neighbours, Simone, and Urs for being my punch ball when I need.

Many thanks also to David, Dino and François for all the no-sense conversations, for all the coffee breaks and all the worst/best ideas for our new start-up!

A particular thanks to 1,3,7-trimethyl-1H-purin-2,6(3H,7H)-dione, all of this couldn't have been possible without you!

Acknowledgement

*“Understand that friends come and go, but with a precious few you should hold on.
Work hard to bridge the gaps in geography and lifestyle,
because the older you get,
the more you need the people who knew you when you were young.”*

The Big Kahuna

I would like to thank all my friends from *Il Branco*. Thank you for keep me company during these years and make me feel like I am still in Sicily.

Fabio, Fefè and Cola (and the daily “oh”), Renzo (and our nerdy discussions about Terminator, Star Wars and so on...), Nena, Giuseppe, Alessia, Fabio, Alice, Stefano, Ninipo and Elena, thanks for the big exodus!

Thank you to all my friends here in Basel. You guys are like my second family. Alessandro, Anna, Berta & Tina my fork-teammates, Carla, Giacomino my gym buddy, Iris, Marina, Salvo, Sirbiuzza, Sofia my dear tandem mate. With all of you around here I always felt I was in great company.

A special thanks to Rosario, my *guru* and my friend, who was always there when I needed someone, and to Elena to be so close despite the distance, and for making the effort to finally meet each other. I feel so lucky to have you guys.

“Happiness is real only when shared.”

Chris McCandless

Thank you Leti, *la mia sorella preferita*, you always supported me and stimulate me since I was a child.

Thank you, Marina, *mi monita*, for making my last PhD year special, I love you, *ed è solo l'inizio*.

Finally, my deepest thanks go to my parents. I am profoundly grateful to you, for helping me to achieve this goal in my life, for your wonderful encouragement and for everything you have done over these years. Thank you.

Infine, il mio ringraziamento più profondo va ai miei genitori. Vi sono immensamente grato per avermi aiutato nel raggiungere questo traguardo della mia vita, per il vostro straordinario incoraggiamento e per tutto quello che avete fatto durante questi anni. Grazie.

Table of contents

List of abbreviations.....	2
Summary.....	3
Aims.....	6
1. Introduction.....	7
1.1. Integrins	
1.2. Integrins as therapeutic targets	
1.3. α L β 2	
1.4. α L β 2 ligands	
1.5. VLA-4 VCAM-1 Natalizumab	
1.6. LAD	
1.7. Efalizumab	
1.8. Progressive multifocal leukoencephalopathy – PML	
1.9. Small Molecule α L β 2 inhibitors	
1.10. Lifitegrast	
1.11. XVA143	
1.12. LFA878	
Paper One.....	27
From virtual screening to highly potent, orally available small molecule inhibitors of the integrin α L β 2	
Paper Two.....	67
Downstream effect profiles discern different mechanisms of integrin α L β 2	
Paper Three.....	82
A novel multi-parameter assay to dissect the pharmacological effects of different modes of integrin α L β 2 inhibition in whole blood	
2. Discussion.....	96
2.1. Back to the future	
2.2. Drug discovery	
2.3. Target identification	
2.4. Target validation	
2.5. Assay development	
2.6. Hit identification	
2.7. Hit to lead	
2.8. Lead optimization	
3. Outlook.....	103
References.....	105
CV.....	117

The research in this thesis is presented in the form of three scientific papers. The first paper is in preparation for submission, the second and the third paper are published. Reference lists for each paper are presented at the end of the relevant section. A reference list covering the general introduction and general discussion is at the end of the thesis.

List of abbreviations

APC, antigen-presenting cell; **CADD**, computer-assisted drug design; **CD**, cluster of differentiation; **CTL**, cytotoxic T lymphocyte; **DED**, dry eye disease; **ECM**, extracellular matrix; **Fc**, fragment crystallisable; **HIV**, human immunodeficiency virus; **HMG-CoA**, hydroxymethylglutaryl coenzyme A; **ICAM**, intercellular cell adhesion molecule; **IFN**, interferon; **Ig**, immunoglobulin; **IL**, interleukin; **IS**, immunological synapse; **ITAM**, immunoreceptor tyrosine-based activation motif; **JAM**, junctional adhesion molecule; **JCV**, John Cunningham virus; **KGD**, Lys-Gly-Asp; **LAD**, leukocyte adhesion deficiency; **LAT**, linker for activation of T cells; **LDV**, Leu-Asp-Val; **LFA-1**, lymphocyte function-associated antigen 1; **LPS**, lipopolysaccharide; **mAb**, monoclonal antibody; **Mac-1**, macrophage-1 antigen; **MAPK**, mitogen-activated protein kinases; **MHC**, major histocompatibility complex; **MIDAS**, metal ion-dependent adhesion site; **NK**, natural killer; **PK**, pharmacokinetic; **PMA**, phorbol 12-myristate 13-acetate; **PML**, progressive multifocal leukoencephalopathy; **RGD**, Arg-Gly-Asp; **SAR**, structure activity relationship; **SMAC**, supramolecular activation cluster; **TCR**, T cell receptor; **Th**, T helper; **TLN**, telencephalin; **TLR**, toll-like receptor; **TM**, transmembrane domain; **TNF**, tumor necrosis factor; **VCAM**, vascular cell adhesion molecule; **VEGF**, vascular endothelial growth factor; **VLA**, very Late Antigen; **vWFA**, Willebrand factor A domain; **WBC**, white blood cell; **ZAP70**, zeta-chain-associated protein kinase 70;

Summary

α L β 2 is expressed on all leukocytes and plays a major role in immune responses by regulating cell adhesion, leukocyte trafficking, T cell costimulation and immunological synapse (IS) formation. This integrin is centrally involved in immune-mediated diseases of high medical need, including chronic plaque psoriasis, multiple sclerosis, rheumatoid arthritis, small vessel vasculitis, dry eye disease and transplantation indications, among other diseases. In several of these diseases, α L β 2 has been validated by biologic therapies as a target of high therapeutic potential.

In the first part (paper) of this thesis we describe the identification and preclinical characterization of a novel class of α L β 2 inhibitors. These novel compounds with an allosteric mechanism of action, (also termed α I allosteric inhibitors), were designed to overcome major unwanted effects of current α L β 2 targeting drugs. Drug candidates derived from this project are foreseen to be assessed clinically in α L β 2-mediated disease of high unmet medical need.

Computer-assisted drug design (CADD) has been used to identify hits that modulate α L β 2 function via binding to the I allosteric site. The CADD approach pursued addressed the task of finding novel hits and leads from two conceptually complementary angles: (1) ligand-based similarity searching from known allosteric α L β 2 modulators but structurally different bioactive compounds, and (2) structure-based similarity searching with the aim to find novel allosteric α L β 2 modulators. A collection of several million commercially available compounds with drug-like properties has been compiled. These virtual screens yielded in ranked lists of compounds.

To determine the activity of these hits, an adhesion assay has been established (V well adhesion assay) to measure the binding of leukocytes (expressing α L β 2) to recombinant intercellular adhesion molecule-1 (ICAM-1), the ligand of α L β 2.

The α I allosteric mode of action of the compounds has been confirmed by quantifying the binding of the anti- α L β 2 mAb R7.1.

The novel and potent α L β 2 silencing compounds identified were chemically derivatized employing also CADD technologies. Based on first SAR data and CADD feedback, the scaffold of the lead compound has been modified.

These newly synthesized α L β 2 inhibitors discovered do not induce “agonistic” effects such as α L β 2 internalization (as observed in some experiments with biologics), induction of α L β 2 activation epitopes (as observed in some experiments with ligand mimetic α/β I allosteric α L β 2 inhibitors), and induction of ZAP70 phosphorylation. Moreover, they do not interfere with the

internalization/recycling of engaged T cell receptor/CD3 complexes and they do not show *in vitro* cytotoxicity.

The lead drug candidate identified, characterized and optimized has been transitioned to preclinical pharmacokinetic (PK) characterization and formulation development *in vivo*.

In the second part (paper) of this thesis we systematically compared different modes of $\alpha\text{L}\beta\text{2}$ inhibition for their $\alpha\text{L}\beta\text{2}$ inhibitory as well as their potential unwanted downstream events, such as paradoxical agonism.

Three major classes of $\alpha\text{L}\beta\text{2}$ inhibitors with distinct modes of action have been described to date: monoclonal antibodies (mAbs), small molecule α/β I allosteric and small molecule α I allosteric inhibitors. All inhibitors assessed were found to potently block $\alpha\text{L}\beta\text{2}$ -mediated leukocyte adhesion in the low nanomolar to picomolar range. None of the inhibitors induced ZAP70 phosphorylation, indicating absence of agonistic outside-in signalling.

Paradoxically, however, the α/β I allosteric inhibitor XVA143 induced conformational changes within $\alpha\text{L}\beta\text{2}$ characteristic for an intermediate affinity state, an effect that was not observed with the α I allosteric inhibitor LFA878 or the anti- $\alpha\text{L}\beta\text{2}$ mAb efalizumab.

On the other hand, efalizumab triggered the unscheduled internalization of $\alpha\text{L}\beta\text{2}$ while LFA878 and XVA143 did not affect or only mildly reduced $\alpha\text{L}\beta\text{2}$ surface expression, respectively.

Moreover, anti- $\alpha\text{L}\beta\text{2}$ mAb efalizumab, in contrast to the small molecule inhibitors, disturbed the fine-tuned internalization/recycling of engaged T cell receptor/CD3 complexes, concomitantly decreasing intracellular ZAP70 expression levels.

In conclusion, different modes of $\alpha\text{L}\beta\text{2}$ inhibition are associated with fundamentally different biologic effect profiles. The differential established here provides important translational guidance for novel $\alpha\text{L}\beta\text{2}$ inhibitors.

In the third part (paper) we described a flow cytometry-based technology that simultaneously quantitates $\alpha\text{L}\beta\text{2}$ conformational change upon inhibitor binding, $\alpha\text{L}\beta\text{2}$ expression and T cell activation at the single-cell level in human blood. Two classes of allosteric low molecular weight inhibitors, designated α I and α/β I allosteric $\alpha\text{L}\beta\text{2}$ inhibitors, were investigated.

The multi-parameter whole blood $\alpha\text{L}\beta\text{2}$ assay described may enable therapeutic monitoring of $\alpha\text{L}\beta\text{2}$ inhibitors in patients' blood. The assay dissects differential effect profiles of different classes of $\alpha\text{L}\beta\text{2}$ inhibitors.

Summary

The flow cytometry-based technology described allows, for the first time, to simultaneously assess and correlate, at the single-cell level, inhibitor-specific $\alpha\text{L}\beta\text{2}$ conformational change, $\alpha\text{L}\beta\text{2}$ expression and T cell activation in human whole blood.

The format, robustness and sensitivity of the assay indicate that it may be suitable for bedside monitoring of newly developed $\alpha\text{L}\beta\text{2}$ inhibitors.

Aims

The first aim of this thesis was the identification and characterisation of novel allosteric $\alpha\text{L}\beta\text{2}$ inhibitors, which stabilize the integrin in its inactive conformation. The second aim was to differentiate these new allosteric inhibitors from other $\alpha\text{L}\beta\text{2}$ inhibitors with different modes of actions. The third aim was to provide novel methods to enable the pharmacodynamic characterization of low molecular weight $\alpha\text{L}\beta\text{2}$ inhibitors.

1. Introduction

1.1. Integrins

Integrins are a superfamily of 24 members known to date. They are heterodimeric cell-surface receptors composed of one alpha subunit and one beta subunit each, non-covalently associated; in vertebrates 18 alpha subunits and 8 beta subunits exist (Fig. 1). Functionally, integrins are cellular adhesion molecules mediating a wide range of cell-cell, cell-extracellular matrix and cell-pathogen interactions (Tan 2012).

The first integrin was identified almost 31 years ago, by Tamkun et al. (Tamkun, et al. 1986) They described the isolation, characterization, and sequence of cDNA clones that encode one subunit of a membrane glycoprotein complex, involved in the transmembrane linkage between fibronectin and actin. They proposed to term this type of glycoprotein complexes *integrin* for their ability to integrate extracellular and cytoskeletal environments (Campbell and Humphries 2011).

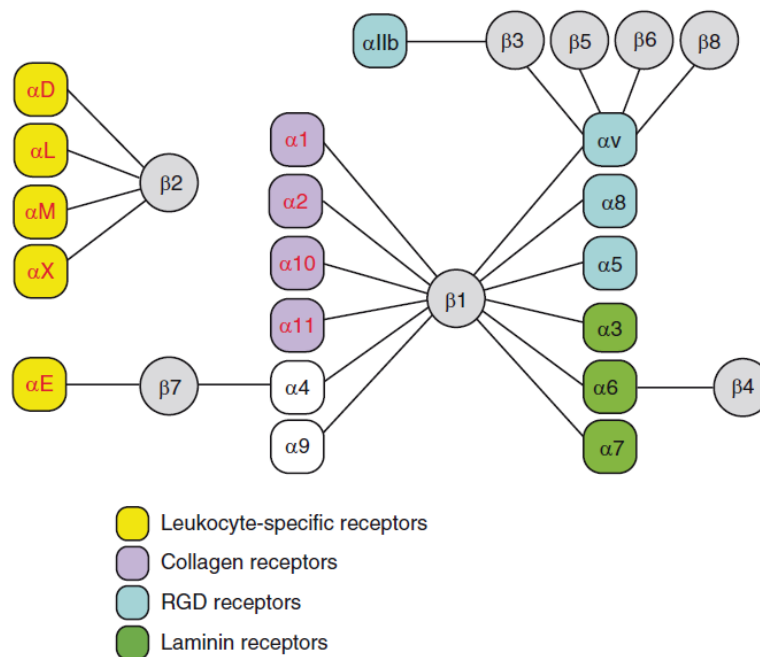


Fig. 1. Classification of integrin family of heterodimers. The nine α domains with “inserted” I domains (1, 2, 10, 11, D, L, M, X, E) are indicated in red (Campbell and Humphries 2011).

Integrins are found in a wide range of organisms: sponges, corals, nematodes, echinoderms and mammals (Burke 1999) and are expressed in a broad variety of cell types. Cells of the immune system express at least 10 members of the integrin family belonging to the $\beta 1$, $\beta 2$ and $\beta 7$. The $\beta 2$ and $\beta 7$ are expressed exclusively on leukocytes while $\beta 1$ integrins are expressed on a wide variety of cells.

The diversity in the subunits and in the combination of the alpha and beta chains make integrins able to interact with several and different ligands (Kern and Marcantonio 1998).

Integrins can bind to extracellular matrix (ECM) glycoproteins including collagens, fibronectins, vitronectin, laminins, plasma proteins, complement factors, C-reactive protein and cellular receptors such as vascular cell adhesion molecule-1 (VCAM-1) and the intercellular cell adhesion molecule (ICAM) family (Fig. 2) (Hynes 2002; Plow, et al. 2000). The amino acid sequence Arg-Gly-Asp (RGD) present in some ligands is a common sequence recognized by several integrins (Ruoslahti and Pierschbacher 1986).

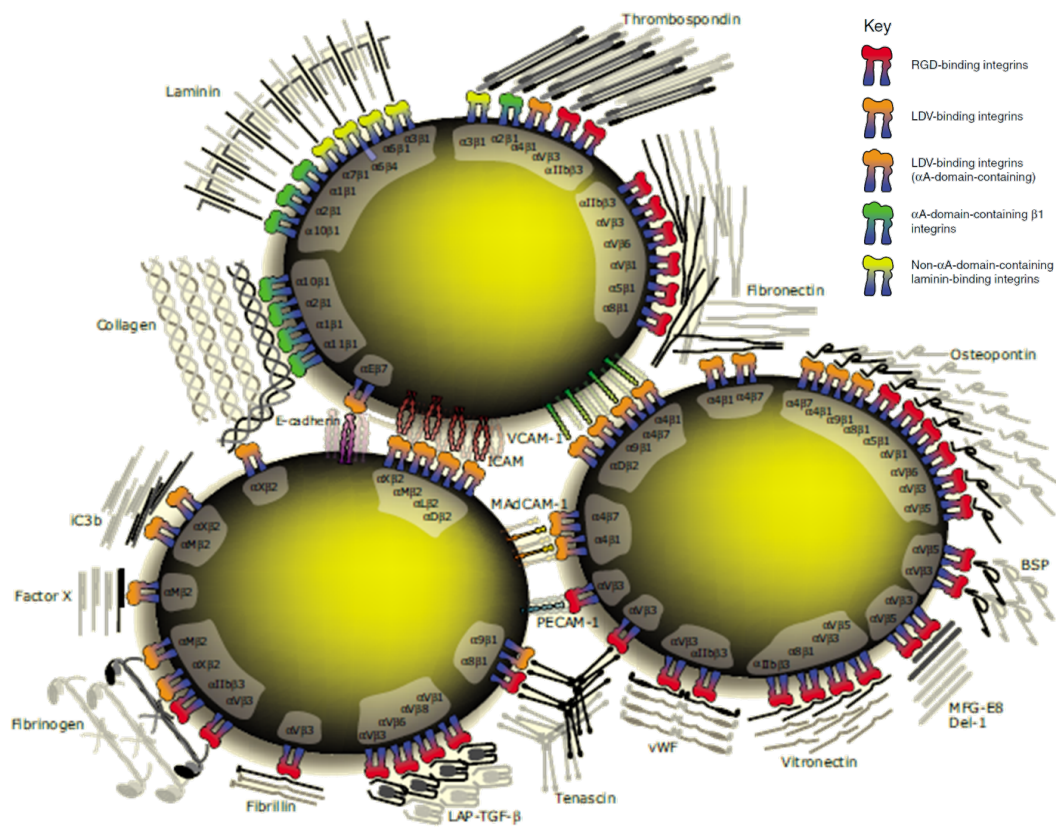


Fig. 2. Classification of integrin ligands and their binding to counterpart integrins. The α A-domain (a von Willebrand factor A domain, vWFA) refers to the “inserted” I domain (Humphries, et al. 2006).

Each integrin heterodimer presents an extracellular domain that binds the extracellular ligands, a transmembrane domain (TM) and an intracellular cytoplasmic domain where the alpha and beta tails undergo to conformational changes to interact with other proteins (Campbell and Humphries 2011). Intriguingly, integrins integrate and transduce signals bidirectionally: “outside-in” and “inside-out” the cell.

Integrins show distinctive activation state on different cell types. They are active in most adherent cells and inactive on platelets or leukocytes (Campbell and Humphries 2011).

In the normal resting, inactive state, integrin extracellular domains do not bind to ligands and exist in a bent conformation. Activation signals from the inside of the cell induce conformational changes within α L β 2 leading to an extended form which is ready to bind ligand (inside-out signalling) (Lau, et al. 2009).

In outside-in signalling the binding of integrins to their ligands results in intracellular signal transduction like proliferation, differentiation and apoptosis (Zaidel-Bar, et al. 2007).

Several integrins interact with their ligands via the inserted I domain on the α chain (Fig. 1). The ligand interaction to the I domain is dependent on divalent cations (Lee, et al. 1995). In humans, the I domain is present in α 1, α 2, α 10, α 11, α D, α E, α L, α M and α X (Fig. 1). The size of the I domain is around 200 a.a. (Johnson and Chouhan 2014).

1.2. Integrins as therapeutic targets

Integrins are interesting therapeutic target for several diseases. Thrombosis was the first disease-related process found to be associated with integrins (Estevez, et al. 2015).

In the mid 1960s Eduard Glanzmann, a Swiss paediatrician, described a disorder now known as Glanzmann thrombasthenia. Patients with this disorder suffer of serious bleeding. Their platelets lack integrin α I**IIb** β 3 (GPIIb/IIIa) and/or have defective α I**IIb** β 3 receptors. As a result, bridging of platelets to other platelets via fibrinogen, the ligand of α I**IIb** β 3, cannot occur, and bleeding times are significantly prolonged (Coller 2014).

To date, six pharmacological inhibitors (antibodies, peptides and peptidomimetics targeting 4 integrins) have been approved (Sawada, et al. 2012) (Holland, et al. 2016). Some other modalities are in clinical development (Table 1) (Chiricozzi, et al. 2016). For example, Abciximab (ReoPro®) is the Fab fragment of the chimeric human-murine mAb 7E3, which binds to the platelet receptor α I**IIb** β 3 and to the vitronectin receptor (integrin α v β 3). Abciximab inhibits platelet aggregation that cause thrombus formation and is used during and after coronary artery procedures (Table 1).

Eptifibatide (Integrilin®) is a cyclic heptapeptide derived from barbourin that contains a KGD sequence. It is a member of the disintegrins. Disintegrins are a class of small proteins that contains an RGD (Arg-Gly-Asp) or KGD (Lys-Gly-Asp) sequence motif. These motifs are able to bind to the α I**IIb** β 3, blocking in this way the binding of fibrinogen to activated α I**IIb** β 3 expressed on platelets (Minoux, et al. 2000) (Ruoslahti and Pierschbacher 1986)

Integrins are also essential protein for the migration and interaction of cells of the immune system. Both β 1 and β 2 integrins are important in immune functions. Mutations in β 2 integrins lead to a rare autosomal recessive disorder, leukocyte adhesion deficiency (LAD) (Hogg and Bates 2000) (Shaw, et al. 2001).

Efalizumab (Raptiva®) is a humanized mAb directed against the α L chain of α L β 2 that was used for the treatment of psoriasis. In 2006 it has been withdrawn from the market because of an association with progressive multifocal leukoencephalopathy (PML) (Keene, et al. 2011). In July 2016, a small molecule α L β 2 inhibitor was approved for dry eye disease (Holland, et al. 2016).

Natalizumab (Tysabri®), a humanized mAb against the α 4 subunit, is effective in the treatment of multiple sclerosis and Crohn's disease (Zohren, et al. 2008).

Integrins are also attractive anticancer targets. During the formation of metastasis, cells become able to migrate and invade other tissues. For this reason, compounds or antibodies that target integrins could be used in combination with other anticancer treatment. Etaracizumab (Abegrin®) is a humanized mAb against α V β 3 recently investigated for the treatment of melanoma (Landen, et al. 2008).

Cilengitide, a cyclic RGD-f-(NMe)V peptide specific for α V β 3 integrin, reached Phase III trials for the treatment of glioblastoma and other brain cancers but it was not efficacious in clinical trials that aimed to limit tumour angiogenesis and progression in patients with glioblastoma (Burke, et al. 2002) (Ley, et al. 2016).

Volociximab is a chimeric mouse/human anti α 5 β 1 mAb. Preclinical studies have shown the ability of volociximab to inhibit tumour neoangiogenesis by blocking the interaction between α 5 β 1 and fibronectin (Ng, et al. 2010) (Almokadem and Belani 2012).

Table 1

Overview of integrin targeting drugs which are approved or in clinical development (Sawada, et al. 2012) (Chiricozzi, et al. 2016) (Holland, et al. 2016).

Target	Product	Company	Indication	Status
α L β 2	Efalizumab	Genentech/Xoma	Plaque psoriasis	Withdrawn
	Lifitegrast	SARcode	Dry eye disease	Approved
	Natalizumab	Biogen Idec	Multiple sclerosis	Approved
α 4 β 1/ α 4 β 7	Firategrast	GSK/MTPC	Crohn's disease	Approved
		Ajinomoto	Multiple sclerosis	Phase II
	AJM300	Ajinomoto	Ulcerative colitis	Phase II
	Vedolizumab	Millennium (Takeda)	Crohn's disease	Approved
α 4 β 7	MLN02		Ulcerative colitis	Approved
			Ulcerative colitis	Phase II
α 3	Abciximab	Centocor/ E Lilly	Acute coronary syndrome	Approved
α 5 β 1	Volociximab	PDL BioPharma	Ovarian cancer	Phase II
	ATN-161	Attenuon LLC	Lung, liver, spleen cancer	Phase I
α 5 β 3	Etaracizumab	Medimmune	Prostate, ovarian cancer	Phase II
α IIb β 3	Tirofiban	Merck/Millennium	Acute coronary syndrome	Approved
	Eptifibatide	Millennium (Takeda)	Acute coronary syndrome	Approved
α V	Intetumumab	Centocor	Melanoma tumourigenesis	Phase II
			Glioblastoma	Phase III
α V β 3/ α V β 5	Cilengitide	Merck Serono	Lung cancer (NSC)	Phase II
			Squamous cell carcinoma	Phase II
			Idiopathic pulmonary fibrosis	Phase II
α V β 6	STX-100	Stromedix/Biogen	Idiopathic pulmonary fibrosis	Phase II

Interestingly, several viral pathogens interact with integrins and use them to be internalized. These viruses display RGD sequences on their viral capsid that can be recognized by integrins. Virus binding induces conformational changes and clustering of the integrins leading to cell-signalling events. As a consequence a rearrangement of the cytoskeleton and an internalization of the virus-integrin complex occurs (Stewart and Nemerow 2007).

Moreover, integrins have an important role in maturation of osteoclasts and thus for the development of the bones. Polymorphisms on the integrin $\alpha V\beta 3$ are associated with increased rate of fractures and osteoporosis (Tofteng, et al. 2007).

Psoriasis is a T cell-mediated autoimmune chronic inflammatory disease. The $\alpha 1\beta 1$ integrin has been shown to be crucial for accumulation of epidermal T cells and the development of psoriasis. It may be possible to prevent the accumulation of epidermal T cells by blocking the interaction of $\alpha 1\beta 1$ with collagen (Conrad, et al. 2007). The interaction of $\alpha L\beta 2$ with ICAM-1 is another target in the treatment of psoriasis (Reisman, et al. 2011).

Uveitis is a disease characterized by an inflammation of the uvea. An early step in the pathogenesis of this inflammatory disease is the adhesion of leukocytes to the vascular wall followed by leukocyte activation, firm adhesion, and transmigration into the interstitial tissue. The accumulation of activated leukocytes in the ocular tissues leads to damage of the uvea.

Several preclinical studies suggest that the integrins VLA-4 and $\alpha L\beta 2$ play major roles in uveitis. VLA-4 blockade by monoclonal anti-rat VLA-4 antibody, clone TA-2, suppresses endotoxin-induced uveitis *in vivo* (Hafezi-Moghadam, et al. 2007). Small-molecule inhibitors of $\alpha 4$ integrins have been shown to be effective in experimental autoimmune uveitis by interfering with cell adhesion events (Martin, et al. 2005). Further, mAbs directed against $\alpha L\beta 2$ or ICAM-1 can be used to protect against experimental uveitis (Uchio, et al. 1994) (Whitcup, et al. 1993) (Whitcup, et al. 1995). Importantly, in a pilot study, efalizumab has been shown to be efficacious in uveitis patients (Faia, et al. 2011b).

1.3. $\alpha L\beta 2$

Within the integrin superfamily, $\alpha L\beta 2$ belongs to the beta 2 integrin subfamily, which is defined by a common beta 2 chain and unique alpha chain. The four members of the beta 2 integrin subfamily are $\alpha L\beta 2$ (LFA-1, CD11a/CD18), $\alpha M\beta 2$ (Mac-1, CD11b/CD18), $\alpha X\beta 2$ (gp 150, CD11c/CD18) and $\alpha D\beta 2$ (CD11d/CD18) (Tan 2012).

In 1981 Davignon et al. used different mAbs to identify important molecules on murine cytotoxic T lymphocytes (CTL). They found that the binding of mAbs to an antigen involved in CTL-mediated

lysis leads to the inhibition of their killing functions. The clone M7/14 defined a cell surface antigen, termed later as leukocyte function-associated antigen 1 (LFA-1) (Davignon, et al. 1981).

In 1982 Sanchez-Madrid et al. identified the human α L β 2 homologue of the previously described mouse α L β 2 antigen. The mouse and human antigens are extremely conserved. Sanchez-Madrid et al. also discovered five different anti- α L β 2 mAbs that inhibit the killing pathway in CTLs (Sanchez-Madrid, et al. 1982).

Given its broad distribution on immunocompetent cells, α L β 2 plays a central role in immune mediated and inflammatory diseases. This has been established extensively in experimental disease in animals, mostly using knock-out mice and anti- α L β 2 antibodies. Anti- α L β 2 therapy led to prolonged graft survival in various models of allograft transplantation (including cardiac, islet and cornea transplantation). Moreover, in several transplantation models, tolerance could be induced with both anti- α L β 2 therapy used alone or in combination with other modalities (Nicolls and Gill 2006) (Arefanian, et al. 2010). In other experimental disease models, for example uveitis, arthritis, multiple sclerosis, diabetes mellitus, asthma and lupus-like disease, animals genetically deficient for α L β 2 or treated with anti- α L β 2 agents were found to be protected against disease (Giblin and Lemieux 2006) (Ke, et al. 2007) (Glawe, et al. 2009) (Lee, et al. 2008) (Suchard, et al. 2010).

α L β 2 has also been identified as a therapeutic target for infectious diseases, including HIV infection (Kapp, et al. 2013).

Beyond, α L β 2 has been described as target receptor for drug delivery or for the delivery of marker molecules such as imaging agents (diagnostic usage) to lymphoma and leukemic cells (Chittasupho, et al. 2010) (Poria, et al. 2006).

Further, α L β 2 plays decisive roles in the differentiation of lymphocyte populations (Verma, et al. 2012) and may be used as a target allowing the selection or expansion of distinct lymphocyte populations *in vitro*, *ex vivo* and *in vivo*. Increases in regulatory lymphocyte populations have been observed in patients treated with anti- α L β 2 antibodies (Faia, et al. 2011a) (Posselt, et al. 2010).

Taken together, it is appreciated that α L β 2 is a receptor involved in inflammatory, immune - mediated and infectious diseases and is overexpressed in certain malignant diseases. These diseases are often severe, chronic disorders often requiring life-long therapy.

The expression of α L β 2 is restricted to leukocytes including T cells, B cells, neutrophils, monocytes, macrophages, dendritic cells, mast cells, eosinophils, and NK cells. The level of expression varies with cell type and differentiation state. α L β 2 is overexpressed in certain lymphomas and leukemias (Poria, et al. 2006) (Chittasupho, et al. 2010).

α L β 2 plays a central role in the innate and adaptive immune response. Firstly, as a cellular adhesion molecule α L β 2 mediates the firm adhesion of leukocytes to inflamed vessel walls and their extravasation into inflamed tissues (Fig. 3).

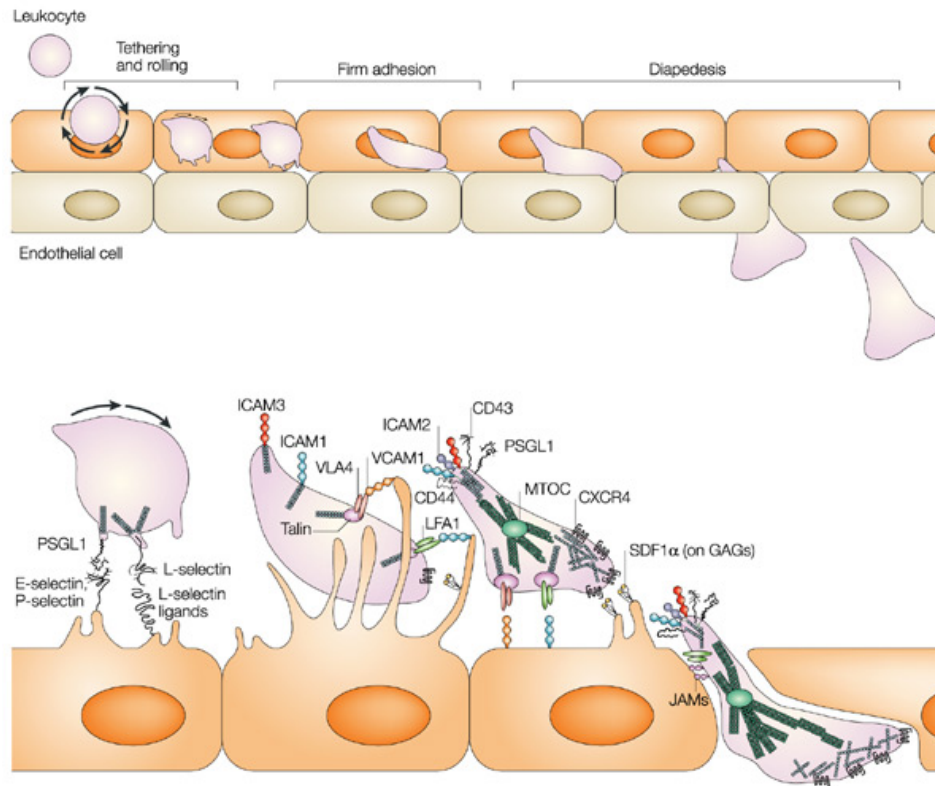


Fig. 3. Leukocyte extravasation into target tissues. Sequential steps of leukocyte extravasation. Tethering of the leukocyte occurs through interactions between selectins and their endothelial ligands. Firm adhesion is mediated by interaction of leukocyte integrins very late antigen 4 (VLA-4) and leukocyte function-associated antigen 1 (LFA-1, α L β 2) with endothelial vascular cell-adhesion molecule 1 (VCAM-1) and intercellular adhesion molecule 1 (ICAM-1), respectively (Vicente-Manzanares and Sanchez-Madrid 2004).

Secondly, α L β 2 is crucial for the activation of immune cells (Fig. 4). In this context, α L β 2 is well-characterized as a costimulatory receptor which is essential for the formation of the immunological synapse (IS) and controls T cell activation and proliferation.

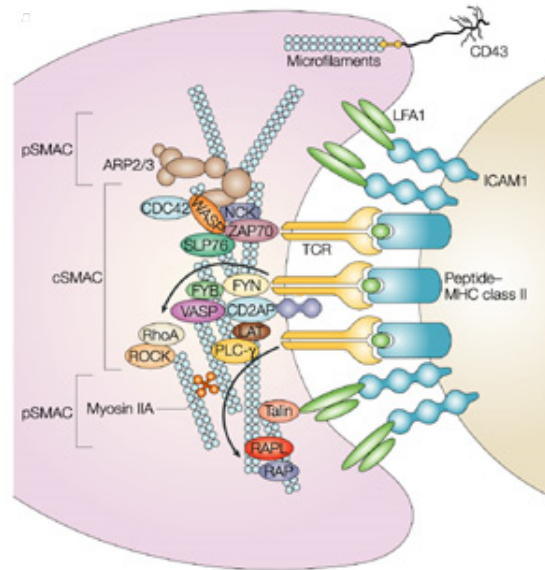


Fig. 4. The lymphocyte cytoskeleton during T cell–APC interactions and the formation of the immunological synapse. In the cSMAC, TCRs interact with APC bearing peptide-MHC complexes. Triggering of TCR leads to the activation of the kinesin LAT, FYN and ZAP70 and to a phosphorylation cascade. In the pSMAC, α L β 2 interacts with ICAM-1 acting as costimulatory receptor (Vicente-Manzanares and Sanchez-Madrid 2004).

Interaction of antigen presenting cells (APC) bearing peptide-MHC complexes with T cell receptor (TCR) leads to the formation of the IS. Already after few seconds, T cells react with a spatial reorganization of proteins and with a chain reaction leading to phosphorylation and dephosphorylation cascades.

The immune synapse is also known as the supramolecular activation cluster or SMAC. This structure is composed of concentric rings each containing segregated clusters of proteins.

In the central ring, cSMAC, there are mainly TCR, the peripheral one, pSMAC, is composed of α L β 2. Studies in mouse models revealed that α L β 2/ICAM-1 interaction is also important for driving Th1 polarization (Mittelbrunn, et al. 2004).

The distal ring, dSMAC, is composed of F-actin microfilaments (Philipsen, et al. 2013). The rearrangement of the actin shows a particular organization called actin cloud that is triggered by α L β 2 outside-in signals. For the actin cloud formation, TCR and ZAP70 appeared to be not essential (Suzuki, et al. 2007).

After the triggering of the TCR, the kinases Lck is activated and can phosphorylate the ITAM sequence on the cytoplasmic domain of the CD3 subunits. ZAP70 can be now recruited to activate the kinase LAT. The phosphorylation cascade will lead to activate T cells through a release of intracellular Ca^{2+} flux and to the activation of the MAPK pathway (Philipsen, et al. 2013).

$\alpha L\beta 2$ is also involved in the organization of cSMAC. The localization of complexes TCR/Class II in the cSMAC has been shown to be $\alpha L\beta 2$ dependent (Graf, et al. 2007).

1.4. $\alpha L\beta 2$ ligands

The ligands of $\alpha L\beta 2$ identified to date belong to the immunoglobulin (Ig) superfamily. They are the intercellular adhesion molecules ICAM-1, -2, -3, -4, and -5 and the junctional adhesion molecule JAM-A (previously JAM-1). These ligands are expressed on various cell types including endothelial cells on the vessel wall, epithelial and tissue resident cells (i.e. keratinocytes, dendritic cells) and leukocytes (Tan 2012).

The five members of the ICAM family express different numbers of Ig-like C2 type domain (Fig. 5) and they have different functions and cell distributions (Xiao, et al. 2013).

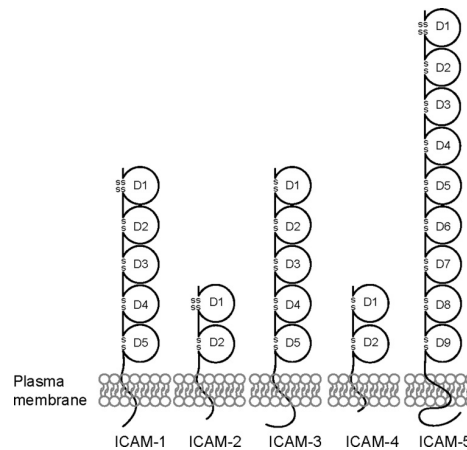


Fig. 5. Schematic primary structures of ICAMs. ICAMs belong to the immunoglobulin superfamily. Each molecule is composed of several Immunoglobulin-like domains in the extracellular region, a short transmembrane region, and a cytoplasmic tail (Xiao, et al. 2013).

In 1986 Rothlein et al. (Rothlein, et al. 1986) identified and characterized ICAM-1 as one of the molecules involved in homotypic aggregation of leukocytes. In their experiments, JY B lymphoblastoid cells were stimulated with phorbol 12-myristate 13-acetate (PMA). PMA stimulation leads to cell aggregation (Rothlein and Springer 1986). Using the mAb RR1/1 a mAb that targets the antigen RR1/1, later defined as ICAM-1, they showed that this antibody prevents cell homotypic aggregation. ICAM-1 is expressed on fibroblasts, endothelial cells and its expression is increased in response to IL-1 and other cytokines (Rothlein, et al. 1986).

LPS, Thrombin, IL-1, PMA, VEGF, and shear stress also induce expression of ICAM-1 (Rahman and Fazal 2009).

In 1987 Corbi et al. showed that ICAM-1 binding to α L β 2 is dependent on the by divalent cations Mg²⁺ and Ca²⁺ at physiologic concentration, in accordance to the activation of the alpha subunit of α L β 2 that presents a divalent cation-binding site (Corbi, Miller et al. 1987). Binding requires also metabolic energy, functional cytoskeleton, and it is temperature depending (Marlin and Springer 1987).

ICAM-1 is a transmembrane heavily glycosylated protein of 532 amino acids. The molecular weight mass ranges from 75 to 115 kDa. The different weights reflect different glycosylation and it is translated in the ability of binding different ligands. ICAM-1, also known as CD54, presents five in tandem immunoglobulin Ig-like domains (Dustin, et al. 1986). ICAM-1 does not contain an RGD sequence (Marlin and Springer 1987), ICAM-1 is also a receptor for human rhinoviruses (Table 2) (Greve, et al. 1989) (Xing, et al. 2003).

Soluble intercellular adhesion molecule-1 (sICAM-1) is the circulating form of ICAM-1. There are evidences that suggest that sICAM-1 can be a candidate marker of vascular inflammation in atherosclerosis and myocardial infarction, although its increased levels were also observed in other diseases affecting the cardiovascular system, such as myocarditis, inflammatory cardiomyopathy and heart failure *per se*.

(Witkowska and Borawska 2004) (Schmidmaier, et al. 2007) (Witkowska 2005). On the other hand, loss of cell surface ICAM-1 from the endothelium may serve a protective function where sICAM-1 acts as a natural inhibitor of α L β 2/ICAM-1 interactions (Zonneveld, et al. 2014).

ICAM-2 was identified in 1991 by Fougerolles et al. as a second α L β 2 ligand. It showed a different and more restricted pattern of distribution compared with ICAM-1. Endothelium and lymphoid cells express ICAM-2. ICAM-2, also known as CD102, is as well a transmembrane protein, with a molecular weight of 55 – 65 kDa and two IgG like domains (de Fougerolles, et al. 1991). ICAM-2 is constitutively expressed in contrast to ICAM-1 where the expression is highly inducible (Table 2) (Xiao, et al. 2013).

In 1994 Fougerolles et al. identified ICAM-3 and characterized its interaction with α L β 2 in the immune synapse. Both ICAM-2 and ICAM-3 have a similar affinity for α L β 2, however their affinities is lower than the affinity of ICAM-1 for α L β 2 ICAM-3, also known as CD50, presents five IgG-like domains and a molecular weight of 120 kDa (de Fougerolles and Springer 1992) (de Fougerolles, et al. 1994). ICAM-3 shows a pivotal role in the immune synapse and in the generation of the immune responses and it is the dominant ligand for α L β 2 on resting lymphocytes (Tab. 2) (Littler, et al. 1997).

ICAM-4 identified in 1940 by Landsteiner and Wiener as part of the human blood group system. It has a molecular weight of 40 – 42 kDa and two IgG-like domains (Bloy, et al. 1989).

In 1994 Bailly et al. aligned the amino sequence of the two IgG like domain of LW protein with the sequences of ICAM-1, -2, -3 showing that they are closely related (Bailly, et al. 1994).

ICAM-4 binds to α L β 2, Mac-1 and α x β 2 (Table 2) (Toivanen, et al. 2008).

ICAM-5, identified in 1994 by Yoshihara et al., has a molecular weight of 130 kDa and nine tandem immunoglobulin-like domains. It also denominated Telencephalin (TLN) because it is expressed exclusively in the telencephalon where it displays two types of binding: homophilic, between neurons, and heterophilic, between neurons and leukocytes (Table 2) (Yoshihara, et al. 1994).

The junctional adhesion molecule A (JAM-A), also known as JAM-1 or F11R interacts with α L β 2 in the early events of the transendothelial migration.

It is expressed as a dimer on the surface of epithelial and endothelial cells, and also hematopoietic cells, such as leukocytes, platelets, and erythrocytes, and it is present in endothelial and epithelial tight junctions of many different tissues (Table 2) (Wojcikiewicz, et al. 2009).

Table 2

Overview of the α L β 2 ligands and their expression pattern and regulation (Xiao, et al. 2013) (Naik, et al. 2001).

α L β 2 Ligands	Cellular Expression	Inducibility
ICAM-1 (CD54)	Leukocytes, epithelial cells, endothelial cells, fibroblasts, Sertoli cells, germ cells	Highly inducible: TNF α , IFN- γ , IL-1a, IL-1b, LPS, phorbol ester, shear stress (by blood flow)
ICAM-2 (CD102)	Leukocytes, platelets, epithelial cells, endothelial cells, Sertoli cells, germ cells	Non-inducible: Down-regulated by TNF α /IL-1 β in HUVECs
ICAM-3 (CD50)	Leukocytes	Inducible: TNF α , retinoic acid, on endothelial cells; down-regulated by PMA and Ca ²⁺ ionophore
ICAM-4 (CD242, LW)	Erythrocytes	Not determined
ICAM-5 (TLN)	Neurons	Non-inducible
JAM-A (JAM-1, F11R)	Leukocytes, platelets, erythrocytes, epithelial cells, endothelial cells	TNF- α and IFN- γ

1.5. VLA-4 VCAM-1 Natalizumab

In 1987 Hemler et al. identified VLA-4 as a new member of the very late antigen (VLA) protein family. VLA-4 (CD49/CD29, α 4 β 1, LPAM-2) is a heterodimeric cell surface integrin with a molecular weight of 115 kDa. VLA-4 shares the beta 1 subunit with VLA-1, -2, -3, and -5 and the α 4 chain with the integrin LPAM-1 (α 4 β 7) (Fig. 1) (Hemler, et al. 1987).

VLA-4 is expressed on peripheral blood B and T cells, thymocytes and monocytes, mast cells, macrophages, basophils and eosinophils, but not neutrophils (Hemler, et al. 1990). VCAM-1 and

fibronectin are the ligands of VLA-4. VCAM-1 was identified as ligand in 1990 by Elices et al. and is a member of the immunoglobulin family. VLA-4 appears to be its major or only receptor (Elices, et al. 1990).

VCAM-1 expression is inducible. Endothelial cells express VCAM-1 in response to cytokines produced in the tissue, high levels of ROS, oxidized low density lipoprotein (oxLDL), 25-hydroxycholesterol, turbulent shear stress, high glucose, and microbial stimulation of endothelial cell TLRs. VCAM-1 can also be released in a soluble form, sVCAM, from the endothelial surface through cleavage by a metalloprotease. The expression of VCAM-1 in lymph nodes and in the bone marrow regulates the homing of leukocyte (Cook-Mills, et al. 2011).

Antibodies against VCAM-1 can interfere with the formation of lamellopodia in monocytes, preventing in this way diapedesis (Ronald, et al. 2001). In 1989 Wayner et al. described VLA-4 as a new fibronectin receptor (Wayner, et al. 1989). Fibronectin is a glycoprotein of the extracellular matrix (ECM) that plays a role in the interaction between cells and ECM (Pankov and Yamada 2002).

The VLA-4/VCAM-1 interaction mediates the tethering, rolling and firm adhesion during an inflammatory response (Labege, et al. 1995).

The synergistic interaction of VLA-4 and α L β 2 to their respective ligands increase the binding of the cells, VCAM-1 binding to VLA-4 results in increased α L β 2-mediated adhesion of T lymphocytes to ICAM-1 via an avidity-dependent mechanism (Chan, et al. 2000).

On the other hand, the occupation of T cell α L β 2 by its ligand ICAM-1 decreases the binding of VLA-4 to ligands fibronectin and VCAM-1 (Porter and Hogg 1997). In contrast to α L β 2, VLA-4 can bind ligands also when it is in its natural resting state. This phenomenon could explain why inhibitors against VLA-4 are usually competitive and not allosteric (Chigaev and Sklar 2012).

VLA-4 is an interesting target for the treatment of several diseases because of the roles it has in different inflammatory processes. Peptides, cyclic peptides derived from ligand, small molecule inhibitors, and monoclonal antibody are used (Yednock, et al. 1992) (Lin and Castro 1998). Finategrast is a small molecule α 4 antagonist developed by Glaxo Smith Kline for the treatment of relapsing remitting multiple sclerosis. It has entered Phase II clinical trials (Millard, et al. 2011).

Heparin is a ligand for VLA-4. In the treatment of metastatic cancers, where the cells are positive for VLA-4, heparin can be used to target this integrin as inhibitor of cancer progression (Fritzsche, et al. 2008) (Schlesinger, et al. 2009) (Chigaev, et al. 2011).

Regarding monoclonal antibodies, Natalizumab was approved by the FDA in 2004 and is used for the treatment of multiple sclerosis and Crohn's disease. Natalizumab is an IgG4k humanized

monoclonal antibody, it binds $\alpha 4$ chain of VLA-4, preventing the transmigration of lymphocytes to the CNS (Lutterotti and Martin 2008).

After IV administration of Natalizumab, the IgG4 isotype antibody engages in Fab-arm exchange with other IgGs present in the serum. This leads to antibodies that are monovalent (Rispen, et al. 2011).

As seen for Efalizumab, treatment with Natalizumab leads to an immunosuppressive state associated with progressive multifocal leukoencephalopathy (PML) (Meira, Sievers et al. 2016). Natalizumab was first withdrawn from markets in 2005 but then relaunched in the USA and European market in 2006 (Lutterotti and Martin 2008) (Benkert, et al. 2012) (Carson, et al. 2009)

1.6. LAD

Leukocytes adhesion deficiency (LAD) is a rare autosomal recessive disorder characterized by immunodeficiency resulting in severe infections. It is caused by deficiency of adhesive glycoproteins on the surfaces of white blood cells (WBCs). This results in lymphocytes, monocytes and granulocytes with defects in their main functions: adhesion to endothelium, phagocytosis, cell-mediated cytotoxicity, and response to specific antigens (Kishimoto, et al. 1987).

LAD is currently divided into three subtypes: LAD-I, LAD-II and LAD-III.

LAD-I has been identified in patients having a deficiency in $\beta 2$ (CD18) integrins. LAD-I is characterized by recurring bacterial and fungal infections, impaired wound healing and severe gingivitis (Hogg and Bates 2000).

In the LAD-II syndrome, there is a lack in fucosylated glycoconjugates. In this form of LAD, neutrophils fail in binding to E-selectin on IL-1 activated endothelial cells (Karsan, et al. 1998).

LAD-III is characterized by defective kindlin-3 production and it is associated with Glanzmann-type bleeding disease. Kindlin-3 deficiency is reported to cause abnormal β integrin activation. Defective function of $\beta 3$ integrin results in platelets that are not capable of binding to each other (Robert, et al. 2011).

1.7. Efalizumab

Efalizumab is a humanized anti-CD11a antibody, the alpha chain of the integrin $\alpha L\beta 2$. Efalizumab, molecular weight 148,841 Da, is an IgG1k isotype antibody with two identical kappa light chains (214 a.a.), and two gamma heavy chains (415 a.a.). Each light chain is linked by disulphide bridge to a heavy chain. The two heavy chains are linked together by disulphide bridge.

Efalizumab was developed as a murine anti-CD11a monoclonal antibody MHM24 (Hildreth and August 1985), and prepared by replacing mouse DNA sequences with human DNA sequences (Boehncke 2007a).

The specificity of efalizumab is restricted to human and chimpanzee CD11a (Champe, et al. 1995) (Reimann, et al. 1994).

M17, a rat IgG2a anti-mouse CD11a monoclonal antibody, shows pharmacological activities that are similar to efalizumab (Nakakura, et al. 1993). Both M17 and Efalizumab bind to the I domain region of the CD11a inhibiting the interaction of α L β 2 with ICAM. The epitope for M17 is within the ICAM binding region, in contrast the epitope for efalizumab is outside the ICAM binding region.

Administration of M17 to mice results in the development of anti-M17 antibodies, for this reason a rat-mouse chimera construct, muM17, was prepared to reduce and overcome the immunogenicity of M17 (Clarke, et al. 2004).

The Fc part of efalizumab is recognised by the Fc γ receptor series (Fc γ RI, Fc γ RIIA, Fc γ RIIB and Fc γ RIIIA). Efalizumab does not show complement-dependent cytotoxicity (CDC), binding poorly to the complement protein C1q (Chetty, et al. 2014) (Brennan, et al. 2010).

Efalizumab inhibits the binding of α L β 2 to ICAM-1, -2, and -3 (Boehncke 2007a), and it is also able to inhibit the mixed lymphocyte response, T cell activation, T-lymphocyte adhesion to human endothelial cells, and trans-endothelial T cell migration (Boehncke 2007b) (Clarke, et al. 2004).

Efalizumab interacts with the alpha I domain, it blocks the binding of ICAM-1 to α L β 2 via steric hindrance. The Fab light chain has spatial conflicts with the domain 2 of ICAM-1 (Li, et al. 2009). After binding to α L β 2, efalizumab is internalized by T cells, translocated to lysosomes and degraded in complex with α L β 2. This process constitutes one of the pathways for *in vivo* clearance of efalizumab (Coffey, et al. 2005).

Efalizumab acts as immunosuppressant, inducing T cell hyporesponsiveness. CD3- and CD2-mediated activation is reduced after treatment with efalizumab, (Guttman-Yassky, et al. 2008) (Major 2010).

In patients the administration of efalizumab leads to the downmodulation of several others surface molecules like CD3, TCR, CD4, CD8, CD28, and the integrin VLA-4 (Guttman-Yassky, et al. 2008) (Major 2010) (Boehncke 2007a).

Efalizumab was commercialized with the name of Raptiva® by Genentech. It was indicated for the treatment of moderate to severe chronic plaque psoriasis where it was able to alleviate signs and symptoms of the disease by inhibiting T-lymphocyte activation in lymph nodes, T-lymphocyte trafficking into psoriatic lesions, T-lymphocyte interaction with keratinocytes, secondary activation

of T-lymphocytes in plaques, and release of pro-inflammatory cytokines (Boehncke 2007a). Raptiva was approved by FDA in 2003 and by EMEA in 2004. In 2009 the antibody was withdrawn from markets because benefits of efalizumab did not outweigh the risks of PML or other serious infections (Carson, et al. 2009).

1.8. Progressive multifocal leukoencephalopathy - PML

PML is a demyelinating disease of the white matter of the human brain caused by the reactivation of latent JC virus, a virus that leads to a lytic infection of oligodendrocytes. It occurs mainly in immune-suppressed patients.

Its highest incidence is in AIDS patients, ~3% of HIV-1-infected individuals. In addition to severe immune suppression, there appear to be synergistic interactions between HIV-1 and JCV that contribute to the higher incidence of PML in AIDS patients (Tyler 2010).

People on chronic immunosuppressive medications, including chemotherapy, are also at increased risk of PML, such as patients with transplants, Hodgkin's Lymphoma, multiple sclerosis, psoriasis and other autoimmune diseases.

Concerning anti-VLA-4 mAb natalizumab, in 2005 it was voluntarily withdrawn from the market because it was linked with three lethal cases of PML (Yousry, et al. 2006). The risk of PML was assessed about 1.0 case per 1,000 patients treated over 18 months, with a possible increased risk in case of additional time treatment (Yousry, et al. 2006). To date, natalizumab is back to the market but the treatment is under a restrictive risk management program (Nijsten, et al. 2009).

In 2009, before the anti- α L β 2 efalizumab was withdrawn, Genentech provided and updated about safety findings with the “U.S. BL 125075/130 Amendment: Efalizumab-Genentech, Inc.”

WARNING:

RISK OF PROGRESSIVE MULTIFOCAL LEUKOENCEPHALOPATHY (PML):

• RAPTIVA increases the risk for PML, a rapidly progressive viral infection of the central nervous system that has no known treatment and that leads to death or severe disability. The risk of PML may markedly increase with longer duration of RAPTIVA exposure. The time dependent threshold when the risk for PML increases is unknown (see WARNINGS).

- Patients on RAPTIVA should be monitored frequently to ensure they are receiving significant clinical benefit, to ensure they understand the significance of the risk of PML, and for any sign or symptom that may be suggestive of PML (see WARNINGS).
- RAPTIVA dosing should be withheld immediately at the first sign or symptom suggestive of PML. For diagnosis, brain magnetic resonance imaging (MRI) and, when indicated, cerebrospinal fluid analyses for JC viral DNA are recommended (see WARNINGS).

RISK OF SERIOUS INFECTIONS

- Infections, including serious infections leading to hospitalizations or death, have been observed in patients treated with RAPTIVA (see WARNINGS and ADVERSE REACTIONS). These infections have included bacterial sepsis, viral meningitis, invasive fungal disease and other opportunistic infections. Patients should be educated about the symptoms of infection and be closely monitored for signs and symptoms of infection during and after treatment with RAPTIVA. If a patient develops a serious infection, RAPTIVA should be discontinued and appropriate therapy instituted.

The incidence of PML in patients treated with efalizumab is estimated to be 1 case per 15,000 person years (Nijsten, et al. 2009). The link between the effects of monoclonal antibody treatments that target proteins of the immune system, adhesion proteins or cell surface markers (Efalizumab- α L β 2, Natalizumab-VLA-4 and Rituximab-CD20) and the occurrence of PML could be explained by the latency of JCV in the bone marrow. Under therapy, bone marrow derived cell carrying latent virus may be released into the circulation and may enter the brain (Seminara and Gelfand 2010).

1.9. Small Molecule α L β 2 inhibitors

Several small molecule inhibitors have been described in patent applications or scientific literature which affect the interaction of α L β 2 with their ligands (Giblin and Lemieux 2006). To date, these compounds can be grouped into two major classes, based on how they bind to α L β 2 and how they influence α L β 2 conformation. One class of inhibitors, termed alpha I allosteric inhibitors, binds to the ligand binding domain (termed I domain) on the α L β 2 alpha chain, however at a site distal to the ligand binding site (termed α L I allosteric site). These inhibitors stabilize α L β 2 in its bent inactive state, preventing the switchblade-like opening of α L β 2 into its extended active state, and the exposure of activation epitopes (Giblin and Lemieux 2006). Furthermore, the binding of alpha I allosteric inhibitors to α L β 2 can be elegantly detected by the loss of the mAb R7.1 epitope (Weitz-Schmidt, et al. 2004). Major chemical classes of alpha I allosteric inhibitors which have been described so far include hydantoin derivatives, statin (or “mevinolin”)-based derivatives, substituted diazepanes and arylthio cinnamide analogues (Giblin and Lemieux 2006) (Kapp, et al. 2013). None of these compounds is reported to be in clinical development, currently.

Another group of inhibitors, termed α/β I allosteric inhibitors, are ligand mimetics, i.e. they are derived from amino acids of the α L β 2 binding region of ICAM (Giblin and Lemieux 2006) (Kapp, et al. 2013). Unexpectedly, these ligand mimetics do not bind to the ligand binding site of α L β 2 located on the alpha chain. Instead, they act via the α L β 2 beta chain by competing with the interaction of an internal ligand. As a result, the binding domain of α L β 2 remains in a low affinity state whereas the rest of α L β 2 adapts an extended, active conformation, exposing activation epitopes (Giblin and Lemieux 2006). Cells treated with these inhibitors exhibit paradoxical activities, i.e. induction of “rolling adhesion” by the inhibitors, in contrast to cells treated with α L I

allosteric inhibitors (Salas, et al. 2004). Paradoxical agonism has also been observed with ligand mimetics targeting other integrin family members including α I**II** β 3 (Ahrens and Peter 2008). Currently, one ligand mimetic α L **β** 2 was approved by FDA for the treatment of the signs and symptoms of dry eye disease (DED) (Sheppard, et al. 2014) (Kapp, et al. 2013) (Holland, et al. 2016).

1.10. Lifitegrast

Lifitegrast is a small molecule peptidomimetic (615.48 Da) which binds to the integrin α L **β** 2 preventing this integrin from interacting with ICAM-1 (Fig. 6) (Zhong, et al. 2012). It belongs to the class of α/β I allosteric α L **β** 2 inhibitors.

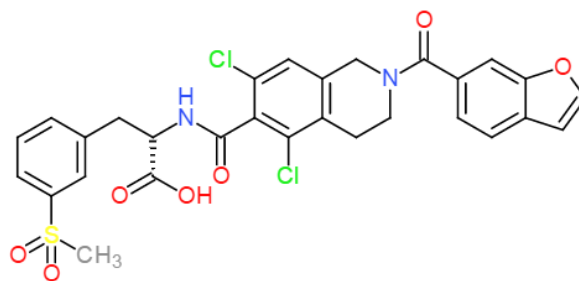


Fig. 6. Lifitegrast

Lifitegrast has been developed by Shire as a treatment for DED.

ICAM-1 is overexpressed in the tissue of the cornea and conjunctiva in DED, and the interaction between ICAM-1 and α L **β** 2 promotes lymphocyte activation and migration and accumulation into the ocular surface (Gao, et al. 2004).

In a Phase II trial, conducted on a total of 230 patients with dry eye, lifitegrast showed a significant improvement in corneal staining score and visual related function and improvements in tear production (Semba, et al. 2012). In a Phase III, trial conducted on 718 patients with dry eye disease, lifitegrast was administered as eye drops (5% solution) or placebo twice a day for 12 weeks, after a 14-day open label placebo run-in period. Lifitegrast showed improvement in eye dryness compared to placebo-treated subjects with significant improvement of secondary symptom end points (Tauber, et al. 2015). In July 2016, lifitegrast was approved by FDA for the treatment of the signs and symptoms of DED (Holland, et al. 2016).

1.11. XVA143

XVA143, a peptidomimetic α L β 2 inhibitor (Fig. 7), with an α/β I-like allosteric inhibitor of α L β 2. XVA143 is not selective for α L β 2, it also inhibits other β 2 integrins including Mac-1 (Welzenbach, et al. 2002).

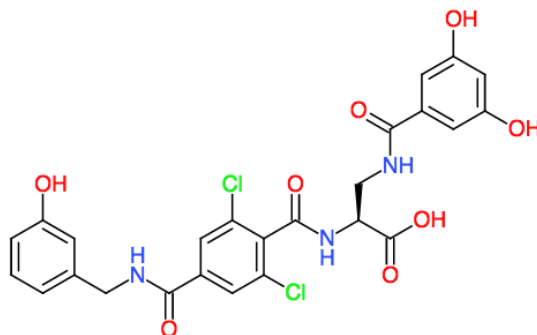


Fig. 7. XVA143.

The binding of XVA143 to the β 2 MIDAS blocks the interaction of the β 2 MIDAS domain itself with the α L-Glu-310. This amino acid is located on the C-linker, which follows the α 7-helix at the C-terminal end of the α I domain and it binds to the MIDAS of the active I domain. Glu-310 can be considered an intrinsic ligand for α L β 2. This interaction leads to downward displacement of the α 7 helix, turning the α I MIDAS into a high-affinity, ligand-binding state (Weitz-Schmidt, et al. 2011). XVA143 binds to the β I domain MIDAS and blocks α I activation by preventing the binding of the intrinsic β 2 MIDAS ligand α L-E310 (Schurpf and Springer 2011) (Yang, et al. 2006).

XVA143 blocks α I activation by disrupting signal transmission between the α I and β I-like domains (Yang, et al. 2004) and in the same time induces the extension of α L β 2 leading to rolling of the cells (Salas, et al. 2004) (Chigaev, et al. 2015). The induction of the β 2 leg extension (Schurpf and Springer 2011) leads to the exposure of KIM127 mAb epitope in the I-EGF-2 domain (Chigaev, et al. 2015) (Nishida, et al. 2006).

XVA143 can also inhibit the homotypic adhesion of NK cells and induce the disaggregation of NK cells (Chen, et al. 2010).

In K562 cells, XVA143 not only extends α L β 2 but also stabilizes the extended low- or intermediate-affinity bonds with ICAM-1 (Feigelson, et al. 2010).

α L β 2 antagonists, interfering with cell-to-cell contact, can affect viral propagation events. XVA143 could inhibit HIV-1 replication, opening to a potential use of this kind of antagonists in combination with traditional therapy (Tardif, et al. 2009).

1.12. LFA878

LFA878 is a statin-derived small compound (MW 596.77) (Fig. 8).

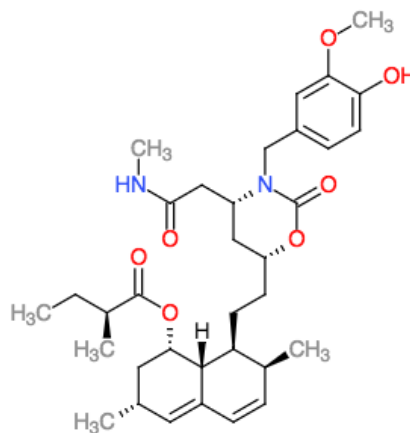


Fig. 8. LFA878.

It binds the α I domain of α L β 2 inhibiting allosterically the binding of α L β 2 to its ligands (Fig. 9). LFA878 lacks the hydroxymethylglutaryl coenzyme A (HMG-CoA) reductase activity. LFA878 has strong anti-inflammatory properties in first place for its direct effect on α L β 2 and then because this results in impaired T cell costimulation (Weitz-Schmidt, et al. 2004).



Fig. 9. X-ray structure of α L β 2 I domain in complex with LFA878 at 2.1Å resolution.

<http://www.rcsb.org/pdb/explore/jmol.do?structureId=1XDG&bionumber=1>

Studies show that LFA878 could also induce cell death in several multiple myeloma cell lines by apoptosis, through the caspase 3 pathway and redistribution of negatively charged phospholipids

transported to the outer cell surface. The induction of apoptosis has not been seen in PBMCs suggesting a disease specific effect (Schmidmaier, et al. 2007). This property was already shown for simvastatin, the statin with the most potent antimyeloma activity (Schmidmaier, et al. 2006).

LFA878 can also target the harmful effects of NK cells, preventing their homotypic adhesion and promoting the disaggregation of existing NK cell clusters (Weitz-Schmidt, et al. 2009).

X-ray crystallography clarified the molecular basis of the binding to the I domain and allowed the design of potent and selective small molecule inhibitors of $\alpha\text{L}\beta\text{2}$.

The engagement and the inhibition of $\alpha\text{L}\beta\text{2}$ by LFA878 through binding of the I domain can be detected in undiluted human blood, that permits to study the role of the I domain under physiological conditions (Weitz-Schmidt, et al. 2001) (Weitz-Schmidt, et al. 2004).

Taken together, it is appreciated that $\alpha\text{L}\beta\text{2}$ is a receptor involved in inflammatory, immune-mediated and infectious diseases and is overexpressed in certain malignant diseases. These diseases are often severe, chronic disorders often requiring life-long therapy. From a clinical perspective, there remains a high need for effective therapies either preventing the conditions or controlling the activity of disease and providing long-term benefit/risk profiles superior to currently available therapies. It is further appreciated that novel $\alpha\text{L}\beta\text{2}$ inhibitors with improved pharmacologic profiles and devoid of side effects observed with earlier $\alpha\text{L}\beta\text{2}$ inhibitors will constitute a therapeutic advance.

In conclusion, based on the status of prior art, there remains a need for novel, improved $\alpha\text{L}\beta\text{2}$ inhibitors of chemical scaffolds different to scaffolds described before. The availability of such inhibitors would provide additional therapeutic and diagnostic options across the spectrum of diseases in which $\alpha\text{L}\beta\text{2}$ is involved or can be employed as a target for drug delivery, given that different chemical structures will be associated with different pharmacologic profiles.

Furthermore, it is appreciated that the function of $\alpha\text{L}\beta\text{2}$ can be modulated in different ways and that unwanted effects/side-effects observed with certain classes of existing $\alpha\text{L}\beta\text{2}$ inhibitors, such as anti- $\alpha\text{L}\beta\text{2}$ monoclonal antibodies, may not be observed with novel types of $\alpha\text{L}\beta\text{2}$ inhibitors.

Paper 1

From virtual screening to highly potent, orally available small molecule inhibitors of the integrin α L β 2

Abbreviations: **ADMIDAS**, adjacent to metal ion-dependent adhesion site; **AK**, adenylate kinase; **AUC**, area under the curve; **AUC_{INF}**, area under the curve from time zero to infinity; **BCECF-AM**, 2',7'-bis-(2-carboxyethyl)-5-(and-6)-carboxyfluorescein, acetoxymethyl ester; **BSA**, bovine serum albumin, **CADD**, computer-aided drug discovery; **CD**, cluster of differentiation; **CL_F**, formation clearance of a drug to a metabolite; **C_{max}**, maximum plasma concentration; **CV**, coefficient of variation; **DMSO**, dimethyl sulfoxide; **EDTA**, ethylenediaminetetraacetic acid; **Fc**, fragment crystallizable; **FCS**, foetal calf serum; **FITC**, fluorescein isothiocyanate; **FSC**, forward scatter; **IC₅₀**, half maximal inhibitory concentration; **ICAM**, intercellular adhesion molecules; **IgG-x**, immunoglobulin G cross-linked; **IgG**, immunoglobulin G; **IL**, interleukin; **IS**, immunological synapse; **IS**, internal standard; **LFA-1**, lymphocyte function-associated antigen-1; **LPS**, lipopolysaccharide; **mAb**, monoclonal antibody; **MFI**, mean fluorescence intensities; **MHC**, major histocompatibility complex; **OD**, optical density; **pAb**, polyclonal antibody; **PAM**, point accepted mutation; **PBMC**, peripheral blood mononuclear cell; **PD**, pharmacodynamic; **PE**, phycoerythrin; **PI**, propidium iodide; **PK**, pharmacokinetic; **PMA**, phorbol 12-myristate 13-acetate; *po*, *per os*; **Rsq**, square of correlation coefficient; **S/N**, signal to noise ratio; **SAR**, structure activity relationship; **SD**, standard deviation; **SSC**, side scatter; **t_{1/2}**, elimination half-life; **TCR**, T cell receptor; **t_{max}**, time to reach maximum concentration; **VCAM-1**, vascular cell adhesion protein-1; **VCAM**, vascular cell adhesion molecule; **VLA-4**, very late antigen-4; **VzF**, apparent volume of distribution during terminal phase after non-intravenous administration; **ZAP70**, zeta-chain-associated protein kinase 70;

Abstract

The integrin lymphocyte function-associated antigen-1 (LFA-1, α L β 2) is expressed on all leukocytes. The interaction between α L β 2 and the intercellular adhesion molecules (ICAMs) is pivotal in cell adhesion, leukocyte trafficking, T cell costimulation and immunological synapse (IS) formation. α L β 2 is centrally involved in immune-mediated diseases of high medical need.

Here we describe the identification, synthesis, *in vitro* structure-activity relationship (SAR) and preclinical characterization of innovative α I allosteric inhibitors that modulate α L β 2 function via binding to the α L I allosteric site. Virtual screening has been used to identify a new chemical scaffold that modulates α L β 2 function. Optimization of this scaffold has resulted in high-affinity inhibitors of the α L β 2/ICAM-1 interaction, with IC₅₀ values in the low nM range. A selected lead compound has been transitioned to preclinical pharmacokinetic (PK) characterization *in vivo*. This

new class of inhibitors is expected to overcome major unwanted effects of current integrin targeting drugs.

1. Introduction

The integrin α L β 2 is expressed on leukocytes. In its activated state α L β 2 mediates the adhesion of leukocytes to each other and to other cells regulating leukocyte trafficking, T cell costimulation and immunological synapse (IS) formation (Hogg, et al. 2011).

In its inactive, bent state, α L β 2 is not capable to mediate cell adhesion and to induce signalling. Upon activation from inside the cell (inside-out signalling) α L β 2 converts into an activated extended state which is able to bind its ligands, intercellular adhesion molecules (ICAMs), to mediate adhesion and induce signalling (outside-in signalling) (Hogg, et al. 2011).

α L β 2 is centrally involved in immune-mediated diseases of high medical need, including chronic plaque psoriasis, multiple sclerosis, rheumatoid arthritis, small vessel vasculitis, dry eye disease and transplantation indications, among other disorders. In several of these diseases, α L β 2 has been validated by biologic therapies as a target of high therapeutic potential (Millard, et al. 2011) (Shimaoka and Springer 2003) (Cox, et al. 2010b).

From a pharmacological perspective, the stabilization of the inactive (bent) state of α L β 2 by low molecular weight compounds constitutes the most elegant approach to therapeutically modulate its function. This approach is also expected to overcome major limitations of current ligand mimetics and biologics targeting integrins. For example, it is anticipated that pharmacological stabilizing of the inactive form of integrins will avoid unwanted agonist-like effects such as the gross downmodulation of major immune receptors (also termed transmodulation) as observed for the anti- α L β 2 mAb efalizumab (Guttman-Yassky, et al. 2008) or paradoxical agonism as observed for various ligand mimetics targeting integrins (Jones, et al. 2010) (Millard, et al. 2011) (Salas, et al. 2004) (Schurpf and Springer 2011).

Previous studies indicate that low molecular weight allosteric modulators of α L β 2, targeting the α L I allosteric site, are able to stabilize α L β 2 in its inactive state and may thereby avoid transmodulation and/or paradoxical agonism. Indeed, we recently demonstrated that inhibitors belonging to the α L I allosteric class can be clearly differentiated from anti- α L β 2 mAbs (i.e. efalizumab) and α L β 2 targeting α / β I allosteric inhibitors in terms of their downstream effects on α L β 2 (Mancuso, et al.2016). Several small molecules which bind to the I allosteric site of α L β 2 have been characterized extensively (Giblin and Lemieux 2006) (Fig. 1) however, none of these compounds meet the pharmacological requirements that would permit their full development into systemically used drugs, i.e. they either provide inadequate pharmacokinetic characteristics and/or

are associated with systemic safety concerns attributable to their chemical scaffold (Cox, et al. 2010a) (Goodman and Picard 2012) (Miller, et al. 2009). As a consequence, currently there is no $\alpha\text{L}\beta\text{2}$ modulator with the intended mode of action on the market.

In collaboration with Gisbert Schneider's group at the ETH Zürich we used a virtual screening approach for the identification of a novel class of $\alpha\text{L I}$ allosteric $\alpha\text{L}\beta\text{2}$ modulators.

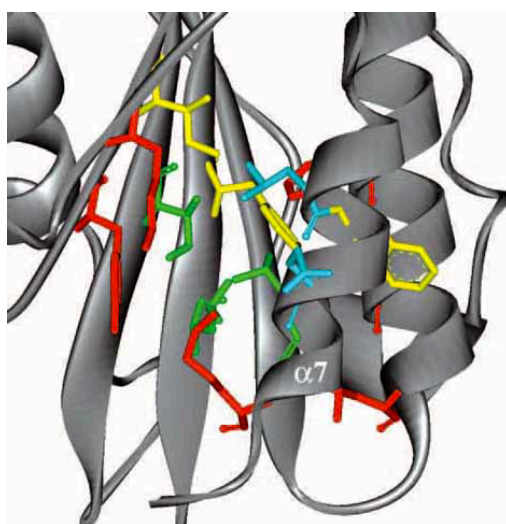


Fig. 1. Close-up view of the $\alpha\text{L I}$ domain allosteric site within the $\alpha\text{L}\beta\text{2 I}$ domain. Indicated in green, red, blue and yellow are the residues of the I allosteric site that are located in close proximity of 4 different classes of alpha I allosteric inhibitors (Source: Giblin and Lemieux 2006).

Three million drug-like, commercially available compounds have been screened and candidates for $\alpha\text{L}\beta\text{2}$ activity testing prioritized, taking known low molecular weight inhibitors as queries for multiple similarity searches and compound ranking.

This virtual screen yielded in ranked lists of compounds. Resulting lists have been combined and analyzed (“data fusion”). Off-targets and potential liabilities of the hits found have been addressed *in silico* by extensive comparison to a set of 672 drug targets using proprietary algorithms for target profile prediction. As the outcome of the first virtual screening triage, approximately 200 commercially available candidate compounds have been submitted for biochemical activity determination. 60 commercially available compounds were purchased.

Here we describe the analysis of these selected 60 compounds, the identification of a hit compound and the chemical derivatization of this hit towards potent lead compounds (collaborative work with Marianne Hürzeler's group at the School of Life Sciences, FHNW Basel) and the detailed

characterisation of the most advanced inhibitor including first pharmacokinetic properties of the compound in rats.

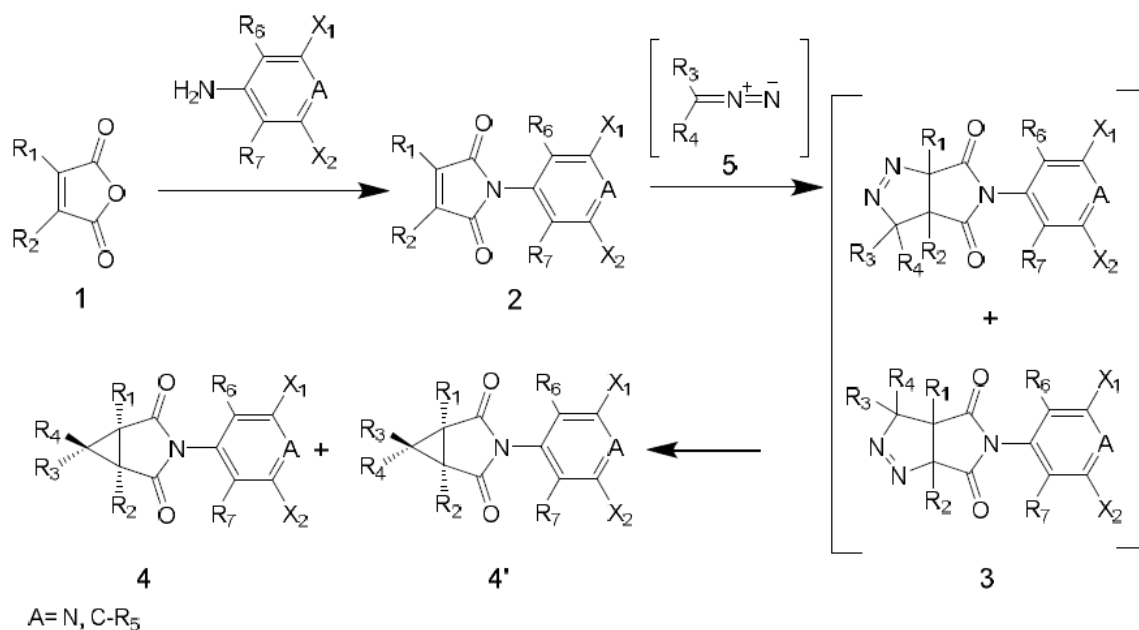
2. Materials and Methods

2.1. Synthesis of chemical compounds

Chemical reagents and solvents were purchased from commercial sources (Sigma-Aldrich, St. Louis, MO, and Bachem, Bubendorf, CH).

The compounds were prepared by the exemplary processes described in detail in the following reaction schemes.

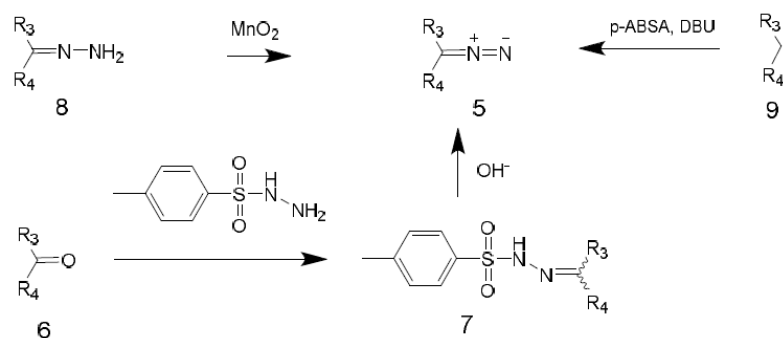
Methods of Scheme A. To a solution of anhydride **1** (1 eq.) in acetic acid amine (1 eq.) was added and the reaction mixture was boiled for 2–10 h. Then the solvent was removed at reduced pressure. The residue was dissolved in DCM and washed with sat. aq. NaHCO₃, aq. 1N HCl and sat. aq. NaCl, dried over Na₂SO₄ and the solvent was removed at reduced pressure. The crude product was purified by silica gel flash chromatography (Shults, et al. 2005). To a solution of maleimide **2** (1 eq.) in DCM or toluene a solution of diazo compound in DCM or toluene was added. The mixture was stirred at room temperature (rt) for 2-10 days until the disappearance of the diazo colour. The precipitate was filtered off and washed with ethanol (Molchanov, et al. 2002). In cases without a precipitate, the solution was used directly in the next step. A mixture of pyrazoline-intermediate **3** and toluene was heated to 100 °C for 1-2 h at 100 °C. The solvent was removed at reduced pressure and the crude product purified by silica gel flash chromatography (Molchanov, et al. 2002).



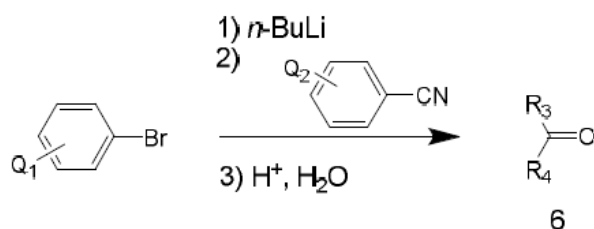
Methods of Scheme B. To the hydrazone **8** (1 eq.) in DCM MnO₂ was added. The suspension was stirred for 15 min at rt and then filtered. The purple solution of **5** was used directly in the next step (Bourget, et al. 2005).

To a stirred suspension of 4-toluenesulfonylhydrazide (1 eq.) and MeOH the aldehyde or ketone **6** (1 eq.) was added. After 1-14 h stirring at different temperatures (rt until 60 °C) the reaction was complete. The suspension was filtered or centrifuged, and then washed with small amounts of MeOH to afford solid **7** (Aggarwal, et al. 2003).

The hydrazone **7** (1 eq.) and TEBAC (0.25 eq.) was stirred in aq. NaOH (15%, 10 eq.) and toluene under nitrogen. After 1-2 h of strong stirring at 70 °C the reaction was usually complete. The deep red/purple organic layer was washed with sat. aq. NH₄Cl, sat. aq. NaCl and dried with Na₂SO₄. This solution of **5** was used directly in the next step (Zhou, et al. 2009). To a solution of the ester **9** (1 eq.) and p-ABSA (1.5 eq.) in 10 mL dry CH₃CN at 0 °C DBU (1.5 eq.) was added over 30 min. After stirring for 1 h at rt, the mixture was partitioned between water and EtOAc. The combined organic extract was dried and concentrated. The residue was purified by silica gel flash chromatography to afford **5** (Taber, et al. 2005).



Method of Scheme C. To the substituted bromobenzene (1 eq.) in THF at $-78\text{ }^\circ\text{C}$ *n*-BuLi (2.5 M in hexane, 1 eq.) was added dropwise and the mixture was stirred at $-78\text{ }^\circ\text{C}$ for 1 h. To the solution of substituted phenyllithium in ether (1 eq.) benzonitrile (1 eq.) in ether was added at $0\text{ }^\circ\text{C}$ and the mixture was stirred at rt overnight. The reaction mixture was poured onto ice (in some cases acidified). The resulting mixture was allowed to warm to rt and was then extracted with ether, dried and concentrated at reduced pressure. The crude product was purified by chromatography on alumina (Cook and Wakefield 1980).



2.2. Preparation of compounds, control compounds and efalizumab

Test compounds were dissolved at 10 mM in DMSO. Control reagents simvastatin, TritonTM X-100, staurosporine, cyclosporine A, amiodarone, procymidone, LPS, PMA and ionomycin were purchased from Sigma-Aldrich, St. Louis, MO, and dissolved at 10 mM in DMSO. Compound RO0505376 was kindly provided by Dr. Paul Gillespie. For the experiments, the compounds were serially pre-diluted in DMSO to avoid precipitation followed by dilution in medium or assay buffer. Final DMSO concentration during the experiments was $\leq 1\%$. No cytotoxicity was detected at this concentration. Efalizumab (obtained from Merck-Serono when product was on the market) was kept at $-80\text{ }^\circ\text{C}$ in RPMI 1640 at a concentration of 10 mg/ml. Serial dilutions were prepared in medium or assay buffer.

2.3. Cell Culture

The human lymphoblastoid cell line Jurkat (European Collection of Cell Cultures, Salisbury, UK), the mouse ovalbumin-specific T cell receptor (TCR)-transgenic cell line OT-1 (gift from Ed Palmer, University Hospital, Basel, CH), the human monocytic cell line THP-1 (gift from Prof. Dr. Jürg Schwaller, University Hospital, Basel, CH) and the human liver cancer cell line HepG2 (ATCC, Manassas, VA) were maintained in a humidified incubator at 37 °C supplied with 5% CO₂. Jurkat cells and THP-1 cells were cultured in RPMI 1640 containing 10% (v/v) heat-inactivated foetal calf serum (FCS), 1% MEM amino acids, amphotericin B 1 µg/ml, gentamycin 10 µg/ml (Gibco Life Technologies, Paisley, UK). OT-1 cells were cultured in RPMI 1640 containing 5% (v/v) heat-inactivated FCS, L-glutamine 2 mM, penicillin 100 U/ml and streptomycin 100 µg/ml (Gibco Life Technologies, Paisley, UK). HepG2 cells were maintained in DMEM containing 10% (v/v) heat-inactivated FCS, 1g/l glucose, 4 mM L-glutamine, 2 mM GlutaMax, 1 mM pyruvate, 10 mM HEPES buffer, 10 mM non-essential amino acid, penicillin 100 U/ml and streptomycin 100 µg/ml (Gibco Life Technologies, Paisley, UK). The density of the cells was maintained below 1 x 10⁶ cells/ml. Every second or third month, the cell cultures were replaced by a new batch of cells with a low passage number.

2.4. Isolation of peripheral blood mononuclear cells (PBMCs)

PBMCs were isolated from EDTA-blood samples via centrifugation in Ficoll-PaqueTM PLUS separating solution according to the manufacturer's protocol (GE Healthcare, Glattbrugg, CH). The blood samples were obtained from healthy donors from the Blood Center SRK of Basel.

2.5. V well adhesion assay ICAM-1 VCAM-1 mICAM-1

The Jurkat/ICAM-1 (human αLβ2 dependent cell adhesion), Jurkat/VCAM-1 (human VLA-4 dependent cell adhesion) and OT-1/ICAM-1 (murine αLβ2 dependent cell adhesion) assays were performed in V-bottom 96-well plates (Sigma-Aldrich, St. Louis, MO) as previously described (Weetall, et al. 2001) (Weitz-Schmidt and Chreng 2012). Briefly, V bottom plates (Sigma-Aldrich, St. Louis, MO) were coated with anti-human IgG mAb (Sigma-Aldrich, St. Louis, MO) diluted in coating buffer (20 mM Tris containing 150 mM NaCl, pH 8) (1 µg/ml) and incubated overnight at 4 °C. The plates were blocked with blocking buffer (50 mM Tris base, 150 mM NaCl, 1.5% BSA (w/v), pH 7.2) at 37 °C for 90 minutes (min). Human ICAM-1/Fc chimera, human VCAM-1/Fc chimera or mouse ICAM-1/Fc chimera (R&D Systems, Abingdon, UK) were immobilized at 0.3 µg/ml in coating buffer. For studies with efalizumab, human ICAM-1 without Fc-tag (R&D Systems, Abingdon, UK) was directly immobilized to V bottom plates without capturing mAb. The

plates were incubated at 37 °C for 90 min and washed with binding buffer (50 mM Tris base, 150 mM NaCl, 1.5% BSA (w/v), 2 mM MgCl₂, 2 mM MnCl₂, 5 mM D-glucose monohydrate, pH 7.2-7.4). The cells were fluorescently labelled with 1 µg/ml of BCECF-AM (Gibco Life Technologies, Paisley, UK) in PBS at 37 °C for 20 min and washed with PBS. The labelled Jurkat cells or OT-1 cells were resuspended in binding buffer and test compounds or solvent controls were added. After 40 min at 37 °C 30,000 cells/well were transferred to the integrin ligand coated V well plates. After 5 min of incubation at rt plates were centrifuged for 4 min at 1,000 rpm using the Centrifuge Eppendorf 10 5810 R (Eppendorf, Schönenbuch, CH), without activating the brake. Non-adherent cells accumulated in the centre of the V-bottom and were quantified using the fluorescence reader Tecan M200 Pro Infinity (Tecan, Mannedorf, CH) (excitation 485 nm / emission at 535 nm). The half maximal inhibitory concentration (IC₅₀) values were calculated using the software GraphPad Prism 6 (GraphPad Software, La Jolla, CA).

2.6. Quantification of mAb R7.1, MEM148 or m24 binding to αLβ2

Conformational changes of αLβ2 upon inhibitor binding were quantified using FITC-labelled anti-αLβ2 mAb R7.1 (ebioscience, Frankfurt, D), PE-labelled anti-αLβ2 mAb MEM148 (Sigma-Aldrich, St. Louis, MO) and Alexa Fluor® 488-labelled anti-αLβ2 mAb m24 (Biolegend, San Diego, CA). For mAb R7.1 binding, Jurkat cells were resuspended in assay buffer (50 mM Tris, 150 mM NaCl, 2 mM MgCl₂, 1.5% BSA and 10 mM D-glucose monohydrate, pH 7.2). For mAb MEM148 and m24 binding, 50 mM Tris, 150 mM NaCl, 1 mM CaCl₂, 1 mM MgCl₂, 5 mM Glucose, 1.5% BSA, pH 7.3). Jurkat cells were transferred in their respective assay buffer to polypropylene tubes containing the compounds, efalizumab, efalizumab cross-linked (efalizumab-x) or respective solvent and IgG controls (Sigma-Aldrich, St. Louis, MO). Multimeric/cross-linked efalizumab was generated by incubation of efalizumab with a goat anti-human IgG (Sigma-Aldrich, St. Louis, MO) at a ratio of 1:1 (10 µg/ml) in assay buffer. The cells were pre-incubated with the compounds at 37 °C for 40 min. In experiments in which the effect of the compounds and the antibody on MnCl₂-induced MEM148 or m24 epitope exposure was studied, cells were pre-incubated in assay buffer containing the inhibitors and the respective controls at 37 °C for 30 min. Then MnCl₂ was added to a final concentration of 2 mM, followed by an incubation of 30 min at 37 °C. After this incubation, the cell suspension was centrifuged, the supernatant discarded. Cells were stained with mAb R7.1 on ice or with mAb MEM148 and mAb m24 at 37 °C for 30 min, respectively (final concentration mAbs 1 - 2 µg/ml). After two wash cycles cells were analyzed by flow cytometry using a FACScalibur (BD, East Rutherford, NJ). Mean fluorescence intensities

(MFI) of FSC/SSC gated events were calculated using the FlowJo software 10.0.8 (Tree Star, Ashland, OR).

2.7. Quantification of mAb R7.1 binding to α L β 2 in whole blood of different species

Conformational change of α L β 2 upon inhibitor binding was also quantified in whole blood of human, rabbit, mouse and pig using FITC-labelled anti- α L β 2 mAb R7.1 (ebioscience, Frankfurt, D). The human blood samples were obtained from healthy donors from the Blood Center SRK of Basel. The mouse blood samples (*Mus musculus*) were obtained from the animal facility of the Department of Biomedicine, Basel. The rabbit blood samples (*Oryctolagus cuniculus*) were kindly provided by Prof. Dr. Ivan Martin, University Hospital Basel. The porcine blood samples (*Sus scrofa*) were kindly provided by Dr. Michele Diana, Hôpital Universitaire de Strasbourg. Blood aliquots (100 μ l) were mixed with the compound solution or DMSO (0.3 μ l) and incubated for 40 min at rt. After this incubation, cells were stained with mAb R7.1 at rt for 30 min. Erythrocytes were then lysed with FACS lysing solution (BD Biosciences, Switzerland). Samples were centrifuged at 200 x g for 5 min and pellets were washed two times in PBS and resuspended in 100 μ l of PBS. Cells were analyzed by flow cytometry using a FACScalibur (BD, East Rutherford, NJ). Mean fluorescence intensities (MFI) of FSC/SSC gated events were calculated using the FlowJo software 10.0.8 (Tree Star, Ashland, OR).

2.8. Cytotoxicity and apoptosis

Cytotoxicity was investigated in Jurkat and HepG2 cells using the ToxiLightTM BioAssay Kit (Lonza, Basel, CH), measuring the release of adenylate kinase (AK), a marker for loss of cell membrane integrity, and CellTiter-Glo[®] Luminescent Cell Viability Assay, determining the number of viable cells in culture based on quantitation of the ATP present, an indicator of metabolically active cells. After 24 h incubation with compounds, or controls, toxicity and viability were determined by plate reader measurements following manufacturer's instructions.

Apoptosis and secondary necrosis were determined by flow cytometry after 24 h incubation with compounds or controls, using Annexin V and propidium iodide (PI) staining kit and following manufacturer's instructions (VybrantTM Apoptosis Assay Kit #2, Gibco Life Technologies, Paisley, UK).

2.9. Cytokine release

IL-6 cytokine concentration was determined by ELISA commercial kit (Biolegend, San Diego, CA); detection limit was 7.8 pg/ml. 50,000 THP-1 cells/well were incubated in 96 well plate in

presence of testing compounds, efalizumab or controls. After 24 h, supernatant was collected and protein concentration was measured by BCA assay.

Nunc Maxisorp™ 96 MicroWell plates were coated with capture antibody and the plates were then incubated at 4 °C overnight. After four washes with PBS pH 7.4 containing 0.05% Tween 20 (washing buffer), nonspecific binding sites were blocked by incubation for 1 h at rt in assay diluent A with shaking at 200 rpm on a plate shaker. After four washes with washing buffer, supernatants or standards diluted in assay diluent A were added. All the samples were in duplicate. Following incubation at rt for 2 h with shaking, and then four washes with washing buffer.

IL-6 was detected with a specific antibody against it. The bound anti-IL-6 antibody was detected with biotinylated-conjugated anti-human IgG by incubation at rt for 1 h with shaking, followed by four washes with washing buffer. An avidin-HRP solution was added to each well and the plate incubated at rt for 30 min with shaking followed by five washes.

100 µl of 1:1 TMB Reagent A and TMB Reagent B solution were added to each well and the plate was incubated at rt for 30 min for colour development. To stop the colour reaction, 100 µl of TMB Stop solution were added. The optical density (OD) was quantified using the fluorescence reader Tecan M200 Pro Infinity (Tecan, Mannedorf, CH) set to 450 nm.

2.10. Analysis of α L β 2 expression and internalization

PBMCs were resuspended in fresh medium (RPMI 1640, 10% FCS) and seeded at 300,000 cells/well into a 24-well plate followed by incubation with test compounds, efalizumab, efalizumab-x or controls for 24 h. After one wash with PBS, PBMCs were stained with PE-labelled anti- α L β 2 mAb TS2/4, FITC-labelled anti-CD4 mAb clone A16A1 and APC-labelled anti-CD8 mAb clone HIT8a (Biolegend, San Diego, CA) or appropriate isotype controls on ice for 25 min and analyzed by flow cytometry. 5,000 events of CD4⁺ or CD8⁺ cells were acquired. MFI were calculated using the FlowJo software.

For imaging α L β 2 localization, treated cells were washed with cold PBS and fixed at rt for 15 min with paraformaldehyde 4% in PBS. Cells were washed, blocked with PBS/2.5% BSA and incubated at rt for 15 min. Then the cells were incubated on ice for 30 min with PE-labelled mAb TS2/4 for α L β 2 staining, Alexa Fluor® 488-labelled anti-CD107a mAb clone H4A3 (Biolegend, San Diego, CA) for lysosomal staining and DAPI (Gibco Life Technologies, Paisley, UK) for nuclear staining. After one washing step with PBS, cells were imaged using the ImageStream X Mark II Imaging flow cytometer (Merck Millipore Schaffhausen, CH). The number of α L β 2 clusters (granular stainings) was quantified using the software ImageJ (NIH, Bethesda, MD). A threshold range of

130 - 1,000 mean intensity was applied to all images. Clusters were defined by pixel area size (4 - 16) plus shape (circularity 0.4 - 1) and were counted as single events.

2.11. Assessment of intracellular ZAP70 phosphorylation or general tyrosine phosphorylation

ZAP70 tyrosine phosphorylation or general tyrosine phosphorylation were determined using phospho-flow analysis. Briefly, PBMCs were rested for 2 h in RPMI containing 2% FCS, 1% MEM NEAA (resting medium). Rested cells in ice cold resting medium were added to 5 ml FACS tubes and incubated with the small molecule α L β 2 inhibitors and DMSO for 30 min and with the control MnCl₂ for 10 min on ice. On the other hand, OKT3 (5 μ g/ml), efalizumab (10 μ g/ml) and respective IgG controls were incubated with the cells for 15 min on ice. After addition of anti-mouse IgG (5 μ g/ml) or anti-human IgG (10 μ g/ml) respectively the incubation on ice was continued for another 15 min. After these incubation steps, all samples were washed once in ice cold resting medium, transferred into a water bath at 37 °C and incubated for 1 min to activate TCR or α L β 2-dependent membrane proximal signalling pathways. Cells were fixed by addition of paraformaldehyde (final concentration 2%) for 10 min at rt. Cells were then washed with ice cold resting medium, permeabilized by treatment with ice cold 100% methanol, for 10 min. Cells were washed twice with excess of ice cold resting medium and stained for 40 min on ice with Alexa Fluor® 488-labelled anti-ZAP70 pY292 (clone J34-602; BD, East Rutherford, NJ) or FITC-labelled anti-phospho-Tyr clone pY20 and APC-labelled anti-CD2 mAb RPA-2.10 (Biolegend, San Diego, CA). Antibody binding was analyzed by flow cytometry as described above.

2.12. Oral application to rats

In vivo study in rats. The animal experiments were conducted according to the animal experimentation guidelines and laws published by the Swiss Federal and Cantonal Authorities.

The goal of the study was to assess the pharmacokinetic characteristic of the compound in adult male rats upon single dose oral administration.

Adult male Sprague-Dawley rats (6 weeks; 200-250 g) (Janvier labs, France) have been fed by oral gavage with the test compound at the dose levels of 30 mg/kg/day. The test compound was suspended in a combination of 60% propylene glycol and 40% macrogol 400. The dose was projected to provide adequate therapeutic exposure. Serial blood samples have been withdrawn from the tail-vein 0 minute (just before dosing), 5 minutes, 30 minutes, 1 hour, 2 hours, 4 hours, 8 hours, 24 hours and 40 hours after dosing for PK analyses. Throughout the dosing interval, animals had free access to water and food and were monitored for their behaviour and clinical signs.

Key pharmacokinetic parameters assessed included the determination of the area under the curve from time zero to infinity (AUC_{inf}), the maximum plasma concentration (C_{max}), the time to reach maximum concentration (t_{max}) and the compound's elimination half-life ($t_{1/2}$). The total blood sampling did not exceed 20% of the total blood volume. The plasma samples were collected after centrifugation and stored at -20 °C until HPLC analysis.

Plasma sample extraction. Plasma samples were thawed at rt and an aliquot of 30 μ l plasma was spiked with acetonitrile (60 μ l), vortexed and incubated for 10 min at 7 °C to precipitate the plasma proteins. The samples were centrifuged at 13,500 rpm for 8 min using the centrifuge Eppendorf 5424 R (Eppendorf, Schönenbuch, CH) and the supernatant was filtered over a syringe filter (PTFE 0.45 μ m, Sigma-Aldrich, St. Louis, MO).

Chromatography conditions. Plasma samples were analyzed on an Agilent/HP 1100 Series HPLC System using a Poroshell 120 EC-C18 column (2.7 μ m, 50 x 4.6 mm), kept at 35 °C. The test compound was detected during a gradient elution at a flow rate of 1.5 ml/min using mobile phase A ($H_2O + 0.1 \%V H_3PO_4$) and mobile phase B (acetonitrile). Details of the gradients are shown below.

Gradient:	t= 0.0 min	95 % Solvent A	5 % Solvent B
	t= 5.5 min	5 % Solvent A	95 % Solvent B
	t= 7.5 min	5 % Solvent A	95 % Solvent B
	t= 8.0 min	95 % Solvent A	5 % Solvent B

The compound was measured at a wavelength of 210 nm.

Standard stock solutions were prepared by dissolving the compound in DMSO at a concentration of 0.5 mg/ml. The stock solution was kept at 4 °C. Working solutions were prepared on the day of analysis by dilution of the stock solutions with the mobile phase solution (3 μ g/ml to 0.015 μ g/ml). Plasma samples were spiked with the working solutions to establish a calibration line from 1000 - 5 ng/ml.

3. Results

3.1. Identification of compound 7130393 as a novel α L β 2 inhibitor by virtual screening

3.1.1. Optimisation of screening assay

For the identification of novel α L β 2 inhibitors derived from virtual screening, we selected the previously published V well adhesion assay technology. Briefly, in the V well adhesion assay, fluorescently labelled leukocytes are allowed to adhere to ICAM-1-coated V well 96-well plates. Adhesion was induced by the α L β 2 activating divalent cation Mn^{2+} . Thereafter, centrifugal force is applied to separate adherent cells from non-adherent cells. Non-adherent cells accumulate in the tip of the V-shaped wells and are quantified using a fluorometer with a narrow aperture. In absence of inhibitors most of the fluorescent cells stick to the wall of the V shaped wells and cannot be detected in the tip of the well, whereas in the presence of inhibitors most of the cells accumulate in the tip and will be detected (Fig. 2A) (Weitz-Schmidt and Chreng 2012). This assay was optimized using Jurkat cells and commercially available recombinant ICAM-1/Fc fusion protein. Fig. 2B shows that increasing concentrations of ICAM-1/Fc resulted in decreasing assay signals, as expected.

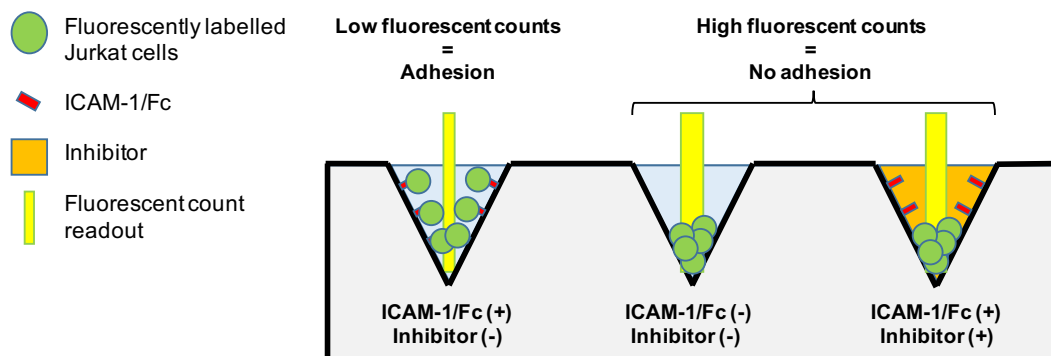


Fig. 2A. Schematic principle of the V well adhesion assay.

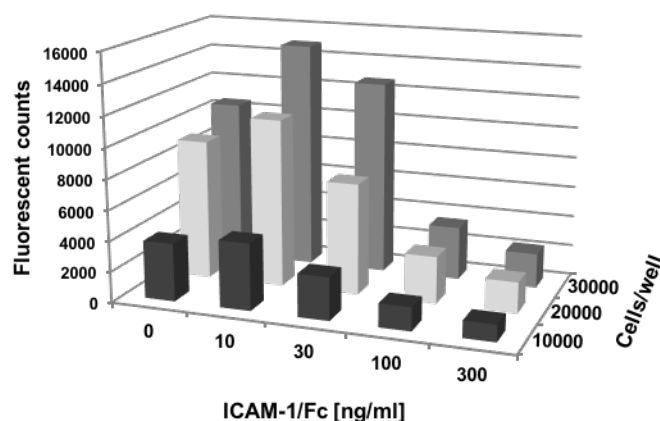


Fig. 2B. Optimisation of the Jurkat cell/ ICAM-1/Fc V well adhesion assay. Anti-human IgG was immobilized on V well microtiter plates at 1 $\mu\text{g/ml}$ and ICAM-1/Fc was added at indicated concentrations. Fluorescently labelled Jurkat cells at indicated numbers were transferred to the wells and adhesion to ICAM-1/Fc was quantified as described under Materials and Methods. The best S/N ratio was obtained by using 300 ng/ml ICAM-1/Fc (15 ng/well) combined with 30,000 cells/well.

Furthermore, the combination of 300 ng/ml ICAM-1/Fc and 30,000 cells/well resulted in acceptable assay properties. In seven independent experiments analyzed, the coefficient of variation (CV) of the assay varied from 5% to 13% for low controls (Jurkat cell binding in presence of ICAM-1/Fc) and from 8% to 14% for high controls (Jurkat cell binding in the absence of ICAM-1/Fc). Signal to noise ratios > 7 were achieved in the assay (Table 1). Based on these properties the assay conditions described above were applied in the search for novel $\alpha\text{L}\beta 2$ inhibitors.

Table 1
Jurkat/ICAM-1/Fc V well assay: coefficients of variation (CV)

	Experiment						
	1	2	3	4	5	6	7
Low controls (100% binding)							
Mean (n = 3)	2776	4118	5006	2974	2599	3469	4115
SD	241	223	374	223	335	226	359
CV%	8.68	5.42	7.47	7.50	12.89	6.51	8.72
High controls (background binding)							
Mean (n = 3)	16 630	22 510	27 474	17 098	16 237	25 588	18 642
SD	1928	3256	3145	2661	1343	3143	2597
CV%	11.59	14.46	11.45	15.56	8.27	12.28	13.93

Mean fluorescent counts \pm SD of low controls (Jurkat cell binding in presence of ICAM-1 Fc) and high controls (Jurkat cell binding in absence of ICAM-1 Fc) run in triplicates of seven independent experiments are shown. % CV= SD /mean x 100.

3.1.2 Screening of compounds

In total, 60 compounds derived from the virtual screening approach were purchased from different suppliers and tested in the V well adhesion assay at 30 μM . This led to the identification of the hit compound 7185446, which inhibited Jurkat cell adhesion to ICAM-1/Fc completely at 30 μM (Fig. 3). The activity of compound 7185446 during initial screening was superior to the previously described $\alpha\text{L}\beta\text{2}$ inhibitor simvastatin (Fig. 3) (Weitz-Schmidt, et al. 2004). All other compounds tested were inactive at 30 μM .

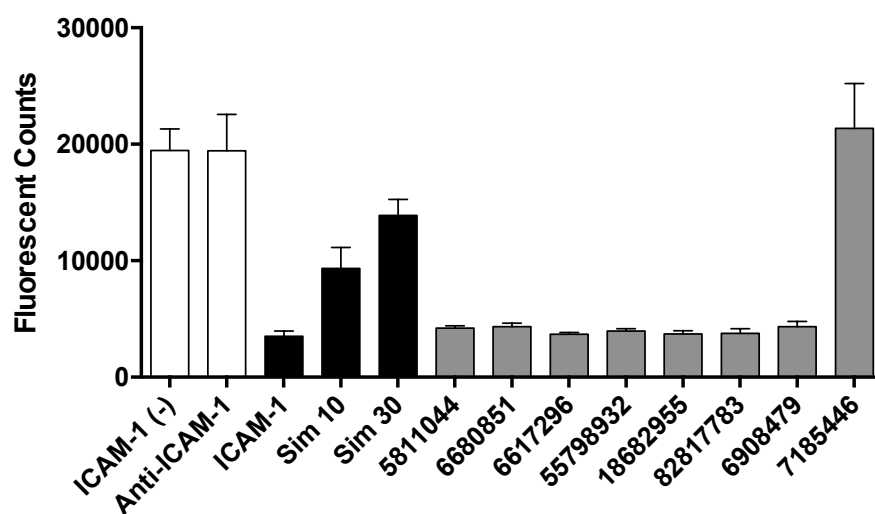


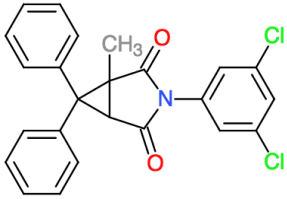
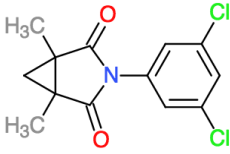
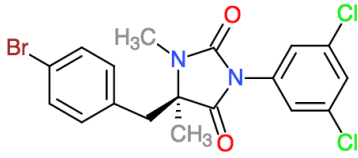
Fig. 3. Identification of $\alpha\text{L}\beta\text{2}$ inhibitor 7185446. Jurkat cell adhesion to ICAM-1/Fc was quantified in the presence of simvastatin at 10 μM and 30 μM (control) and CADD derived compounds at 30 μM using the V well technology as described under Materials and Methods. Compound 7185446 completely inhibited adhesion to ICAM-1 at 30 μM . ICAM-1 (-): Wells without ICAM-1/Fc (no adhesion); anti-ICAM-1: Wells treated with the anti-ICAM-1 mAb (10 $\mu\text{g}/\text{ml}$) (inhibited adhesion); ICAM-1: Wells with ICAM-1/Fc (100% adhesion); DMSO solvent control 1%. Sim: simvastatin; 5811044, 6680851, 6617296, 55798932, 18682955, 82817783, 6908479: compounds selected by CADD.

3.1.2. Chemical structure and physico-chemical properties of screening hit

The 'hit' identified belongs to the chemical class of succinimides (Table 2). The structure of 7185446 exhibits similarity with the fungicide procymidone (Campos, et al. 2016) and the hydantoin class of $\alpha\text{L}\beta\text{2}$ inhibitors (Table 2) (Giblin and Lemieux 2006).

Table 2

Chemical structures of 7185446, procymidone and BIRT-377

7185446	Procymidone	BIRT-377
		
Succinimide	Succinimide	Hydantoin
3-(3,5-dichlorophenyl)-1-methyl-6,6-diphenyl-3-azabicyclo[3.1.0]hexane-2,4-dione	3-(3,5-dichlorophenyl)-1,5-dimethyl-3-azabicyclo[3.1.0]hexane-2,4-dione	5(R)-(4-Bromobenzyl)-3-(3,5-dichlorophenyl)-1,5-dimethylimidazolidine-2,4-dione

A closer inspection of compound 7185446 revealed that it passes almost all criteria of Lipinski's "rule of five" (i.e. $c\text{Log}P$ does not exactly meet target value) which predicts oral absorption (Table 3) and the possibility to be derivatized towards patentable compounds.

Table 3

Physico-chemical properties*.

	7185446	"Rule of five" criteria
Molecular weight (Da)	422	< 500
$c\text{Log}P$	5.42	< 5
Rotatable bonds	3	-
H donor	0	< 5
H acceptor	2	<10
Form	White solid powder	-

* data retrieved from the Chembridge database.

3.1.3 Further characterization of 7185446 and preliminary SAR data

To obtain preliminary SAR data, commercially available close derivatives of compound 7185446 were purchased (Table 4). When tested under standard conditions in BSA-containing binding buffer, compound 7185446 inhibited Jurkat cell binding to ICAM-1/Fc with an IC_{50} value of $1.865 \pm 1.269 \mu\text{M}$ (Fig. 4). Under the same conditions, the reference $\alpha\text{L}\beta 2$ inhibitors simvastatin (natural statin) (Weitz-Schmidt, et al. 2001) was considerably less active than compound 7185446 (Table 4). Moreover, compound 7130393, a close derivative of compound 7185446, inhibited $\alpha\text{L}\beta 2$ with an IC_{50} value of $7.9 \mu\text{M}$ whereas all other close derivatives analyzed were found to be inactive at $10 \mu\text{M}$ (Fig. 4, Table 4). This limited structure-activity-relationship (SAR) suggests that the 3,5

dichloro residue of compound 7185446 is essential for activity. The 3,5 dichloro residue has also been shown to be crucial for α I allosteric α L β 2 inhibitors of the hydantoin class (Giblin and Lemieux 2006).

It needs to be noted at this point that both, 7185446 and 7130393, were more active when tested in the presence of 1.5% or 10% FCS instead of 1.5% BSA (Table 4). This result provides evidence that the compounds are sequestered by BSA (to different extends) decreasing their apparent concentration in the assay.

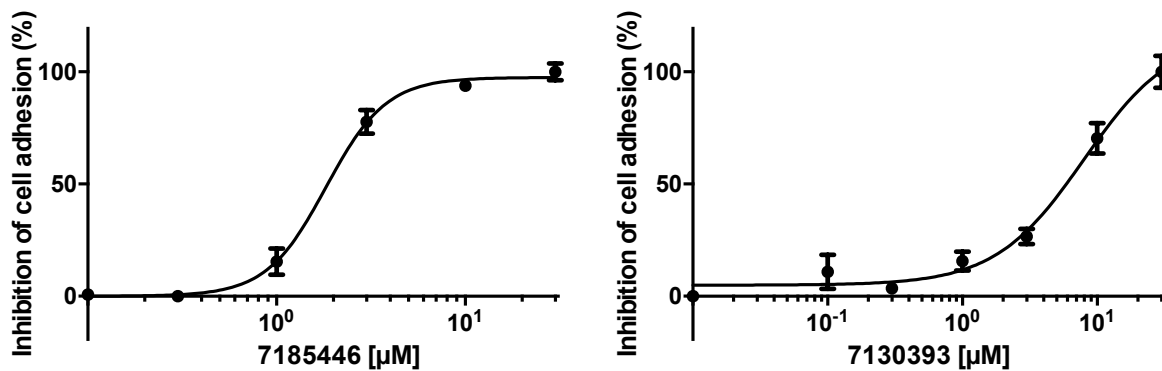
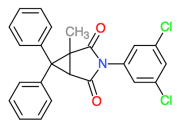
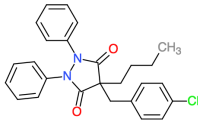
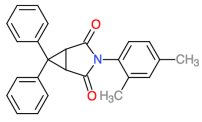
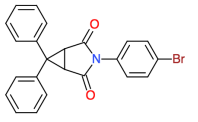
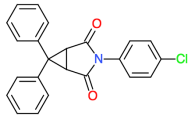
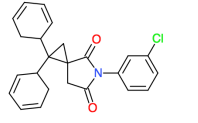
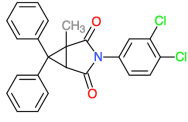
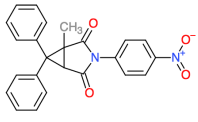
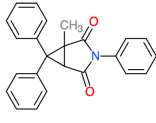
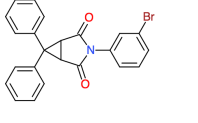
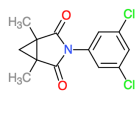
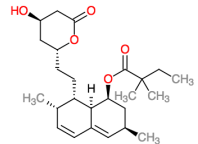


Fig. 4. 7185446 and 7130393 inhibit Jurkat cell binding to ICAM-1/Fc in a dose-dependent manner. Binding of Jurkat cells to recombinant ICAM-1/ Fc was quantified in the V well adhesion assay in the presence of increasing concentrations of 7185446 or 7130393 as described under Materials and Methods. Representative experiments are shown. Each point represents the mean value of triplicates \pm SD.

Table 4

Compound 7185446 and close derivatives: Structure-activity relationship.

Compound	IC ₅₀ [μM] 1.5% BSA	IC ₅₀ [μM] 1.5% FCS	IC ₅₀ [μM] 10% FCS	Compound	IC ₅₀ [μM] 1.5% BSA	IC ₅₀ [μM] 1.5% FCS	IC ₅₀ [μM] 10% FCS
7185446 	1.865 ± 1.269	0.325	0.244 0.304	6908479 	> 10		
6369678 	> 10			6370020 	>10		
6370940 	>10			7037690 	>10		
7130393 	7.948		0.835	7137311 	>10		
7145474 	>10			7208094 	>10		
Procymidone 	>10			Simvastatin 	7.726		

Chembridge database ID; IC₅₀ values of independent experiments run in triplicates shown; some compounds were tested in presence of FCS or BSA at different concentrations.

3.1.4. Selectivity of compounds 7185446 and 7130393

To assess the selectivity of 7185446 and 7130393 over other members of the integrin family, the effect of the compounds on VLA-4-mediated cell adhesion was assessed. VLA-4 is a non-I domain containing integrin which mediates lymphocyte adhesion to its ligand VCAM-1. For this purpose, the V well technology described above was adapted to the VLA-4/VCAM-1 integrin/ligand pair by measuring Jurkat cell binding to recombinant VCAM-1/Fc immobilized onto V well plates. Jurkat cells express both integrins, αLβ2 and VLA-4. The assay was validated with the potent VLA-4 inhibitor RO0505376 which blocked cell adhesion with an IC₅₀ of 9.5 nM (Fig. 5B). In contrast,

7185446 and 7130393 were inactive in the VLA-4 adhesion assay at 30 μ M demonstrating high selectivity of the compounds for α L β 2 over the integrin VLA-4 (Fig. 5A).

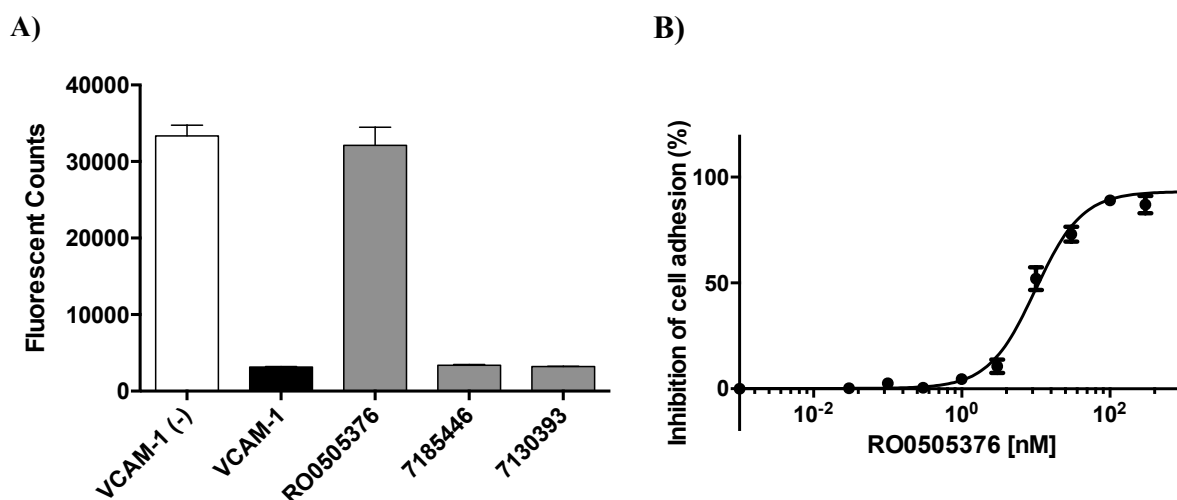


Fig. 5. 7185446 and 7130393 did not affect VLA-4-mediated adhesion. **(A)** The adhesion of fluorescently labelled Jurkat cells to recombinant VCAM-1/Fc immobilized onto V well plates was quantified in presence of solvent control, the VLA-4 inhibitor RO0505376 at 3 μ M and the α L β 2 inhibitors 7185446 and 7130393 at 30 μ M. The assay was performed as described under Material and Methods. Each bar represents the mean value \pm SD of triplicates. VCAM-1 (-): Wells without immobilized VCAM-1; VCAM-1: VCAM-1/Fc coated well containing 1% DMSO (solvent control); **(B)** IC₅₀ determination of VLA-4 inhibitor RO0505376.

3.1.5. Reversible inhibition of the α L β 2/ICAM-1 interaction by 7185446

To assess whether 7185446 is a reversible or irreversible inhibitor of the α L β 2/ICAM-1 interaction, Jurkat cells were treated with compound or solvent (DMSO), washed and then assayed for ICAM-1 binding in the V well adhesion assay. As shown in Fig. 6, binding was restored after washing. This demonstrates that 7185446 is a reversible inhibitor of α L β 2-mediated adhesion.

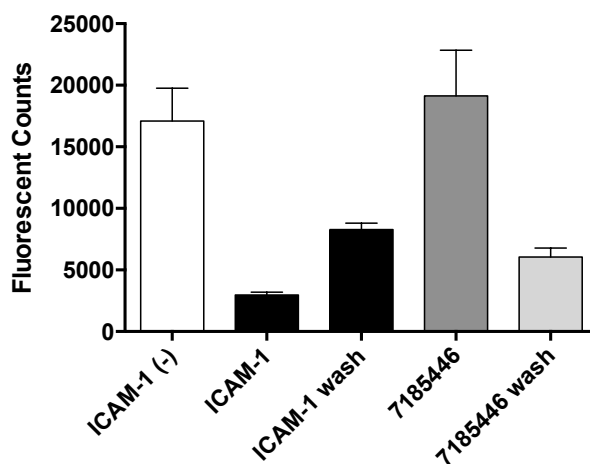


Fig. 6. 7185446 is a reversible inhibitor of the Jurkat/ICAM-1 interaction. Fluorescently labelled Jurkat cells were simultaneously activated with Mn^{2+} and treated with the $\alpha L\beta 2$ inhibitors 7185446 at 10 μM or solvent (DMSO 0.1%) for 30 min. After treatment one group was immediately tested for binding to ICAM-1/Fc immobilized onto V well plates in presence of the compounds or DMSO whereas the “wash” group were rinsed three times with binding buffer and then tested for adhesion as described under Materials and Methods. Data shown are the mean values of triplicates \pm SD. ICAM-1 (-): Control wells without ICAM-1/Fc.

3.1.6. Effect of 7185446 on cell viability

The effect of 7185446 on cell viability was assessed using the ToxiLight™ Bioassay Kit and the CellTiter-Glo® Luminescent Cell Viability Assay. Jurkat cells were incubated for 24 h with the compound at 0.1 μM , 1 μM and 10 μM . 7185446 did not induce toxicity and did not impair cell viability up to 10 μM (Fig. 7A and B). In the same experiments cyclosporine A at 10 μM significantly induced toxicity by 2.3 fold compared to solvent control (DMSO 0.1%) (Fig. 7A) and reduced cell viability by 78.7% at 10 μM after 24 h of exposure (Fig. 7B). Triton X and amiodarone were used as positive controls for cytotoxicity.

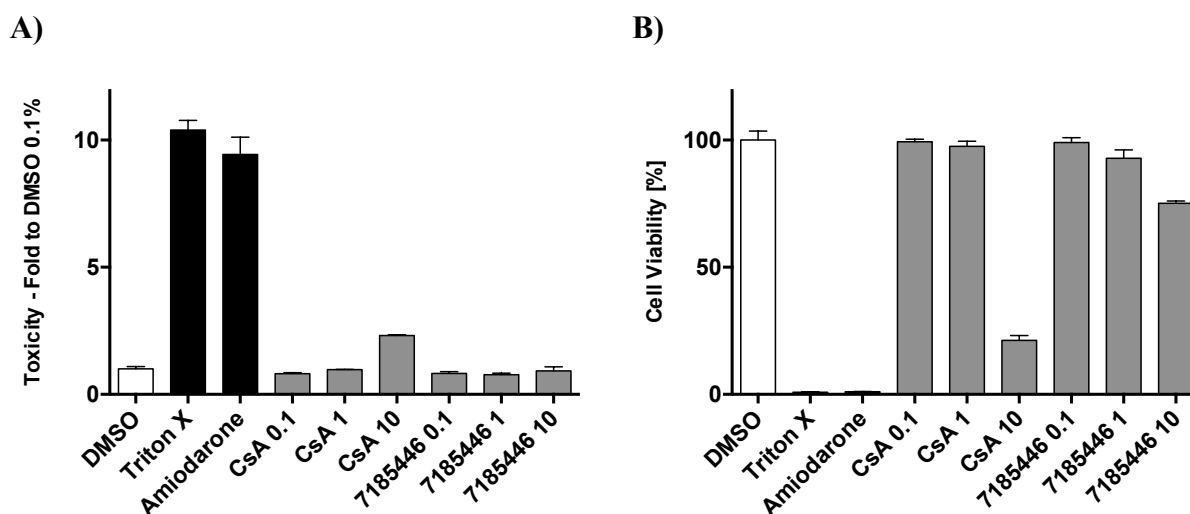


Fig. 7. Cytotoxicity was evaluated by measuring the release of adenylate kinase (A), and the intracellular content of ATP (B) in Jurkat after 24 h of incubation. In both assays, 7185446 is not cytotoxic at 0.1, 1 and 10 μM . DMSO 0.1% solvent control; Triton X 0.5%; amiodarone 50 μM ; CsA: cyclosporine A 0.1, 1, 10 μM . Each bar represents the mean value \pm SD of triplicates.

3.1.7. Compound 7185446 belongs to the class of α I allosteric inhibitors

7185446 was identified by ligand-based similarity searching from known αL I allosteric $\alpha L\beta 2$ modulators (Giblin and Lemieux 2006). αL I allosteric inhibitors are known to impair the reactivity

of the anti- α L β 2 mAb R7.1 (Weitz-Schmidt, et al. 2004) but not the reactivity of the anti- α L β 2 mAb TS2/4 (Weitz-Schmidt, et al. 2011).

mAb R7.1 recognizes a combinational epitope that requires both the α L I and the β propeller domain on the α L chain for full reactivity (Weitz-Schmidt, et al. 2011).

Therefore, we investigated the effect of 7185446 on R7.1 and TS2/4 binding to α L β 2. 7185446 reduced the reactivity of mAb R7.1 in a concentration-dependent manner whereas the binding of the mAb TS2/4 was not affected by the compound (Fig. 8A and B). This result further substantiates that 7185446 belongs to the class of α L I allosteric modulators which are known to stabilize integrins in their inactive state.

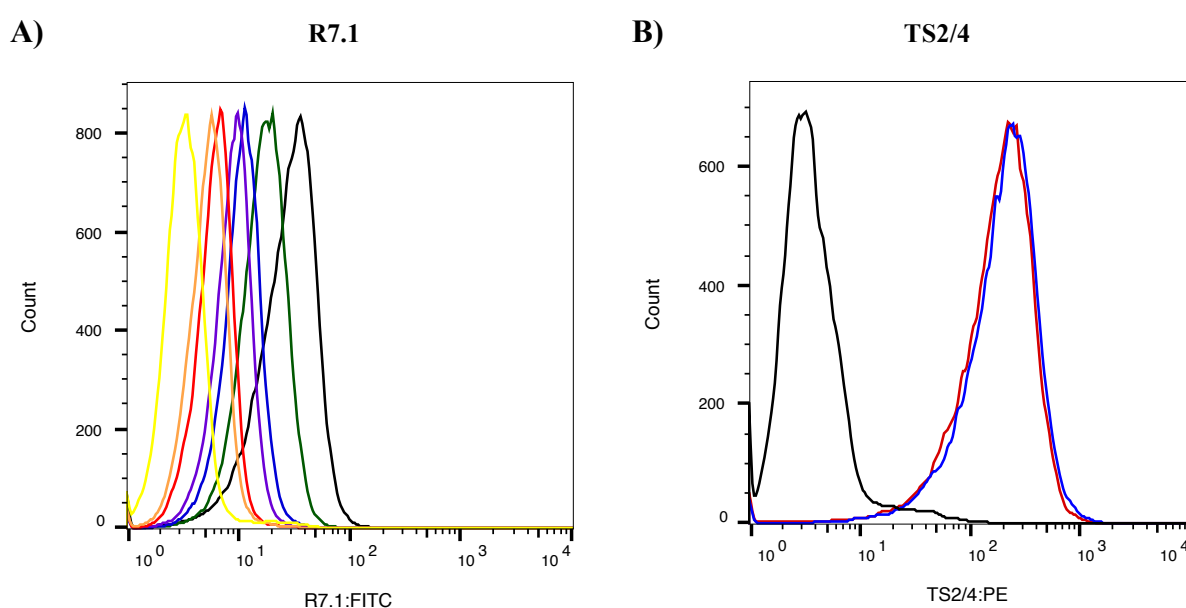


Fig. 8. Inhibition of mAb R7.1 binding to Jurkat cell α L β 2 by 7185446. **(A)** Jurkat cells were incubated with FITC-labelled mAb R7.1 in the presence of DMSO (1%) or increasing concentrations of 7185446. The experiment was performed in the presence of Mn^{2+} and Mg^{2+} . Bound antibody was quantified by flow cytometry. Yellow line: isotype control; orange line: 7185446 10 μ M, red line: 7185446 3 μ M; violet line: 7185446 1 μ M; green line: 7185446 0.3 μ M; black line: DMSO 1%.

(B) Jurkat cells were incubated with PE-labelled mAb TS/4 in the presence of 1% DMSO or 30 μ M 7185446. The experiment was performed in assay buffer containing Mn^{2+} and Mg^{2+} . Bound antibody was quantified by flow cytometry. A representative experiment out of two independent experiments is shown. Black line: isotype control; blue line: DMSO 1%; red line: 7185446 30 μ M.

In conclusion, the first hit which emerged from the CADD approach fulfilled the criteria of inhibition of α L β 2-dependent adhesion, lack of cytotoxicity, allosteric mode of action, molecular weight < 500 Da, and drugability. This prompted us to initiate a chemistry program with the goal to improve the activity and the physicochemical properties of the hit compound 7185446.

3.1.8. Hit optimisation and SAR

Compound 7185446 was modified based on the preliminary SAR data described in section 3.1.3. and CADD feedback. The chemical derivatisation program was conducted in order to optimize activity and physicochemical properties of the hit compounds while maintaining a molecular weight of ~ 500 Da. The synthesis of the derivatives is depicted in Fig. 9.

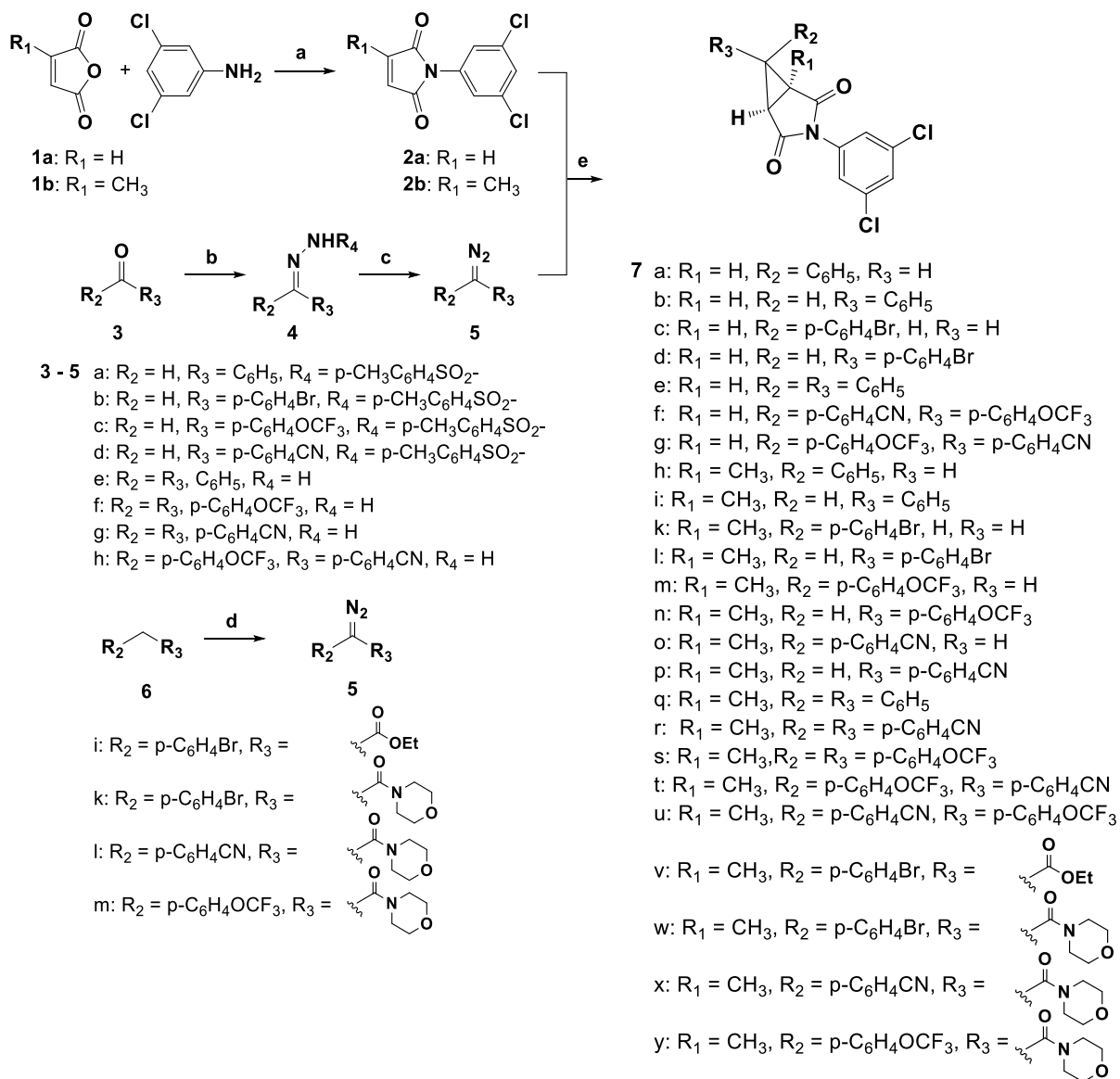
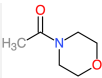
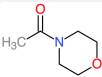
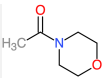


Fig. 9. Synthesis of $\alpha L\beta 2$ antagonists 7a-y. Reagents and conditions: a) acetic acid, reflux, 5 h, **1a**: 66%, **1b**: 67%; b) for **4a- 4d**: 4-toluenesulfonylhydrazide, MeOH, rt; for **4e- 4h**: hydrazine, EtOH, reflux; c) for **5a- 5d**: 15% NaOH, toluene; for compounds **5e – 5h**: MnO_2 , CH_2Cl_2 , 30 min. rt; d) 4-acetamidobenzenesulfonylazide, DBU, MeCN, rt; e) toluene, 80 °C; If $R_2 \neq R_3$, a mixture of two diastereomers was obtained. The diastereoisomers were separated by chromatography. If R_2 is phenyl or a substituted aromatic ring, the H-NMR signals for the H_2 and the H_6 -proton of the dichloroaniline group, are shifted from 7.5 ppm (**2a** or **2b**) to 6.2 – 6.5 ppm. Compounds **7h – 7y** are racemates.

Starting from the hit compound **7q** (=7185446) the influence of the substituents R_1 , R_2 and R_3 on the activity was tested (Table 5). The influence of the methyl function (R_1) at the succinimide ring revealed the following: if one proton at the succinimide ring is replaced by a methyl function, the activity is enhanced (i.e. 8-fold in case of compound **7t** ($R_1 = \text{CH}_3$, $\text{IC}_{50} [\mu\text{M}] = 0.016$) and **7g** ($R_1 = \text{H}$, $\text{IC}_{50} [\mu\text{M}] = 0.132$)) (Table 5). The SAR analysis for substituent R_2 revealed that there is a need for aryls in the endo position at the three membered ring. This is reflected by the observation that the activity of the compounds **7a**, **7c**, **7h**, **7k**, **7m** or **7o** is in the range of 0.147 to 3.3 μM whereas the respective diastereomers **7b**, **7d**, **7i**, **7l**, **7n** and **7p** where R_2 is H, are inactive (Table 5). It needs to be noted that the endo configuration is consistent with a chemical shift of the dichloroaniline protons H_2 and H_6 from 7.5 ppm to 6.2 - 6.5 ppm. Next, we investigated the impact of the substituent R_3 at the three membered ring on the activity of the compounds. Compounds with $R_3 = \text{H}$, aryl, CO_2Et or morpholine amide were measured. Table 5 and 6 show that no definite trends for $R_3 = \text{H}$, ester or amide were detected. However, it can be clearly observed, that if R_3 is an aryl substituent, the activity is improved (Table 5).

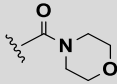
Further, according to the $\text{cLog}P$ values the chemical derivatization program resulted in less lipophilic compounds as compared to the hit compound **7q**. $\text{cLog}P$ values were reduced from 5.42 (hit compound **7q**) to 2.83 (compound **7x**) by introducing solubilizing groups such as carboxyethyl (compound **7v**), nitrile (compound **7r**) or morpholine amide (compound **7x**) (Table 5).

Table 5
Chemical structure, MW, cLogP and biological activity of novel α L β 2 inhibitors

Code	MW (Da)	cLogP	R ₁	R ₂	R ₃	IC ₅₀ [μ M]
7a	332.18	3.67	H	C ₆ H ₅	H	2.753, 1.587
7b	332.18	3.67	H	H	C ₆ H ₅	> 10
7c	411.08	4.42	H	p-C ₆ H ₄ Br	H	3.326
7d	411.08	4.42	H	H	p-C ₆ H ₄ Br	> 10
7e	408.28	5.19	H	C ₆ H ₅	C ₆ H ₅	9.119 \pm 3.722 (n=3)
7f	516.28	5.87	H	p-C ₆ H ₄ CN	p-C ₆ H ₄ OCF ₃	0.963
7g	516.28	5.87	H	p-C ₆ H ₄ OCF ₃	p-C ₆ H ₄ CN	0.132
7h	346.21	3.96	CH ₃	C ₆ H ₅	H	1.544 \pm 0.646 (n=3)
7i	346.21	3.96	CH ₃	H	C ₆ H ₅	> 10
7k	425.10	4.69	CH ₃	p-C ₆ H ₄ Br	H	0.472 \pm 0.180 (n=5)
7l	425.10	4.69	CH ₃	H	p-C ₆ H ₄ Br	> 10
7m	430.21	5.08	CH ₃	p-C ₆ H ₄ OCF ₃	H	0.495 \pm 0.213 (n=3)
7n	430.21	5.08	CH ₃	H	p-C ₆ H ₄ OCF ₃	> 10
7o	371.22	3.77	CH ₃	p-C ₆ H ₄ CN	H	0.471 \pm 0.407 (n=3)
7p	371.22	3.77	CH ₃	H	p-C ₆ H ₄ CN	> 10
7q	422.30	5.42	CH ₃	C ₆ H ₅	C ₆ H ₅	1.865 \pm 1.269 (n=21)
7r	472.33	4.88	CH ₃	p-C ₆ H ₄ CN	p-C ₆ H ₄ CN	0.045 \pm 0.014 (n=3)
7s	590.30	7.33	CH ₃	p-C ₆ H ₄ OCF ₃	p-C ₆ H ₄ OCF ₃	0.101
7t	531.31	6.10	CH ₃	p-C ₆ H ₄ OCF ₃	p-C ₆ H ₄ CN	0.016 \pm 0.012 (n=10)
7u	531.31	6.10	CH ₃	p-C ₆ H ₄ CN	p-C ₆ H ₄ OCF ₃	0.595, 0.530
7v	497.17	4.72	CH ₃	p-C ₆ H ₄ Br	CO ₂ Et	0.375 \pm 0.204 (n=3)
7w	538.22	3.80	CH ₃	p-C ₆ H ₄ Br		3.496
7x	484.33	2.83	CH ₃	p-C ₆ H ₄ CN		0.636
7y	543.32	4.08	CH ₃	p-C ₆ H ₄ OCF ₃		0.480

The activity of the compounds was determined in the α L β 2-dependent V well adhesion assay. IC₅₀ values \pm SD of > 3 independent experiments run in triplicates or IC₅₀ values of a single experiment run in triplicates are shown. cLogP values were calculated using the online tool ALOGPS (<http://www.vcclab.org/lab/alogps/>).

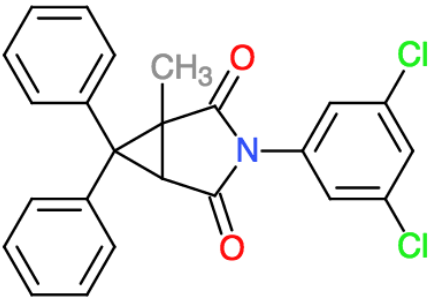
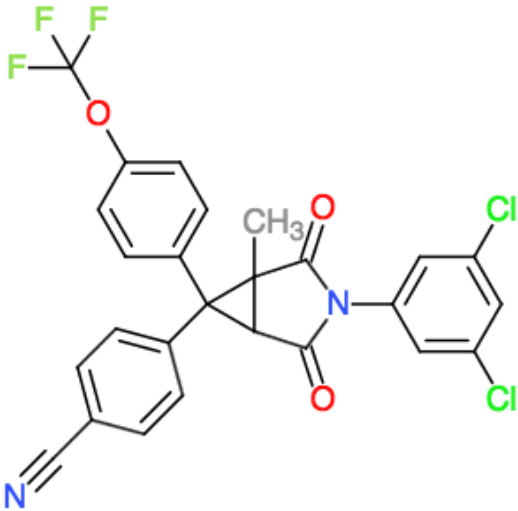
Table 6Influence of the substituent R₃ on the activity.

R ₂ \ R ₃	H	CO ₂ Et		p-C ₆ H ₄ CN	p-C ₆ H ₄ OCF ₃
p-C ₆ H ₄ Br	0.472	0.375	3.496	-	0.076*
p-C ₆ H ₄ CN	0.471	-	0.636	0.045	0.562
p-C ₆ H ₄ OCF ₃	0.495	-	0.480	0.016	0.101

R₁ = CH₃; IC₅₀ [μM]; *IC₅₀ value derived from the diastereomer mixture.

The racemate of the hit compound **7q** and the most active compound **7t** were separated by chromatography on a chiral column. We found that enantiomer I was 2 or 100 times more active than enantiomer II, respectively (Table 7). Moreover, enantiomer I of compound **7t** was > 300 fold more potent than enantiomer I of compound **7q** (Table 7).

Table 7From hit compound **7q** (=7185446) to lead compound **7t**

	
7q	7t
IC ₅₀ [μM]: 1.865 ± 1.269 (racemate) (= compound 7185446)	IC ₅₀ [μM]: 0.016 ± 0.013 (racemate) (=Compound 1)
IC ₅₀ [μM]: 1.544 ± 0.646 (n=3) (enantiomer I)	IC ₅₀ [μM]: 0.005, 0.004 (enantiomer I)
IC ₅₀ [μM]: 3.690, 5.360 (enantiomer II)	IC ₅₀ [μM]: 0.573 (enantiomer II)

Several derivatives shown in Table 4 represent promising novel αLβ2 inhibitors. Below the properties of compound **7t**, also termed “Compound 1”, are described in more detail. The activity, selectivity, cytotoxicity and first PK data of this compound are presented. Moreover, studies are described which address potential unwanted agonist-like downstream effects of Compound 1 such

as induction of activation epitopes, unwanted outside-in signalling, cytokine release or α L β 2 internalization.

3.2. α L β 2 inhibitor Compound 1

3.2.1. Characterization of α L β 2 inhibitor Compound 1

Compound 1 blocked α L β 2 mediated Jurkat cell adhesion to immobilized ICAM-1 with an IC₅₀ of 0.016 ± 0.012 μ M (Table 8).

In the selectivity Jurkat/VCAM-1 adhesion assay Compound 1 did not impair the adhesion indicating selectivity for α L β 2 over VLA-4 (Table 8).

Moreover, profiling in a mouse specific α L β 2 adhesion assay revealed that the α I allosteric inhibitor Compound 1 exhibited ~ 40 fold greater potency towards inhibition of human versus murine α L β 2 (Table 8). Such limited cross-species reactivity have been also observed for LFA878, another α I allosteric α L β 2 inhibitors (Mancuso, et al.2016).

Compound 1 was not cytotoxic to Jurkat cells or the liver cell line HepG2 after 24 h of incubation as determined by the release of the enzyme AK from damaged cells (Table 8). Moreover, Compound 1 did not induce apoptosis and/or necrosis in Jurkat cells after 24 h of exposure, in contrast to the control compounds staurosporine and amiodarone (Table 8) (Felser, et al. 2013).

Table 8
Activity profile of α L β 2 Compound 1.

Assay	Compound 1 IC ₅₀ [μ M]
Activity (αLβ2) Jurkat/ICAM-1	0.016 ± 0.012
Selectivity (VLA-4) Jurkat/VCAM-1	> 10
Cross-reactivity (mouse αLβ2) OT-1/mICAM	0.629 ± 0.100
Cytotoxicity (AK release) Jurkat cells	> 10
Cytotoxicity (AK release) HepG2 cells	> 10
Cytotoxicity (Annexin V / PI) Jurkat	> 10 (n=3)

Data were generated as described under Material and Methods. Mean values \pm SD of ≥ 3 independent experiments run in triplicates or single values run in triplicates are shown.

3.2.2. Quantification of mAb R7.1 to α L β 2 in whole blood of different species

Next, we were interested to determine the binding of Compound 1 to α L β 2 in the presence of all blood components. For this investigation, we utilized a recently validated whole blood technology which determines mAb R7.1 mAb to α L β 2 (Welzenbach, et al. 2015). We applied this technology not only to human but also to whole blood of rabbits. We found that Compound 1 reduced the binding of mAb R7.1 to α L β 2 in a concentration-dependent manner on lymphocytes, monocytes and granulocytes. Compound 1 showed potent activity with IC₅₀s in the range of low micromolar (Table 9). Surprisingly, first data indicate that Compound 1 was more active in blood samples from rabbit than from human (Table 9). These findings together suggest that Compound 1 efficiently binds to α L β 2 in the presence of all blood components. Further, they show that Compound 1 fully cross-reacts with rabbit α L β 2. Compound 1 shares this property with other α I allosteric inhibitors (Weitz-Schmidt, et al. 2004).

The effect of Compound 1 on the binding of mAb R7.1 in whole blood from mice and pigs could not be assessed because R7.1 did not cross-react with mouse α L β 2 (shown previously) or with pig α L β 2 (shown here for the first time), respectively.

Table 9
Binding of mAb R7.1 in whole blood from different species.

	Allosteric mode of action - REMA IC ₅₀ [μ M]			
	<i>Hs</i>	<i>Oc</i>	<i>Ss</i>	<i>Mm</i>
Lymphocytes	0.247 \pm 0.141	-	-	-
Monocytes	0.158 \pm 0.069	0.049	-	-
Granulocytes	0.247 \pm 0.141	0.055	-	-

IC₅₀ \pm SD of three independent experiment (*Homo sapiens*, *Hs*) or single IC₅₀ determination (*Oryctolagus cuniculus*, *Oc*) are shown. *Sus scrofa* (*Ss*), *Mus musculus* (*Mm*).

3.2.3. Compound 1: impact on α L β 2 conformations

The allosteric mode of action of Compound 1 was confirmed by quantifying the binding of the anti- α L β 2 mAb R7.1 to Jurkat cells. Under resting conditions, Compound 1 and simvastatin (the statin was included in the experiment as a positive control) induced R7.1 epitope loss on the α chain as expected for α I allosteric inhibitors (Fig. 10A). The IC₅₀ value measured for Compound 1 in the R7.1 epitope loss assay was IC₅₀ 2 \pm 2 nM (Fig. 10B), and thus in the range of the IC₅₀ determined in the α L β 2 V well adhesion assay (Table 8).

The conformational state of α L β 2 upon Compound 1 binding was further studied using two other well-characterized, conformation-sensitive mAbs mapping to distinct sites of α L β 2. MEM148 recognizes an epitope on the hybrid domain of the β 2 chain that becomes exposed when the integrin

adopts an extended, active conformation (Tang, et al. 2005). The epitope of the second mAb m24 is uncovered when the $\beta 2$ I-like domain is activated, i.e. mAb m24 epitope exposure is characteristic for the activated conformation of this domain (Chen, et al. 2010a). We found that both epitopes were not induced in presence of Compound 1 (Fig. 10C and E) demonstrating that Compound 1 does not mediate $\alpha L\beta 2$ extension and $\beta 2$ -I-like domain activation, in contrast to what has been observed for α/β I allosteric $\alpha L\beta 2$ inhibitors (Mancuso, et al. 2016) (Shimaoka, et al. 2003). Interestingly, under Mn^{2+} activating conditions (Mn^{2+} is known to increase integrin affinity by replacing Ca^{2+} at the ADMIDAS site of the $\beta 2$ I-like domain (Chen, et al. 2010b)), a differential effect of Compound 1 on MEM148 and m24 epitope exposure was noted. Compound 1 suppressed Mn^{2+} -induced MEM148 epitope expression (Fig. 10D) but allowed Mn^{2+} -mediated mAb 24 epitope exposure (Fig. 10F). This finding indicates that the α I allosteric inhibitor Compound 1 stabilizes the bent conformation of $\alpha L\beta 2$ not only under resting but also under activating conditions (Shimaoka, et al. 2003) (Sen, et al. 2013b). However, the result also shows that Compound 1 allows Mn^{2+} -induced $\beta 2$ I-like domain activation (as monitored by m24 epitope expression) in the absence of extension (Fig. 10F). Remarkably, a similar ‘cocked’ conformation with $\beta 2$ I-like domain activation, despite the presence of a bent conformation has been also noted in a crystal structure of the closely related integrin $\alpha X/\beta 2$ (Sen, et al. 2013a). Moreover, the $\alpha L\beta 2$ conformational states observed in this study for Compound 1 resembles those observed upon binding of the α I allosteric $\alpha L\beta 2$ inhibitor LFA878 (statin derivative) (Mancuso, et al. 2016), indicating that the distinct conformations observed in this study are characteristic for the α I allosteric mode of action.

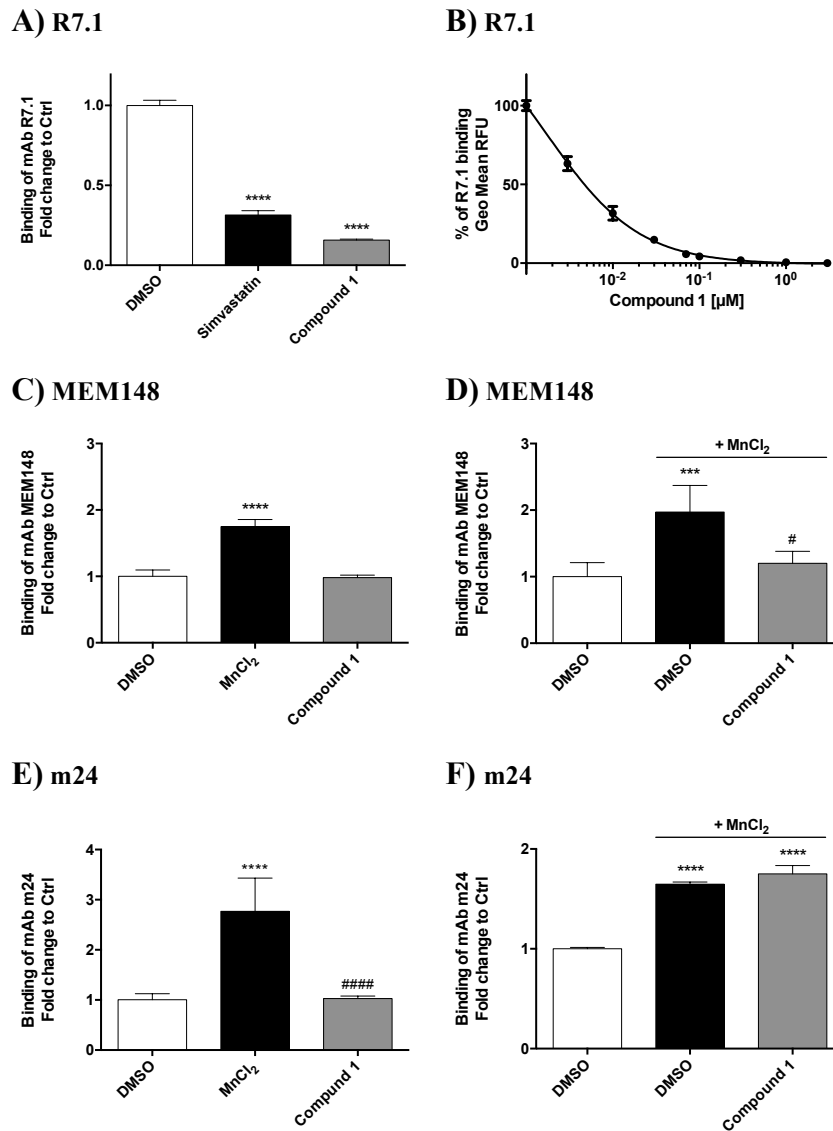


Fig. 10. Effect of Compound 1 on the conformational status of α L β 2 under resting and Mn²⁺ activating conditions. **(A)** Cells were exposed to DMSO (0.1%), Simvastatin (100 μ M) and Compound 1 (10 μ M), for 40 min. At 40 min the binding of mAb R7.1 (reports α I allosteric inhibitor binding to α L/ β 2) was quantified by flow cytometry. Each bar represents the mean value \pm SD of triplicates. **(B)** R7.1 epitope loss was quantified by flow cytometry in the presence of indicated concentrations of Compound 1. Each point represents the mean value \pm SD of three independent experiments.

(C) The binding of mAb MEM148 (reports α L/ β 2 extension) or **(E)** mAb m24 (reports β 2 I-like domain activation) was quantified by flow cytometry. Each bar represents the mean values \pm SD of \geq three independent experiments. **(D)** Jurkat cells were exposed to Compound 1 in the presence of Mn²⁺ and control in the presence and absence of Mn²⁺ for 24 h at above indicated concentrations. The binding of mAb MEM148 and **(F)** mAb m24 was determined by flow cytometry. Each bar represents the mean value \pm SD of four independent experiments (D) or of triplicates (F).

Fold change to control was calculated as the ratio of the geometric MFI (gMFI) value of the test sample and gMFI value of the respective control. The ratio of controls was set to 1. Statistical significance was determined using one-way analysis (ANOVA) (***p* < 0.001 and *****p* < 0.0001 vs DMSO control; # *p* < 0.05 vs second comparison).

3.2.4. Compound 1 does not induce protein tyrosine phosphorylation

After proving that Compound 1 does not induce α L β 2 activation epitopes, we investigated the effect of the compound on α L β 2 mediated outside-in signalling. We reasoned that the lack of agonistic effects such as activation epitope induction will also translate into an absence of (unwanted) outside-in signalling.

In order to prove this hypothesis, we assessed zeta-chain-associated protein kinase of 70 kDa (ZAP70) tyrosine phosphorylation in PBMCs treated with Compound 1. ZAP70 is an established early mediator of α L β 2 outside-in signalling and constitutively associated with α L β 2 (Evans, et al. 2011). PBMCs were used for this study instead of Jurkat cells to avoid the limitations inherent to T-leukemic cells lines when studying signalling events. We found that Compound 1 did not trigger detectable ZAP70 Y292 phosphorylation in CD2⁺ T cells, in contrast to the integrin activating cation Mn²⁺ or cross-linked anti-CD3 mAb OKT3 (OKT3-x) (Fig. 11A). mAb OKT3 binds to CD3 of the TCR/CD3 complex and is used to induce signalling pathway normally triggered upon binding of the natural ligand peptide antigen-major histocompatibility complex (pMHC) to the TCR (Houtman, et al. 2005). These signalling pathways lead to phosphorylation of various proteins on tyrosine residues including ZAP70 (Houtman, et al. 2005). Moreover, in agreement with the above data, Compound 1 did not lead to detectable general protein tyrosine phosphorylation in CD2⁺ T cells, in contrast to Mn²⁺ and OKT3-x (Fig. 11B, Table 10).

Taken together, under experimental conditions tested, Compound 1 did not induce α L β 2 mediated outside-in signalling as assessed via protein tyrosine phosphorylation.

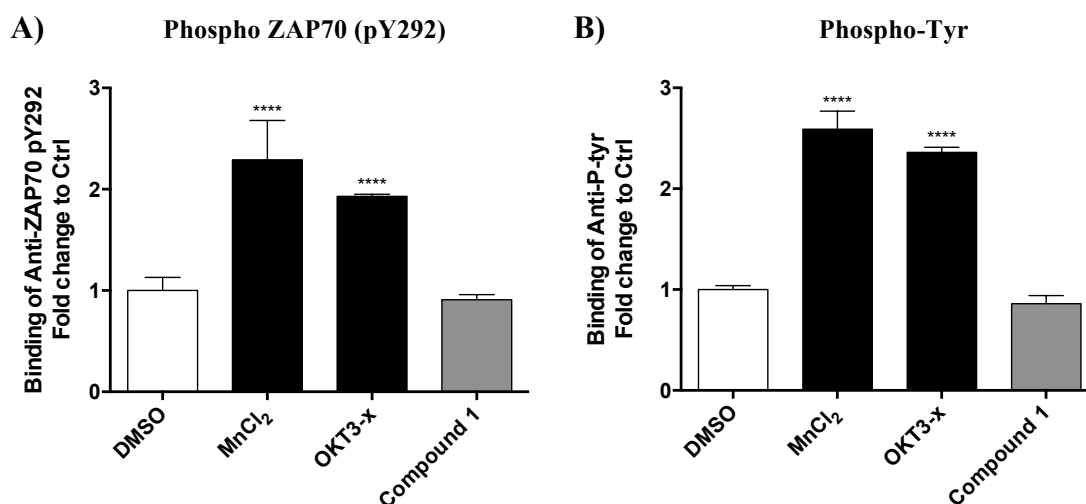


Fig. 11. Effect of Compound 1 on the phosphorylation state of ZAP70 or protein tyrosine phosphorylation in general. PBMCs were treated with Compound 1 (10 μ M), controls DMSO (0.1%), MnCl₂ (2mM)/DMSO (0.1%) (Mn²⁺ activates α L β 2) or cross-linked anti-CD3 mAb OKT3 (OKT3-x; 5 μ g/ml) (activates the TCR signalling pathway) were pre-incubated on ice and then activated for 1 min at 37 $^{\circ}$ C. The binding of (A) anti-ZAP70 pY292 (J34-602) mAb and (B) anti-pTyr (PY20) mAb was quantified in CD2+ lymphocytes by flow cytometry. Each bar represents the mean value \pm SD of three independent experiments (different donors, single determinations each). Statistical significance was determined using one-way analysis (ANOVA) (**** $p < 0.0001$ vs DMSO).

3.2.5. Cytokine release

Subjects treated with the anti- α L β 2 mAb efalizumab showed an increase of IL-6 plasma level by 90-fold after two hours of administration (Prater, et al. 2014). This increase was still detectable after two days. This prompted us to assess whether a small molecule α L β 2 inhibitor, such as Compound 1 could also induce unwanted cytokine release. THP-1 cells were treated with Compound 1, efalizumab or respective controls for 24 h. PMA/Ionomycin and LPS were used as positive control stimuli (Jones, et al. 2003). After 24 hours of incubation Compound 1 did not induce IL-6 release in THP-1 (Fig. 12, Table 10). In contrast, there was a clear trend towards IL-6 induction in presence of efalizumab alone and cross-linked, confirming the observation made in patients treated with efalizumab.

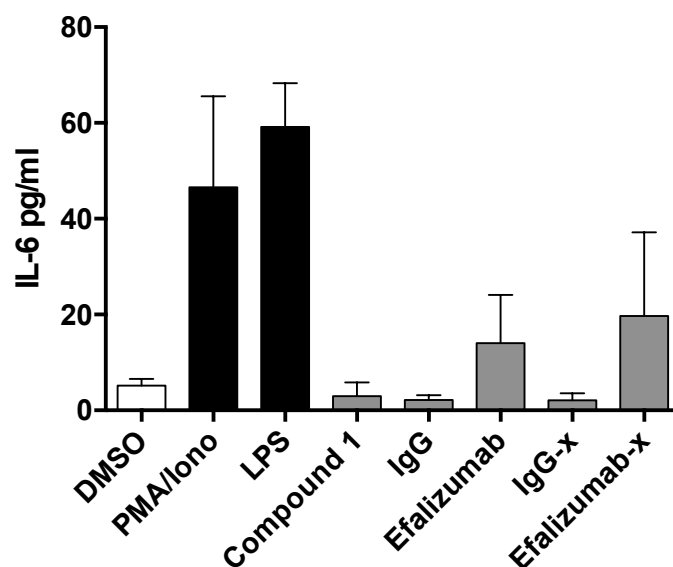


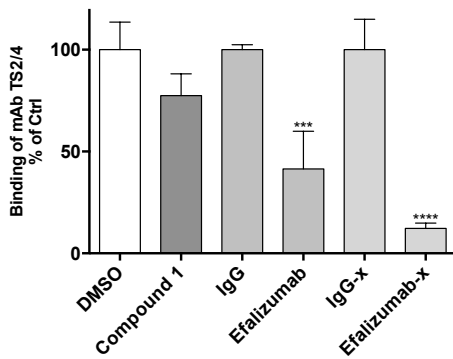
Fig. 12. Compound 1 did not induce IL-6 release. THP-1 cells were untreated or were treated with Compound 1, (10 μ M) and the control DMSO (0.1%), efalizumab (10 μ g/ml) or efalizumab-x (10 μ g/ml) and the respective controls IgG (10 μ g/ml) and IgG-x (10 μ g/ml). PMA (10 ng/ml), Ionomycin (Iono) (1 μ M) and LPS (1 μ g/ml) served as assay controls. Mean values \pm SD of nine independent experiments are shown.

3.2.6. Compound 1 does not affect α L β 2 expression

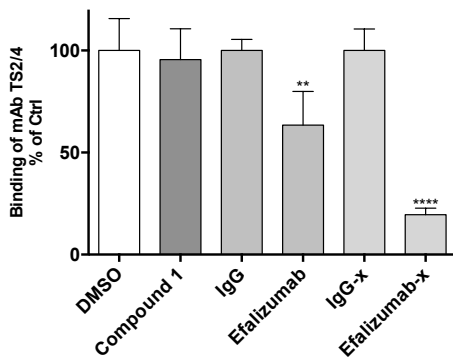
Previous data show that α L β 2 engagement by efalizumab induces a rapid downmodulation of α L β 2 in psoriasis patients by more than 70% in T cells (Vugmeyster, et al. 2004) (Mortensen, et al. 2005) (Guttman-Yassky, et al. 2008). Thus, we investigated the effect of Compound 1 on α L β 2 surface expression using resting PBMCs. The cells were treated for 24 h with inhibitors and α L β 2 expression was determined on CD4⁺ and CD8⁺ T cells. In agreement with previous observations in psoriasis patients, efalizumab led to a downmodulation of α L β 2 in CD4⁺ and CD8⁺ T cells which became more evident when the antibody was cross-linked (Fig. 13A and B). In contrast, even high concentrations of Compound 1 (> 500 \times IC₅₀ value) did not significantly affect α L β 2 surface expression (Table 10).

Moreover, consistent with previously published data (Coffey, et al. 2004) cross-linked efalizumab induced α L β 2 clustering, internalization and co-localisation within the lysosomal compartment (Fig. 13 C, F and G). In contrast, α L β 2 cell surface expression and lysosomal localization in presence of Compound 1 was indistinguishable from the respective solvent control (Fig. 13C, D and E). Taken together these data point towards fundamental differences between Compound 1 and efalizumab regarding the effect on α L β 2 internalization, and lysosomal degradation.

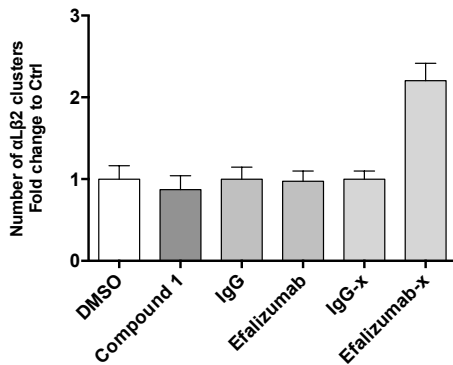
A) CD4+



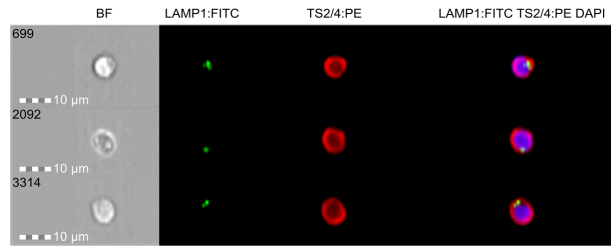
B) CD8+



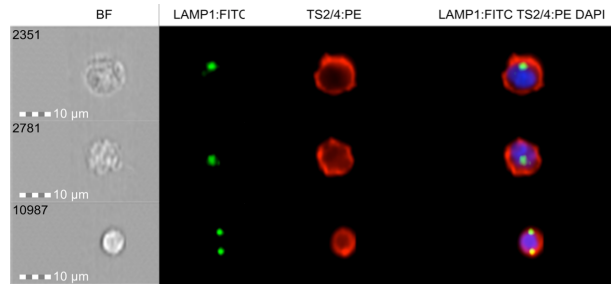
C) PBMCs



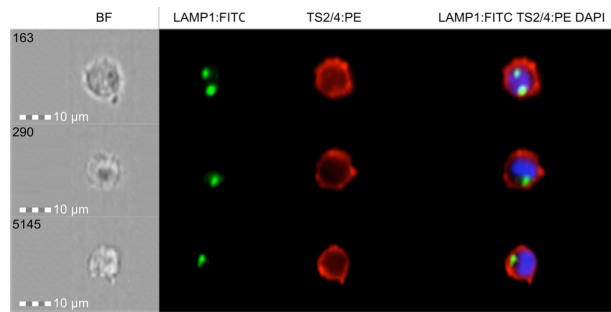
D) DMSO



E) Compound 1



F) IgG-x



G) Efalizumab-x

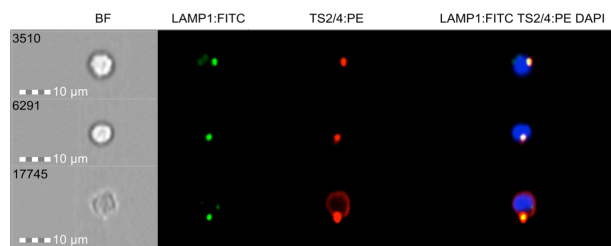


Fig. 13. Effect of Compound 1 and efalizumab on the localisation of α L β 2. PBMCs were treated with Compound 1 (10 μ M), efalizumab (10 μ g/ml) or efalizumab-x (10 μ g/ml) and the respective controls DMSO (0.1%), IgG (10 μ g/ml) and IgG-x (10 μ g/ml) for 24 h. After 24 h α L β 2 surface expression on (A) CD4⁺ and (B) CD8⁺ T cells was determined by the binding of fluorescently labelled mAb TS2/4 using flow cytometry. Each bar represents the mean value \pm SD of three independent experiments. Statistical significance was determined using one-way analysis (ANOVA) (* $p < 0.05$, ** $p < 0.01$, *** $p < 0.001$ and **** $p < 0.0001$ vs respective controls). (C) α L β 2 clusters (granular stainings) were quantified in inhibitor-treated PBMCs by flow-based imaging and image analysis. Clusters were defined by pixel area size (4-16) plus shape (circularity 0.4-1) and were counted as single events. Each bar represents the mean value \pm SEM of 1,000 images analyzed. A representative experiment out of two independent experiments is shown. (D) Localisation of α L β 2 in presence of DMSO, (E) Compound 1, (F) IgG-x or (G) efalizumab-x was visualized using flow-based imaging. α L β 2 was labelled with mAb TS2/4-PE (red), lysosomes with anti-LAMP-1 mAb H4A3-FITC (green) and the

nucleus with DAPI (blue). Co-location of α L β 2 and LAMP-1 staining is indicated in yellow. Individual cells are displayed by multispectral imaging of brightfield (BF). Representative images are shown.

In conclusion, Compound 1 is a potent α I allosteric α L/ β 2 inhibitor which apparently lacks unwanted agonist-like effects observed with other α L/ β 2 pharmacologies. The profile of Compound 1 is summarized in Table 10.

Table 10

Overview of *in vitro* effect profiles of Compound 1.

αLβ2 inhibitor	Compound 1
Mode of action	α I allosteric
Selectivity of mode of action	α L β 2
Inhibition of α L β 2 adhesion	+
Induction of α L β 2 activation epitopes	-
ZAP70 phosphorylation	-
Tyrosine phosphorylation	-
α L β 2 internalization	-
Cytokines release induction	-

+: effect, -: no effect

3.2.7. Oral application study

On the basis of its exceptional *in vitro* profile, Compound 1 was evaluated *in vivo*. Adult male Sprague-Dawley rats were fed by oral gavage with the test compound at the dose levels of 30 mg/kg/day. A summary of the PK parameters obtained following po dose of Compound 1 to rats is shown in Table 11. The plot of the mean Compound 1 plasma concentrations over time is shown in Fig. 14.

In summary, this initial single oral dose PK study in rats showed that Compound 1 at a dose level of 30 mg/kg was orally available, achieving exposure levels well in excess of the expected human effective dose (estimated based on human IC₅₀ *in vitro*). The high volume of distribution suggested an at least 2-compartmental distribution. Drug clearance was close to hepatic drug flow. HPLC analyses of the PK samples identified a single peak without major peaks indicative of major metabolites. Treatment was well-tolerated without gross abnormalities in animal behaviour.

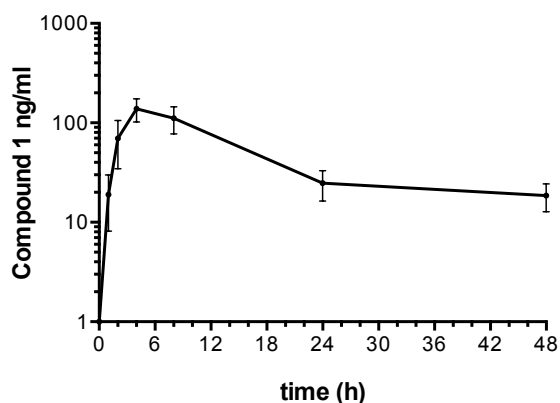


Fig. 14. Pharmacokinetic profiles after a single oral (po) dose of Compound 1. Each point represents the mean Compound 1 plasma concentrations of three different animals \pm SD.

Table 11

Pharmacokinetic parameters for Compound 1.

Species	Rat
Cmpd	Compound 1
Route	PO
Dose	30 mg/kg
Rs_q	1
t_{1/2}	58 h
t_{max}	4 h
C_{max}	138 ng/ml
C_{max}/D	4.61 (ng/ml)(mg/kg)
AUC_{INF}	3930 h*ng/ml
AUC_{INF}/D	131 (h*ng/ml)(mg/kg)
V_{ZF}	639 L/kg
CL_F	7.64 L/h/kg

4. Discussion

Computer aided drug design (CADD) is an important tool in drug discovery and development that can reduce time and expense requested for the development of new drugs.

In the current study, we conducted a virtual screening approach to identify a novel class of small molecule α L β 2 inhibitors of an α I allosteric mode of action, taking advantage of the published structural information for this leukocyte integrin. The α I allosteric mode of action was pursued because it promises to introduce strict α L β 2 target selectivity and to avoid paradoxical agonism, i.e. to potentially resolve unwanted phenomena alternative α L β 2 targeting modes of action were found to be associated with.

The hit molecule identified by virtual screening exhibited micromolar activity, displayed selectivity over the integrin VLA-4, exhibited reversible binding and was free from cytotoxicity in the assays applied. The subsequent derivatisation program had three major objectives: (1) to improve the activity and (2) to enhance the hydrophilicity of the chemical scaffold while (3) maintaining a low molecular weight in the order of 500 Da. Several compounds fulfilling these objectives were synthesized. The most active compound identified so far (enantiomer of Compound 1) exhibits an IC₅₀ value in the single-digit nanomolar range in a cell-based adhesion assay, representing one of the most active α L β 2 inhibitors described to date. Importantly, first data indicate that Compound 1 is able to efficiently bind to α L β 2 in the whole blood compartment, supporting the expectation of biologic effect in a clinically relevant compartment. Further, the compound was shown to be orally available. When delivered to rats at 30 mg/kg it resulted in plasma levels over the human IC₅₀ value

(*in vitro* data) for up to 24 h. This property favourably differentiates Compound 1 from some other α I allosteric inhibitors and α/β I allosteric inhibitors which exhibit poor oral bioavailability (Zhong, et al. 2012).

However, we also noted limited cross-species reactivity when we profiled our compounds in the mouse specific α L β 2-dependent OT-1 adhesion assay. This limited cross-species reactivity has been also observed with other α I allosteric inhibitors and may be explained by the difference in the amino acids sequence of the I domain (Mancuso, et al. 2016). This limited cross-species reactivity needs to be taken into account when selecting experimental animal diseases for assessing potential therapeutic effects of the compounds.

In line with our previous study (Mancuso, et al. 2016) we could also demonstrate that the novel class of α I allosteric inhibitors described here does not exhibit unwanted agonist-like effects typically observed for α L β 2 targeting antibodies or α/β I allosteric α L β 2 inhibitors. Our study further underlines that α I allosteric α L β 2 inhibitors can be favourably differentiated from these inhibitor classes in terms of their downstream effects.

Taken together these results show that we discovered a new class of α L β 2 inhibitors with an encouraging *in vitro* profile and with promising properties to be investigated *in vivo* towards potential drug candidate selection and further development.

5. References

- Aggarwal, Varinder K., et al.
2003 A New Protocol for the In Situ Generation of Aromatic, Heteroaromatic, and Unsaturated Diazo Compounds and Its Application in Catalytic and Asymmetric Epoxidation of Carbonyl Compounds. Extensive Studies To Map Out Scope and Limitations, and Rationalization of Diastereo- and Enantioselectivities. *Journal of the American Chemical Society* 125(36):10926-10940.
- Bourget, Cécile, et al.
2005 Biotin-phenyldiazomethane conjugates as labeling reagents at phosphate in mono and polynucleotides. *Bioorganic & medicinal chemistry* 13(5):1453-1461.
- Campos, M., et al.
2016 Novel insights into the metabolic pathway of iprodione by soil bacteria. *Environ Sci Pollut Res Int*.
- Chen, W., J. Lou, and C. Zhu
2010a Forcing switch from short- to intermediate- and long-lived states of the alphaA domain generates LFA-1/ICAM-1 catch bonds. *J Biol Chem* 285(46):35967-78.
- Chen, X., et al.
2010b Requirement of open headpiece conformation for activation of leukocyte integrin alphaXbeta2. *Proc Natl Acad Sci U S A* 107(33):14727-32.
- Coffey, G. P., et al.
2004 In vitro internalization, intracellular transport, and clearance of an anti-CD11a antibody (Raptiva) by human T-cells. *J Pharmacol Exp Ther* 310(3):896-904.
- Cook, Lawrence S., and Basil J. Wakefield
1980 Enamidines. Part 1. Synthesis of enamidines and dihydrtriazines by the reaction of organolithium and organomagnesium compounds with aromatic nitrites. *Journal of the Chemical Society, Perkin Transactions 1* (0):2392-2397.
- Cox, D., M. Brennan, and N. Moran
2010a Integrins as therapeutic targets: lessons and opportunities. *Nat Rev Drug Discov* 9(10):804-20.
- Cox, Dermot, Marian Brennan, and Niamh Moran
2010b Integrins as therapeutic targets: lessons and opportunities. *Nat Rev Drug Discov* 9(10):804-820.
- Evans, R., et al.
2011 The integrin LFA-1 signals through ZAP-70 to regulate expression of high-affinity LFA-1 on T lymphocytes. *Blood* 117(12):3331-42.
- Felser, A., et al.
2013 Mechanisms of hepatocellular toxicity associated with dronedarone--a comparison to amiodarone. *Toxicol Sci* 131(2):480-90.
- Giblin, P. A., and R. M. Lemieux
2006 LFA-1 as a key regulator of immune function: approaches toward the development of LFA-1-based therapeutics. *Curr Pharm Des* 12(22):2771-95.
- Goodman, S. L., and M. Picard
2012 Integrins as therapeutic targets. *Trends Pharmacol Sci* 33(7):405-12.
- Guttman-Yassky, E., et al.
2008 Blockade of CD11a by efalizumab in psoriasis patients induces a unique state of T-cell hyporesponsiveness. *J Invest Dermatol* 128(5):1182-91.
- Hogg, Nancy, Irene Patzak, and Frances Willenbrock
2011 The insider's guide to leukocyte integrin signalling and function. *Nat Rev Immunol* 11(6):416-426.
- Houtman, J. C., et al.

- 2005 Early phosphorylation kinetics of proteins involved in proximal TCR-mediated signaling pathways. *J Immunol* 175(4):2449-58.
- Hyun, Young-Min, Craig T. Lefort, and Minsoo Kim
2009 Leukocyte integrins and their ligand interactions. *Immunologic research*:10.1007/s12026-009-8101-1.
- Jones, M. L., et al.
2010 RGD-ligand mimetic antagonists of integrin α IIb β 3 paradoxically enhance GPVI-induced human platelet activation. *J Thromb Haemost* 8(3):567-76.
- Jones, Michael A., et al.
2003 Induction of Proinflammatory Responses in the Human Monocytic Cell Line THP-1 by *Campylobacter jejuni*. *Infection and Immunity* 71(5):2626-2633.
- Mancuso, R. V., et al.
2016 Downstream effect profiles discern different mechanisms of integrin α L β 2 inhibition. *Biochem Pharmacol*.
- Millard, M., S. Odde, and N. Neamati
2011 Integrin targeted therapeutics. *Theranostics* 1:154-88.
- Miller, Meredith W., et al.
2009 Small-molecule inhibitors of integrin α 2 β 1 that prevent pathological thrombus formation via an allosteric mechanism. *Proceedings of the National Academy of Sciences* 106(3):719-724.
- Molchanov, Alexander P, et al.
2002 Double Addition of Diphenylcyclopropenone to Azomethine Imines Generated from 6-Aryl-1,5-diazabicyclo[3.1.0]hexanes. *European Journal of Organic Chemistry* 2002(3):453-456.
- Mortensen, D. L., et al.
2005 Pharmacokinetics and pharmacodynamics of multiple weekly subcutaneous efalizumab doses in patients with plaque psoriasis. *J Clin Pharmacol* 45(3):286-98.
- Prater, E. F., et al.
2014 A retrospective analysis of 72 patients on prior efalizumab subsequent to the time of voluntary market withdrawal in 2009. *J Drugs Dermatol* 13(6):712-8.
- Salas, A., et al.
2004 Rolling adhesion through an extended conformation of integrin α L β 2 and relation to α I and β I-like domain interaction. *Immunity* 20(4):393-406.
- Schurpf, T., and T. A. Springer
2011 Regulation of integrin affinity on cell surfaces. *Embo j* 30(23):4712-27.
- Sen, M., K. Yuki, and T. A. Springer
2013a An internal ligand-bound, metastable state of a leukocyte integrin, α X β 2. *J Cell Biol* 203(4):629-42.
- Sen, Mehmet, Koichi Yuki, and Timothy A. Springer
2013b An internal ligand-bound, metastable state of a leukocyte integrin, α (X) β (2). *The Journal of Cell Biology* 203(4):629-642.
- Shimaoka, M., et al.
2003 Small molecule integrin antagonists that bind to the β 2 subunit I-like domain and activate signals in one direction and block them in the other. *Immunity* 19(3):391-402.
- Shimaoka, Motomu, and Timothy A. Springer
2003 Therapeutic antagonists and conformational regulation of integrin function. *Nat Rev Drug Discov* 2(9):703-716.
- Shults, E.E., et al.
2005 Thebaine Adducts with Maleimides. *Synthesis and Transformations. Russian Journal of Organic Chemistry* 41(8):1132-1144.
- Taber, D. F., R. B. Sheth, and P. V. Joshi

- 2005 Simple preparation of alpha-diazo esters. *J Org Chem* 70(7):2851-4.
- Tang, R. H., et al.
2005 Epitope mapping of monoclonal antibody to integrin alphaL beta2 hybrid domain suggests different requirements of affinity states for intercellular adhesion molecules (ICAM)-1 and ICAM-3 binding. *J Biol Chem* 280(32):29208-16.
- Vugmeyster, Y., et al.
2004 Efalizumab (anti-CD11a)-induced increase in peripheral blood leukocytes in psoriasis patients is preferentially mediated by altered trafficking of memory CD8+ T cells into lesional skin. *Clin Immunol* 113(1):38-46.
- Weetall, M., et al.
2001 A homogeneous fluorometric assay for measuring cell adhesion to immobilized ligand using V-well microtiter plates. *Anal Biochem* 293(2):277-87.
- Weitz-Schmidt, G., and S. Chreng
2012 Cell adhesion assays. *Methods Mol Biol* 757:15-30.
- Weitz-Schmidt, G., T. Schurpf, and T. A. Springer
2011 The C-terminal alphaI domain linker as a critical structural element in the conformational activation of alphaI integrins. *J Biol Chem* 286(49):42115-22.
- Weitz-Schmidt, G., et al.
2004 Improved lymphocyte function-associated antigen-1 (LFA-1) inhibition by statin derivatives: molecular basis determined by x-ray analysis and monitoring of LFA-1 conformational changes in vitro and ex vivo. *J Biol Chem* 279(45):46764-71.
- Weitz-Schmidt, Gabriele, et al.
2001 Statins selectively inhibit leukocyte function antigen-1 by binding to a novel regulatory integrin site. *Nat Med* 7(6):687-692.
- Welzenbach, K., et al.
2015 A novel multi-parameter assay to dissect the pharmacological effects of different modes of integrin alphaLbeta2 inhibition in whole blood. *Br J Pharmacol* 172(20):4875-87.
- Zhong, Min, et al.
2012 Discovery and Development of Potent LFA-1/ICAM-1 Antagonist SAR 1118 as an Ophthalmic Solution for Treating Dry Eye. *ACS Medicinal Chemistry Letters* 3(3):203-206.
- Zhou, Yibo, et al.
2009 Catalytic Reactions of Carbene Precursors on Bulk Gold Metal. *Journal of the American Chemical Society* 131(33):11734-11743.

Paper 2



Contents lists available at ScienceDirect

Biochemical Pharmacology

journal homepage: www.elsevier.com/locate/biochempharm

Downstream effect profiles discern different mechanisms of integrin α L β 2 inhibition



Riccardo V. Mancuso^a, Karl Welzenbach^b, Peter Steinberger^c, Stephan Krähenbühl^a, Gabriele Weitz-Schmidt^{d,*}

^aDivision of Clinical Pharmacology and Toxicology and Department of Research, University Hospital, CH-4031 Basel, Switzerland

^bNovartis Pharma AG, Novartis Institutes of Biomedical Research, CH-4002 Basel, Switzerland

^cInstitute of Immunology, Medical University of Vienna, Lazarettgasse 19, 1090 Vienna, Austria

^dAlloCyte Pharmaceuticals AG, Hochbergerstrasse 60C, CH-4057 Basel, Switzerland

ARTICLE INFO

Article history:

Received 8 July 2016

Accepted 2 September 2016

Available online 6 September 2016

Keywords:

Integrin

LFA-1

Allosteric inhibitor

Paradoxical agonism

TCR

ABSTRACT

The integrin leucocyte function-associated antigen-1 (α L β 2, LFA-1) plays crucial roles in T cell adhesion, migration and immunological synapse (IS) formation. Consequently, α L β 2 is an important therapeutic target in autoimmunity. Three major classes of α L β 2 inhibitors with distinct modes of action have been described to date: Monoclonal antibodies (mAbs), small molecule α/β I allosteric and small molecule α I allosteric inhibitors. The objective of this study was to systematically compare these three modes of α L β 2 inhibition for their α L β 2 inhibitory as well as their potential agonist-like effects. All inhibitors assessed were found to potently block α L β 2-mediated leucocyte adhesion. None of the inhibitors induced ZAP70 phosphorylation, indicating absence of agonistic outside-in signalling. Paradoxically, however, the α/β I allosteric inhibitor XVA143 induced conformational changes within α L β 2 characteristic for an intermediate affinity state. This effect was not observed with the α I allosteric inhibitor LFA878 or the anti- α L β 2 mAb efalizumab. On the other hand, efalizumab triggered the unscheduled internalization of α L β 2 in CD4+ and CD8+ T cells while LFA878 and XVA143 did not affect or only mildly reduced α L β 2 surface expression, respectively. Moreover, efalizumab, in contrast to the small molecule inhibitors, disturbed the fine-tuned internalization/recycling of engaged TCR/CD3, concomitantly decreasing ZAP70 expression levels. In conclusion, different modes of α L β 2 inhibition are associated with fundamentally different biologic effect profiles. The differential established here is expected to provide important translational guidance as novel α L β 2 inhibitors will be advanced from bench to bedside.

© 2016 Elsevier Inc. All rights reserved.

Abbreviations: ADMIDAS, adjacent to metal ion-dependent adhesion site; AK, adenylate kinase; APC, allophycocyanin; BCECF, AM, 2',7'-bis-(2-carboxyethyl)-5-(and-6)-carboxyfluorescein, acetoxymethyl ester; CD, cluster of differentiation; DAPI, 4',6-diamidino-2-phenylindole; DMSO, dimethyl sulfoxide; ED₅₀, median effective dose; efalizumab-x, efalizumab cross-linked; Fc, fragment crystallizable; FCS, foetal calf serum; FITC, fluorescein isothiocyanate; FSC, forward scatter; FDA, food and drug administration; IC₅₀, half maximal inhibitory concentration; IgG, immunoglobulin G; IgG-x, immunoglobulin G cross-linked; IL, interleukin; IS, immunological synapse; ICAM-1, intercellular adhesion molecule-1; LFA-1, leucocyte function-associated antigen-1; mAb, monoclonal antibody; MFI, mean fluorescence intensity; MHC, major histocompatibility complex; MIDAS, metal ion-dependent adhesion site; PBMC, peripheral blood mononuclear cell; PE, phycoerythrin; PI, propidium iodide; SD, standard deviation; SEM, standard error of the mean; SSC, side scatter; TCR, T cell receptor; TNF, tumour necrosis factor; VCAM-1, vascular cell adhesion protein-1; VLA-4, very late antigen-4; ZAP70, zeta-chain-associated protein kinase 70.

* Corresponding author at: AlloCyte Pharmaceuticals AG, Hochbergerstrasse 60C, CH-4057 Basel, Switzerland.

E-mail addresses: gabriele.weitz-schmidt@unibas.ch, gabriele.weitz@alloyte-pharma.com (G. Weitz-Schmidt).

<http://dx.doi.org/10.1016/j.bcp.2016.09.002>

0006-2952/© 2016 Elsevier Inc. All rights reserved.

1. Introduction

The leucocyte cell surface receptor leucocyte function-associated antigen-1 (LFA-1, α L β 2, CD11a/CD18) is a member of the integrin family of at least 24 α/β heterodimeric receptors which mediate cell-to-cell or cell-to-extracellular matrix adhesion. Integrins are unique in that they are normally expressed on the cell surfaces in a resting, bent state in which they do not bind ligand and do not signal. Intracellular signalling (inside-out signalling) is required to convert integrins into active, extended states with different ligand binding affinities. Upon ligand binding integrins transmit signals back into the cells (outside-in signalling) that regulate cell shape, migration, growth and differentiation. When present, the I (inserted) domain of the integrin α subunit serves as the ligand binding domain. Integrins which lack this domain on the α

subunit utilize the I-like domain on the β subunit to bind ligand [1,2].

Integrins are well-characterized and attractive therapeutic targets that offer the potential to modulate the function of distinct cell populations and to selectively target cellular processes known to drive various diseases including malignant, thrombotic as well as autoimmune disorders, among others [3,4]. However, so far only six pharmacological inhibitors (antibodies and ligand mimetics) targeting three different integrins are currently approved for clinical use. These are natalizumab ($\alpha 4$ -integrin, $\alpha 4\beta 1$ and $\alpha 4\beta 7$), vedolizumab (integrin $\alpha 4\beta 7$), abciximab, eptifibatid and tirofiban (integrin $\alpha II\beta 3$). Even these integrin inhibitors remain associated with major limitations. Due to their antibody or peptidomimetic natures they need to be administered intravenously. Some of them are associated with the risk of paradoxical effects, i.e. induction of effects they were designed to prevent. This phenomenon of paradoxical agonism is of major concern and has been described mostly for ligand mimetic integrin inhibitors [5,6]. Ligand mimetics bind to the ligand binding site in a manner similar to the natural ligands, which can then cause unwanted outside-in signalling and cell activation. Further, currently used ligand mimetics are known to exhibit various levels of cross-reactivities to other integrin receptors, i.e. these inhibitors are not strictly selective for a single target integrin [6].

The rather modest success of integrin targeting medications to date is contrasted by an overwhelming wealth of data regarding integrin structure and function. The understanding of integrin-ligand interaction at atomic levels, on the one hand, and the detailed elucidation of the role of integrins in health and disease, on the other, provide an intriguing opportunity to develop novel approaches towards integrin modulation introducing differentiated types of inhibitors. Allosteric inhibition of ligand binding to integrins has been put forward as one such approach in order to overcome major limitations of previous integrin targeting strategies [5,6]. The leucocyte integrin $\alpha L\beta 2$ offers a unique opportunity to further validate this concept because $\alpha L\beta 2$ is the only integrin for which small molecule allosteric inhibitors with different modes of action have been described, in addition to competitive acting antibody approaches [7,8].

$\alpha L\beta 2$ belongs to the $\beta 2$ integrin family, sharing the $\beta 2$ subunit with Mac-1 ($\alpha M\beta 2$), $\alpha X\beta 2$ and $\alpha D\beta 2$ [1]. Expressed on all leucocytes, $\alpha L\beta 2$ mediates cell adhesion and migration [2]. Moreover, $\alpha L\beta 2$ plays a pivotal role in immunological synapse (IS) formation and thus T cell activation, and in directing the fate of naïve T cells towards disease-driving (“pro-inflammatory”) or protective (“regulatory”) populations [9,10]. The major ligand of $\alpha L\beta 2$ is intercellular adhesion molecule-1 (ICAM-1), which is upregulated by pro-inflammatory stimuli on endothelial cells and leucocytes. $\alpha L\beta 2$ is a validated therapeutic target in autoimmune disorders (e.g. psoriasis) as well as in transplant rejection [8]. More recently, $\alpha L\beta 2$ has been also implicated in the development of Alzheimer’s disease [11]. The best-characterized therapeutic mAb targeting $\alpha L\beta 2$ is efalizumab. Efalizumab binds close to the ICAM-1 binding site, the so-called metal ion-dependent adhesion site (MIDAS), located on the αL I domain, thereby blocking the binding of $\alpha L\beta 2$ to ICAM-1 competitively via steric hindrance (Fig. 1) [12]. The antibody has been utilized therapeutically for the treatment of >46,000 patients with moderate to severe psoriasis until it was withdrawn from markets in 2009 following four cases of progressive multifocal leukoencephalopathy (PML) [13]. The two small molecule $\alpha L\beta 2$ inhibitor classes with an allosteric mode of action are termed α I allosteric and α/β I allosteric inhibitors. The α I allosteric inhibitors have been demonstrated to bind underneath the C-terminal $\alpha 7$ helix of the αL I domain, located distant from the ligand binding site [1]. By this interaction α I allosteric inhibitors prevent a downward axial shift of the $\alpha 7$ helix which is crucial

for the conformational activation of $\alpha L\beta 2$ (Fig. 1). Natural statins such as lovastatin or simvastatin have been described first to interact with this $\alpha L\beta 2$ allosteric pocket [14]. All known α I allosteric $\alpha L\beta 2$ inhibitors are still at pre-clinical stage. Interestingly, α/β I allosteric inhibitors (the second class of small molecule $\alpha L\beta 2$ inhibitors) have been derived from the key amino acids of ICAM-1 responsible for its interaction with $\alpha L\beta 2$ [15]. As ligand mimetics this type of inhibitors were expected to bind to the ligand binding site of the αL I domain. Surprisingly, however, in depth studies revealed that these compounds follow an allosteric mode of action [16]. α/β I allosteric inhibitors apparently bind to the MIDAS of the I-like domain of the $\beta 2$ subunit as mimetics of an intrinsic ligand located in the C-terminal α I domain linker of the αL chain thereby leaving the α I domain in its default inactive conformation (Fig. 1). Of note, α/β I allosteric inhibitors have been demonstrated to also target other members of the $\beta 2$ integrin family, such as Mac-1 and $\alpha X\beta 2$, in contrast to the selectively acting α I allosteric inhibitors [17,18]. Currently, the most advanced small molecule inhibitor with an α/β I allosteric mode of action, liftegrast, has completed phase III clinical trials as a topical treatment for dry eye syndrome [19,20], enabling recent approval by US FDA.

In the present study we determined the activity profiles of allosterically acting $\alpha L\beta 2$ inhibitor classes side by side with the anti- $\alpha L\beta 2$ mAb efalizumab. For the first time, we systematically investigated potential agonist-like effects associated with the respective pharmacologies and identified hitherto unknown downstream effects which may be of therapeutic relevance, in the future.

2. Materials and methods

2.1. Cell culture

The human lymphoblastoid cell line Jurkat (European Collection of Cell Cultures, Salisbury, UK), the mouse ovalbumin specific T cell-receptor (TCR)-transgenic cell line OT-1 (gift from Ed Palmer, University Hospital, Basel, CH) and the human liver cancer cell line HepG2 (ATCC, Manassas, VA) were maintained in a humidified incubator at 37 °C supplied with 5% CO₂. Jurkat cells were cultured in RPMI 1640 containing 10% (v/v) heat-inactivated foetal calf serum (FCS), 1% MEM amino acids, amphotericin B 1 µg/ml, and gentamycin 10 µg/ml. OT-1 cells were cultured in RPMI 1640 containing 5% (v/v) heat-inactivated FCS, L-glutamin 2 mM, Penicillin 100 U/ml and Streptomycin 100 µg/ml. HepG2 cells were maintained in DMEM containing 10% (v/v) heat-inactivated FCS, 1 g/l glucose, 4 mM L-glutamine, 2 mM GlutaMax, 1 mM pyruvate, 10 mM HEPES buffer, 10 mM non-essential amino acid, penicillin 100 U/ml and streptomycin 100 µg/ml. The density of the cells was maintained below 1 × 10⁶ cells/ml. Every second or third month, the cell cultures were replaced by a new batch of cells with a low passage number. All cell culture media and reagents were purchased from Gibco Life Technologies, Paisely, UK.

2.2. Isolation of peripheral blood mononuclear cells (PBMCs)

PBMCs were isolated from EDTA-blood samples via centrifugation in Ficoll-Paque™ PLUS separating solution according to the manufacturer’s protocol (GE Healthcare, Glattbrugg, CH). The blood samples were obtained from healthy donors from the Blood Center SRK of Basel.

2.3. Preparation of $\alpha L\beta 2$ inhibitors, control compounds and efalizumab

Test compounds LFA878 (supplied by Dr. Berndt Oberhauser, Novartis Pharma Basel AG, CH) (PubChem CID: 449170) and

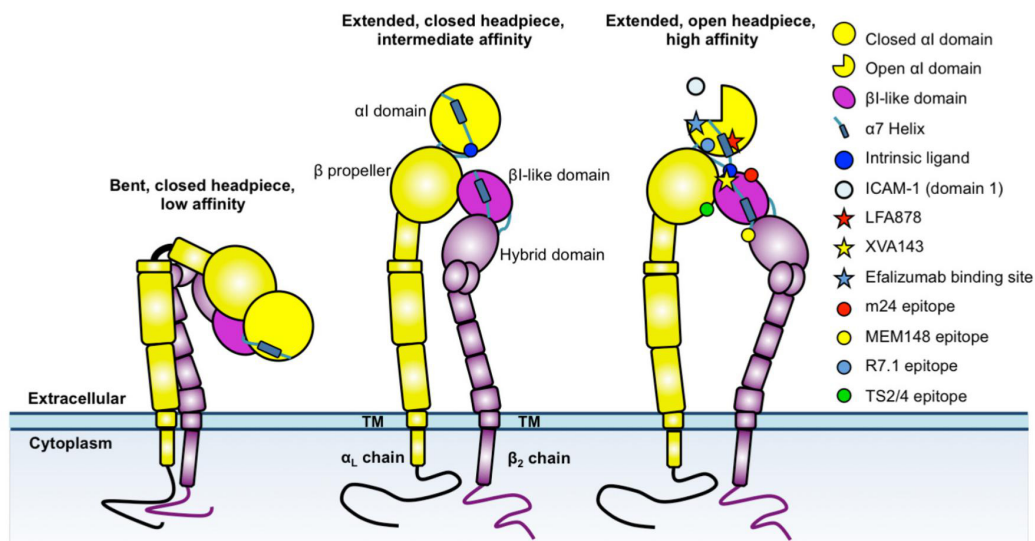


Fig. 1. Schematic of $\alpha\text{L}\beta\text{2}$ activation states, with different epitopes and inhibitor binding sites indicated. The inactive, bent conformation with a closed headpiece (left), the semi-active extended conformation with a closed headpiece (middle) and the active, extended conformation with an open headpiece (right) are illustrated. The binding site of LFA878 (αI allosteric inhibitor), the putative binding site of XVA143 ($\alpha/\beta\text{I}$ allosteric inhibitor) and the binding site of the anti- αL mAb efalizumab plus the epitopes of mAbs m24, MEM148, R7.1 and TS2/4 are indicated in the active extended conformation.

XVA143 (=R00281607-000 provided by Dr. Paul Gillespie, Hoffmann-La Roche Inc., Nutley, US) (PubChem CID: 9872589) were dissolved at 10 mM in DMSO (Sigma-Aldrich, St. Louis, MO, USA). Control compounds simvastatin, staurosporine, cyclosporine and amiodarone were purchased from Sigma-Aldrich, St. Louis, MO, USA and dissolved at 10 mM in DMSO. For the experiments, the compounds were serially pre-diluted in DMSO to avoid precipitation followed by dilution in medium or assay buffer. Final DMSO concentration during the experiments was $\leq 1\%$. No cytotoxicity was detected at this concentration. Efalizumab (obtained from Merck-Serono when product was on the market) was kept at -80°C in RPMI 1640 at a concentration of 10 mg/ml. Serial dilutions were prepared in medium or assay buffer.

2.4. V well cell adhesion assays

The human Jurkat/ICAM-1 ($\alpha\text{L}\beta\text{2}$ -dependent), the Jurkat/VCAM-1 ($\alpha\text{4}\beta\text{1}$ -dependent) and the murine OT-1/ICAM-1 ($\alpha\text{L}\beta\text{2}$ -dependent) assays were performed in V-bottom 96-well plates (Sigma-Aldrich, St. Louis, MO, USA) as previously described [21,22]. Briefly, V bottom plates were coated with anti-human IgG antibody (Sigma-Aldrich, St. Louis, MO, USA) diluted in coating buffer (20 mM Tris containing 150 mM NaCl, pH 8) (1 $\mu\text{g}/\text{ml}$) and incubated overnight at 4°C . The plates were blocked with blocking buffer (50 mM Tris base, 150 mM NaCl, 1.5% BSA (w/v), pH 7.2) at 37°C for 90 min (min). Human ICAM-1/Fc chimera, human VCAM-1/Fc chimera or mouse ICAM-1/Fc chimera (R&D Systems, Abingdon, UK) were immobilized at 0.3 $\mu\text{g}/\text{ml}$ in coating buffer. For studies with efalizumab, human ICAM-1 without Fc-tag (R&D Systems, Abingdon, UK) was directly immobilized to V bottom plates without capturing mAb. The plates were incubated at 37°C for 90 min and washed with binding buffer (50 mM Tris base, 150 mM NaCl, 1.5% BSA (w/v), 2 mM MgCl_2 , 2 mM MnCl_2 , 5 mM D-glucose monohydrate, pH 7.2–7.4). The cells were fluorescently labelled with 1 $\mu\text{g}/\text{ml}$ of BCECF-AM (Gibco Life Technologies, Paisley, UK) in phosphate-buffered saline (PBS; Gibco Life Technologies, Paisley, UK) at 37°C for 20 min and washed with PBS. The labelled Jurkat cells or OT-1 cells were re-suspended in binding buffer and test

compounds or solvent controls were added. After 40 min at 37°C 30,000 cells/well were transferred to the integrin ligand coated V well plates. After 5 min of incubation at room temperature (rt) plates were centrifuged for 4 min at 1000 rpm (in case of efalizumab at 500 rpm) using the Centrifuge Eppendorf 10 5810 R (Eppendorf, Schönenbuch, CH), setting the brake off. Non-adherent cells that accumulated in the centre of the V bottom were quantified using the fluorescence reader Tecan M200 Pro Infinity (Tecan, Mannedorf, CH) (excitation 485 nm/emission at 535 nm). The half maximal inhibitory concentration (IC_{50}) values were calculated using the software GraphPad Prism 6 (GraphPad Software, La Jolla, CA, USA). All buffer reagents used in the V well cell adhesion assay were obtained from Sigma-Aldrich, St. Louis, MO, USA.

2.5. Quantification of mAb R7.1, MEM148 or m24 binding to $\alpha\text{L}\beta\text{2}$

Conformational changes of $\alpha\text{L}\beta\text{2}$ upon inhibitor binding were quantified using FITC-labelled anti- $\alpha\text{L}\beta\text{2}$ mAb R7.1 (ebioscience, Frankfurt, D), PE-labelled anti- $\alpha\text{L}\beta\text{2}$ mAb MEM148 (Sigma-Aldrich, St. Louis, MO, USA) and Alexa Fluor[®] 488-labelled anti- $\alpha\text{L}\beta\text{2}$ mAb m24 (Biolegend, San Diego, CA, USA). For mAb R7.1 binding Jurkat cells were re-suspended in assay buffer I (50 mM Tris, 150 mM NaCl, 2 mM MgCl_2 , 1.5% BSA and 10 mM D-glucose monohydrate, pH 7.2). For mAbs MEM148 or m24 binding assay buffer II (50 mM Tris, 150 mM NaCl, 1 mM CaCl_2 , 1 mM MgCl_2 , 5 mM D-glucose monohydrate, 1.5% BSA, pH 7.3) was used. The Jurkat cell suspensions were transferred to polypropylene tubes containing the compounds, efalizumab, efalizumab cross-linked (efalizumab-x) or solvent and IgG controls (Sigma-Aldrich, St. Louis, MO, USA). Multimeric efalizumab-x was generated by incubation of efalizumab with goat anti-human IgG (Sigma-Aldrich, St. Louis, MO, USA) at a ratio of 1:1 (10 $\mu\text{g}/\text{ml}$) in the respective assay buffer. The cells were pre-incubated with the $\alpha\text{L}\beta\text{2}$ inhibitors and respective controls at 37°C for 40 min. In experiments in which the effect of the $\alpha\text{L}\beta\text{2}$ inhibitors on MnCl_2 -induced MEM148 or m24 epitope exposure was studied, cells were pre-incubated in assay buffer II containing inhibitors and controls at 37°C for 30 min. Then MnCl_2 was added to a final concentration of 2 mM,

followed by an incubation of 30 min at 37 °C. After this incubation, the cell suspensions were centrifuged and the supernatants discarded. Cells were stained with mAb R7.1 on ice or with mAb MEM148 and mAb m24 at 37 °C for 30 min, respectively. After two wash cycles cells were analysed by flow cytometry using a FACScalibur (BD, East Rutherford, NJ, USA). Mean fluorescence intensities (MFI) of FSC/SSC gated events were calculated using the FlowJo software 10.08 (Tree Star, Ashland, OR). All buffer reagents used in the flow cytometry assays described above were purchased from Sigma-Aldrich, St. Louis, MO, USA.

2.6. Analysis of cytotoxicity and apoptosis

Cytotoxicity was investigated in Jurkat and HepG2 cells using the ToxiLight™ BioAssay Kit (Lonza, Basel, CH). This assay measures the release of adenylate kinase (AK), a marker for loss of cell membrane integrity. Cell cultures were treated with the compounds, antibody and controls for 24 h (h). Then 20 µl cell culture supernatant was mixed with 100 µl AK detection reagent. Luminescence was measured after incubation in the dark for 5 min, using the Tecan M200 Pro Infinity plate Reader to determine cytotoxicity. Apoptosis and secondary necrosis were determined by flow cytometry using the Annexin V and propidium iodide (PI) staining kit, following manufacturer's instructions (Vybrant™ Apoptosis Assay Kit #2, Gibco Life Technologies, Paisley, UK).

2.7. Analysis of α L β 2 expression and internalization

PBMCs were resuspended in fresh medium (RPMI 1640, 10% FCS) and seeded at 300,000 cells/well into a 24-well plate followed by incubation with α L β 2 inhibitors or controls for 24 h. After one wash with PBS the cells were stained with PE-labelled anti- α L β 2 mAb TS2/4, FITC-labelled anti-CD4 mAb clone A16A1 and APC-labelled anti-CD8 mAb clone HIT8a (Biolegend, San Diego, CA, USA) or appropriate isotype controls on ice for 25 min (min) and analysed by flow cytometry. 5,000 events of CD4+ or CD8+ cells were acquired. MFI were calculated using the FlowJo software.

For imaging α L β 2 localization, treated cells were washed with cold PBS and fixed at rt for 15 min with paraformaldehyde 4% (Sigma-Aldrich, St. Louis, MO, USA) in PBS. Cells were washed, blocked with PBS/2.5% BSA and incubated at rt for 15 min. Then the cells were incubated on ice for 30 min with PE-labelled mAb TS2/4 for α L β 2 staining, Alexa Fluor® 488-labelled anti-CD107a mAb clone H4A3 (Biolegend, San Diego, CA, USA) for lysosomal staining and DAPI (Gibco Life Technologies, Paisley, UK) for nuclear staining. After one washing step with PBS, cells were imaged using the ImageStream X Mark II Imaging flow cytometer (Merck Millipore Schaffhausen, CH). The number of α L β 2 clusters (granular stainings) was quantified using the software ImageJ (NIH, Bethesda, MD). A threshold range of 130–1,000 mean intensity was applied to all images. Clusters were defined by pixel area size (4–16) plus shape (circularity 0.4–1) and were counted as single events.

2.8. Analysis of CD3 and TCR surface expression

Internalization of surface CD3 or TCR α/β chains induced by mAb OKT3 in presence or absence of α L β 2 inhibitors or controls was quantified by flow cytometry. Freshly isolated PBMCs were resuspended in RPMI 1640 containing 10% FCS. Anti-CD3 mAb OKT3 (Biolegend, San Diego, CA, USA) was added at 50 ng/ml for 24 h. PBMCs were washed once with PBS and stained with FITC-labelled anti-CD3 mAb clone UCHT1 or FITC-labelled anti-TCR α/β mAb clone IP26 (Biolegend, San Diego, CA, USA) on ice for 25 min. Antibody binding was quantified by flow cytometry as described above, analysing the % CD3+ or % TCR+ events within

the lymphocyte population. Of note, the anti-CD3 mAbs UCHT1 utilized for the detection of CD3 surface expression did not compete with OKT3 for CD3 binding under conditions applied (data not shown).

2.9. Assessment of ZAP70 phosphorylation or general tyrosine phosphorylation

ZAP70 tyrosine phosphorylation or general tyrosine phosphorylation was determined using phospho-flow analysis. Briefly, PBMCs were rested for 2 h in RPMI containing 2% FCS, 1% MEM NEAA (resting medium). Rested cells in ice cold resting medium were added to 5 ml FACS tubes and incubated with the small molecule α L β 2 inhibitors for 30 min and with MnCl₂/DMSO for 10 min on ice. On the other hand OKT3 (5 µg/ml), efalizumab (10 µg/ml) and respective IgG controls were incubated with the cells for 15 min on ice. After crosslinking of OKT3 and efalizumab with anti-mouse IgG (5 µg/ml) or anti-human IgG (10 µg/ml) respectively the incubation on ice was continued for another 15 min. After these incubation steps all samples were washed once in ice cold resting medium, transferred into a water bath at 37 °C and incubated for 1 min to activate TCR or α L β 2-dependent membrane proximal signalling pathways. Cells were fixed by addition of paraformaldehyde (final concentration 2%) for 10 min at rt. Cells were then washed with ice cold resting medium, permeabilized by treatment with ice cold 100% methanol (Sigma-Aldrich, St. Louis, MO, USA), for 10 min. Cells were washed twice with excess of ice cold resting medium and stained for 40 min on ice with Alexa Fluor® 488-labelled anti-ZAP70 pY292 (clone J34-602; BD, East Rutherford, NJ, USA) or FITC-labelled anti-phospho-Tyr clone pY20 and APC-labelled anti-CD2 mAb RPA-2.10 (Biolegend, San Diego, CA, USA). Antibody binding was analysed by flow cytometry as described above.

2.10. Analysis of intracellular ZAP70 protein expression

PBMCs were resuspended in RPMI 1640 containing 10% FCS at a concentration of 4×10^6 cells/ml and incubated with test compounds and controls for 24 h. After 24 h cells were transferred to polystyrene tubes, washed once with PBS, resuspended in BD Cytofix/Cytoperm™ (BD, East Rutherford, NJ, USA) and incubated for additional 20 min at 4 °C. Cells were washed and resuspended in permeabilization buffer (PBS, digitonin 20 µg/ml, BSA 0.5%; buffer reagents obtained from Sigma-Aldrich, St. Louis, MO, USA). Intracellular ZAP70 in the lymphocyte population was quantified by flow cytometry using a PE-labelled anti-ZAP70 mAb (clone 1E7.2, Biolegend, San Diego, CA, USA).

2.11. Statistical analysis

Data are represented as mean \pm standard deviation (SD) or mean \pm standard error of the mean (SEM). GraphPad Prism 6 (GraphPad Software, La Jolla, CA) was used for calculation of *p*-values by one-way ANOVA. A value of *p* < 0.05 was considered to be significant.

3. Results

3.1. Activity profile of α L β 2 inhibitors

For the present study we utilized the well-characterized α I allosteric inhibitor LFA878, the α/β I allosteric inhibitor XVA143 and the anti- α L β 2 mAb efalizumab [16,23,24] (Table 1). All inhibitors potently blocked α L β 2 mediated Jurkat cell adhesion to immobilized ICAM-1 (CD54) in a concentration-dependent manner

Table 1
Chemical structure of α L β 2 inhibitors LFA878, XVA143, and efalizumab, molecular weight (Da) and mode of action.

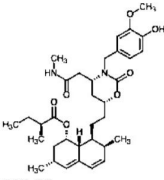
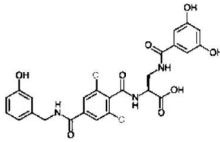

Parameter	LFA878	XVA143	Efalizumab
Chemical structure			
Molecular weight (Da)	596.77	562.36	~150,000
Mode of action	α I allosteric	α/β I allosteric	Competitive

Table 2
Activity profile of α L β 2 inhibitors.

Assay	LFA878 IC ₅₀ [μ M]	XVA143 IC ₅₀ [μ M]	Efalizumab [μ g/ml]
Activity (αLβ2)	0.096 \pm 0.036	0.0007 \pm 0.0005	0.064, 0.059
Jurkat/ICAM-1	(n = 4)	(n = 3)	
Selectivity (α4β1)	>10	>10	>10
Jurkat/VCAM-1			
Cross-reactivity (mouse αLβ2)	10.78 \pm 0.21	0.0019 \pm 0.0014	n.d.
OT-1/mICAM	(n = 3)	(n = 3)	
Cytotoxicity (AK release)	>10	>10	n.d.
Jurkat cells			
Cytotoxicity (AK release)	>10	>10	n.d.
HepG2 cells			
Cytotoxicity (Annexin V/PI)	>10	>10	>10
Jurkat cells	(n = 3)	(n = 3)	(n = 3)

Mean values \pm SD of \geq three independent experiments or single values run in triplicates are shown; n.d.: not determined.

(Table 2, Fig. 2A–C). In contrast, Jurkat cell adhesion mediated by a related leucocyte integrin, very late antigen-4 (VLA-4; α 4 β 1; CD49d/CD29), was not impaired in presence of the inhibitors, indicating selectivity for α L β 2 over α 4 β 1 (Table 2). Moreover, profiling in the mouse specific α L β 2-dependent OT-1 adhesion assay revealed that the α I allosteric α L β 2 inhibitor LFA878 exhibited greater inhibitory potency towards human than murine α L β 2 (Table 2, Fig. 2A and D). Such limited cross-species reactivity has been also observed for α I allosteric α L β 2 inhibitors other than LFA878 [25,26]. Interestingly, in contrast to α I allosteric inhibitors the α/β I allosteric inhibitor XVA143 fully cross-reacted with murine α L β 2 (Table 2, Fig. 2B and E). This observation is in agreement with studies indicating that α/β I allosteric inhibitors such as XVA143 interact with the MIDAS of the β 2 I-like domain, a region which is 100% conserved between human and mouse [16,27]. In contrast, the α L I domain which contains the binding site of α I allosteric inhibitors is less well conserved. The identity of the I domain between human and mouse is 74.7% (Table 3). Moreover, the alignment of the human and mouse amino acid sequences revealed that the main contact sites of LFA878 (as determined by the X-ray structure of the human α L I domain in complex with LFA878 [23]) include four un-matched residues with two located in the α 7 helix of the I domain (Table 3). These findings provide a straightforward explanation for the limited cross-reactivity of α I allosteric inhibitors with mouse α L β 2. Efalizumab does not bind to murine α L β 2 [28] and thus was not tested in the mouse assay. Neither of the compounds was cytotoxic to Jurkat cells or the liver cell line HepG2 after 24 h of incubation as determined by the release of the enzyme adenylate kinase from damaged cells (Table 2). Moreover, none of the α L β 2 inhibitors induced apoptosis

and/or necrosis in Jurkat cells after 24 h of exposure, in contrast to the control compounds cyclosporine A, staurosporine and amiodarone [29] (Table 2, Fig. 3).

3.2. α L β 2 inhibitors differentially impact α L β 2 conformations

The conformational state of α L β 2 upon inhibitor binding was studied using three well-characterized, conformation-sensitive mAbs mapping to distinct sites of α L β 2. MEM148 recognizes an epitope on the hybrid domain of the β 2 chain that becomes exposed when the integrin adopts an extended, active conformation [30]. The epitope of the second mAb m24 is uncovered when the β 2 I-like domain is activated, i.e. mAb m24 epitope exposure is characteristic for the activated conformation of this domain [31]. The third antibody, mAb R7.1, recognizes a combinational epitope that requires both the α L I and the β propeller domain on the α L chain for full reactivity [32]. This epitope is known to be lost upon α I allosteric inhibitor binding [23] (Fig. 1).

In resting Jurkat cells, the α/β allosteric inhibitor XVA143 induced both the MEM148 and m24 epitope by 2.3 and 3.8 fold respectively, in contrast to α I allosteric inhibitors and efalizumab alone or cross-linked with anti-human IgG antibody (to mimic engagement of the Fc part of the antibody with Fc receptors). Moreover, XVA143-induced MEM148 and m24 epitope expression was more pronounced than exposure levels induced by the integrin activating cation Mn²⁺ (Fig. 4A and B). Mn²⁺ is known to increase integrin affinity by replacing Ca²⁺ at the ADMIDAS site of the β 2 I-like domain [31]. These results confirm that α/β I allosteric inhibitors such as XVA143 induce an extended conformation of α L β 2, (associated with an activated β 2 I-like domain) which is characteristic for the semi-active form of α L β 2 [16]. They also confirm that α I allosteric inhibitors such as LFA878 do not induce α L β 2 extension upon binding [16]. Interestingly, efalizumab alone or cross-linked did not affect the bent conformation of α L β 2 under resting conditions (Fig. 4A and B). This observation is in line with the finding that the crystal structure of the α L I domain in complex with efalizumab adopts the inactive conformation as seen in the unliganded form of α L β 2 [12].

Differential effects of the α L β 2 inhibitor classes on MEM148 and m24 epitope exposure were also noted under Mn²⁺ activating conditions. LFA878 was able to suppress Mn²⁺-induced MEM148 epitope expression (Fig. 4C). This result confirms that α I allosteric inhibitors stabilize the bent conformation of α L β 2 not only under resting but also under activating conditions [16]. On the other hand however, LFA878 allowed Mn²⁺-induced β 2 I-like domain activation (as monitored by m24 epitope expression) (Fig. 4D). Remarkably, a similar 'cocked' conformation with β 2 I-like domain activation, despite the presence of a bent conformation has been also noted in a crystal structure of the closely related integrin α X/ β 2 [33]. XVA143 enhanced both MEM148 and mAb24 epitope exposure by Mn²⁺, suggesting that the compound is able to sub-

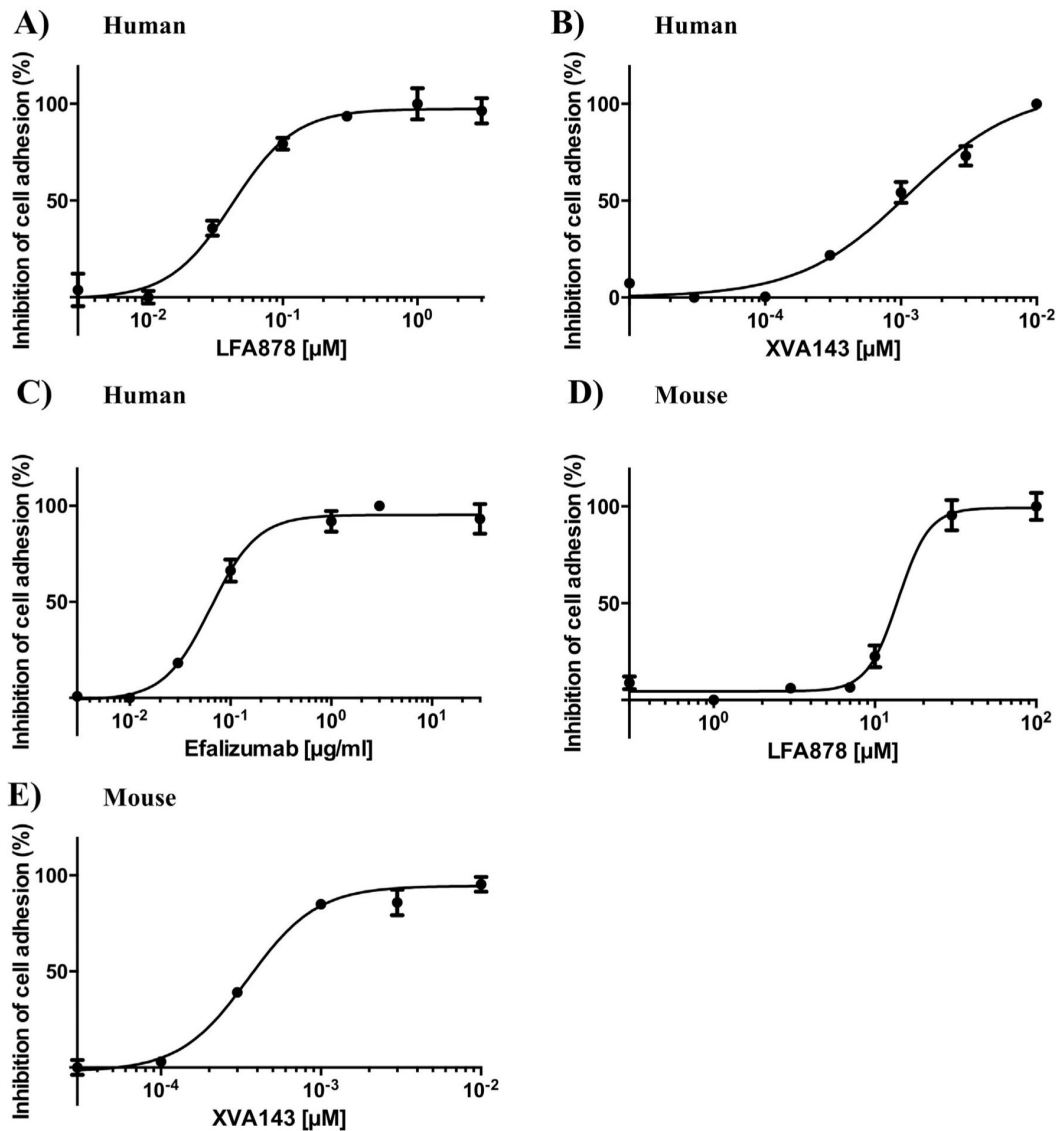


Fig. 2. Concentration-dependent inhibition of human or mouse α L β 2-mediated cell adhesion. The effect of indicated α L β 2 inhibitors on the binding of fluorescently labelled human Jurkat cells (A, B, C) or mouse OT-1 cells (D, E) to immobilized human ICAM-1/Fc or mouse ICAM-1/Fc, respectively was determined using the V well adhesion assay. Each point represents the mean value \pm SD of triplicates. Representative experiments out of four (A), three (B, D, E) and two (C) independent experiments run in triplicates are shown.

stantially augment α L β 2 extension and β 2 I-like domain activation (Fig. 4C and D). This observation underlines the strong agonist-like effect of XVA143 already observed under resting conditions. In contrast to LFA878 and XVA143, efalizumab did not alter (i.e. neither prevent nor augment) Mn²⁺-induced α L β 2 extension according to the degree of mAb MEM148 binding (Fig. 4C). However, similar to XVA143, efalizumab augmented Mn²⁺-induced activation of the β 2 I-like domain (Fig. 4D). This observation establishes that the Mn²⁺-induced activation of the β 2 I-like domain and the Mn²⁺-induced α L β 2 extension represent distinct conformational changes which can be influenced differentially. This interpretation of Mn²⁺-mediated β 2 I-like domain activation and extension representing distinct processes is in line with the observation that LFA878 allows for normal Mn²⁺-induced I-like domain activation but prevents α L β 2 extension (Fig. 4C and D). In addition, we assessed the impact of the inhibitors on the R7.1 epitope under

resting conditions. The α I allosteric inhibitor LFA878 and simvastatin (included as an assay control) induced R7.1 epitope loss on the α L chain as expected whereas XVA143 and efalizumab did not significantly affect the R7.1 epitope (Fig. 4E). The effect of the inhibitors on the R7.1 epitope under Mn²⁺-activating conditions was not investigated.

Of note, the XVA143-induced MEM148 and m24 epitope exposure was concentration-dependent with ED₅₀ values of 2 ± 1 nM and 0.55 ± 0.07 nM, respectively (Fig. 4F and G). Interestingly, these ED₅₀ values correlated well with the IC₅₀ value measured for XVA143 in the functional α L β 2 V well adhesion assay (Table 2 and Fig. 4F and G). Similarly, the IC₅₀ value measured for LFA878 in the R7.1 epitope loss assay (IC₅₀: 24 ± 7 nM) was in the range of the IC₅₀ determined in the α L β 2 V well adhesion assay (Table 2 and Fig. 4H). These correlations suggest that α / β I allosteric inhibitor-induced MEM148 or m24 epitope gain or α I allosteric inhibitor

Table 3
Comparison of human and mouse α L I domain amino acid sequences.

Species	a.a. Sequence I domain																						
Human	130	V	D	L	V	F	L	F	D	G	S	M	S	L	Q	P	D	E	F	Q	K	140	
Mouse		V	D	L	V	F	L	F	D	G	S	Q	S	L	D	R	K	D	F	E	K		
		*	*	*	*	*	*	*	*	*	*	*	*	*	:	.	:	*	:	*			
Human	150	I	L	D	F	M	K	D	V	M	K	K	L	S	N	T	S	Y	Q	F	A	160	
Mouse		I	L	E	F	M	K	D	V	M	R	K	L	S	N	T	S	Y	Q	F	A		
		*	*	:	*	*	*	*	*	*	*	*	*	*	*	*	*	*	*	*	*	*	
Human	170	A	V	Q	F	S	T	S	Y	K	T	E	F	D	F	S	D	Y	V	K	R	180	
Mouse		A	V	Q	F	S	T	D	C	R	T	E	F	T	F	L	D	Y	V	K	Q		
		*	*	*	*	*	*	.	:	*	*	*	*	*	*	*	*	*	*	*	*	:	
Human	190	-	K	D	P	D	A	L	L	K	H	V	K	H	M	L	L	L	T	N	T	200	
Mouse		N	K	N	P	D	V	L	L	G	S	V	Q	P	M	F	L	L	T	N	T		
		*	*	:	*	*	.	:	*	*	*	*	*	*	*	*	*	*	*	*	*	*	
Human	210	F	G	A	I	N	Y	V	A	T	E	V	F	R	E	E	L	G	A	R	P	220	
Mouse		F	R	A	I	N	Y	V	V	A	H	V	F	K	E	E	S	G	A	R	P		
		*	*	*	*	*	*	*	.	:	.	*	*	:	*	*	*	*	*	*	*	*	
Human	230	D	A	T	K	V	L	I	I	I	T	D	G	E	A	T	D	S	G	N	I	240	
Mouse		D	A	T	K	V	L	V	I	I	T	D	G	E	A	S	D	K	G	N	I		
		*	*	*	*	*	*	:	*	*	*	*	*	*	*	:	*	*	*	*	*	*	
Human	250	D	A	A	K	D	I	I	R	Y	I	I	G	I	G	K	H	F	Q	T	K	260	
Mouse		S	A	A	H	D	I	T	R	Y	I	I	G	I	G	K	H	F	V	S	V		
		.	*	*	:	*	*	*	*	*	*	*	*	*	*	*	*	*	*	*	:	*	
Human	270	E	S	Q	E	T	L	H	K	F	A	S	K	P	A	S	E	F	V	K	I	280	
Mouse		Q	K	Q	K	T	L	H	I	F	A	S	E	P	V	E	E	F	V	K	I		
		:	.	*	*	*	*	*	*	*	*	*	*	*	.	.	*	*	*	*	*	*	
Human	290	L	D	T	F	E	K	L	K	D	L	F	T	E	L	Q	K	R	I	Y	V	300	
Mouse		L	D	T	F	E	K	L	K	D	L	F	T	E	L	Q	R	K	I	Y	A		
		*	*	*	*	*	*	*	*	*	*	*	*	*	*	*	*	*	*	*	*	*	
Human	310	I	E	G	T	S	K	Q	D	L	T	S	F	N	M	E	L	S	S			320	
Mouse		I	E	G	T	N	R	Q	D	L	T	S	F	N	M	E	L	S	S				
		*	*	*	*	.	*	*	*	*	*	*	*	*	*	*	*	*	*	*	*	*	

LFA878 contact points to the I allosteric site are shown in yellow, the α 7 helix sequence is shown in bold. A point accepted mutation (PAM250) was used to score matrix for sequence comparison. Conserved sequences are marked with (*), conservative mutations with scoring >0.5 in the PAM250 matrix are marked with (:), semi-conservative mutations with scoring \leq 0.5 in the PAM250 are marked with (.), and non-conservative mutations are marked with (.) . Sequence data and software BLAST for alignment are derived from <http://www.uniprot.org/>.

triggered R7.1 epitope loss can be used to predict the functional activity of the compounds *in vitro* or *ex vivo* in whole blood assays [34].

3.3. α L β 2 inhibitors do not induce protein tyrosine phosphorylation

We reasoned that the differential effects of the inhibitor classes on the conformational status of α L β 2 may directly translate into differential (unwanted) outside-in signalling. In order to prove this hypothesis we assessed ζ – chain-associated protein kinase of 70 kDa (ZAP70) tyrosine phosphorylation in PBMCs treated with inhibitors. ZAP70 is an established early mediator of α L β 2 outside-in signalling and constitutively associated with α L β 2 [35]. PBMCs were used for this study instead of Jurkat cells to avoid the limitations inherent to T-leukaemic cells lines when studying signalling events. We show here for the first time that none of the small molecule α L β 2 inhibitors triggered detectable ZAP70 Y292 phosphorylation in CD2+ T cells, in contrast to the integrin activating cation Mn²⁺ or cross-linked anti-CD3 mAb OKT3 (OKT3-x) (Fig. 5A). mAb OKT3 binds to CD3 of the TCR/CD3 complex and is used to induce signalling pathways normally triggered upon binding of the natural ligand peptide antigen-major histocompatibility complex (pMHC) to the TCR [36]. These signalling pathways lead to phosphorylation of various proteins on tyrosine

residues including ZAP70 [36]. Moreover, in agreement with the above data, none of the compounds led to detectable general protein tyrosine phosphorylation in CD2+ T cells, in contrast to Mn²⁺ and OKT3-x (Fig. 5B). Interestingly, this observation indicates that the extended conformation of α L β 2 stabilized by α / β I allosteric inhibitors does not mediate signals into the cells although this conformational status of α L β 2 represents a semi-active form of LFA-1 [37,38]. In addition, efalizumab alone or cross-linked did not evoke ZAP70 or general protein tyrosine phosphorylation in PBMCs (Fig. 5A and B). This observation was surprising because crosslinking of integrins with blocking antibodies has been reported to elicit signals similar to ligand binding [39,40]. Taken together, under experimental conditions tested, the α L β 2 inhibitors did not induce α L β 2 mediated outside-in signalling as assessed via protein tyrosine phosphorylation.

3.4. α L β 2 inhibitors differentially affect α L β 2 expression

Previous data show that α L β 2 engagement by efalizumab induces a rapid downmodulation of α L β 2 in psoriasis patients by more than 70% in T cells [41–43]. Thus, we investigated the effects of the α L β 2 inhibitors on α L β 2 surface expression using resting PBMCs. The cells were treated for 24 h with inhibitors and α L β 2 expression was determined on CD4+ and CD8+ T cells. In

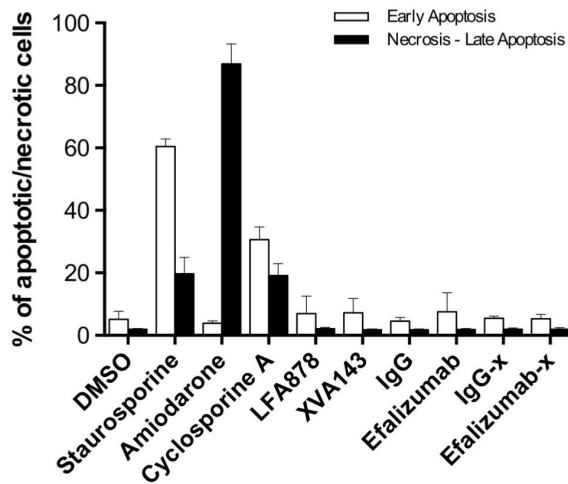


Fig. 3. α L β 2 inhibitors did not induce apoptosis and/or necrosis. Jurkat cells were left untreated or were treated with the α L β 2 inhibitors LFA878 (10 μ M), XVA143 (10 μ M), efalizumab (10 μ g/ml) and efalizumab cross-linked (efalizumab-x) (10 μ g/ml), the respective controls DMSO (0.1%), IgG (10 μ g/ml), IgG cross-linked (IgG-x) (10 μ g/ml) for 24 h. At 24 h cells were labelled with Annexin V/PI, and analysed by flow cytometry to evaluate early and late apoptosis. Cyclosporine A (10 μ M), staurosporine (200 nM) and amiodarone (100 μ M) served as assay controls. Mean values \pm SD of three independent experiments with single determinations each are shown.

agreement with previous observations in psoriasis patients efalizumab led to a downmodulation of α L β 2 in CD4+ and CD8+ T cells which became more evident when the antibody was cross-linked (Fig. 6A and B). Further, the effect of efalizumab on CD4+ T cells was slightly more pronounced than on CD8+ T cells (Fig. 6A and B). In contrast, even high concentrations of LFA878 ($>100 \times$ IC₅₀ value) did not significantly affect α L β 2 surface expression in both T cell subpopulations while the α/β I allosteric inhibitor XVA143 significantly reduced α L β 2 expression in CD4+ cells but not in CD8+ cells. These data suggest that both XVA143 and efalizumab are able to differentially affect α L β 2 expression in CD4+ and CD8+ T cells. Interestingly, variability in α L β 2 downmodulation among cell types has also been observed in patients treated with efalizumab [42]. Moreover, cross-linked efalizumab induced α L β 2 clustering and co-localization within the lysosomal compartment, in contrast to efalizumab alone, XVA143 or LFA878 (Fig. 6C and D). This result is in agreement with the previous finding that efalizumab-x is consistent with a previous study showing that upon crosslinking fluorescently labelled efalizumab localizes to the lysosome [44]. Taken together our study points towards fundamental differences between the inhibitor classes regarding their effect on α L β 2 clustering, internalization, and lysosomal degradation.

3.5. Effect of α L β 2 inhibitors on the internalization of engaged TCR/CD3

Based on the results described above we speculated that in activated T cells inhibitor-induced α L β 2 internalization may disturb the downmodulation of engaged TCR/CD3 from the cell surface, a phenomenon thought to play a role in T cell desensitization. It is well established that upon pMHC or mAb OKT3 binding to the TCR/CD3 complex both TCR and CD3 are simultaneously downregulated as a result of increased internalization, decreased recycling and, increased degradation [45]. Moreover, it has been shown that the regulation of TCR/CD3 and α L β 2 recycling pathways are linked in activated T cells [46]. To investigate the hypothesis that

efalizumab-induced α L β 2 internalization may affect TCR/CD3 downmodulation PBMCs were treated for 24 h with α L β 2 inhibitors in presence of mAb OKT3 which provokes TCR/CD3 internalization. We found that in unstimulated cells (in the absence of mAb OKT3) none of the inhibitors or respective controls induced a significant change in cell surface CD3 or TCR expression as assessed by the frequency of CD3+ or TCR+ PBMCs (Fig. 7A and B, left panels). When treated with mAb OKT3 for 24 h, both CD3 and TCR molecules were virtually completely downregulated. α I and α/β I allosteric inhibitors and controls (DMSO, IgG and IgG-x) did not significantly alter the mAb OKT3-induced downmodulation of the TCR/CD3 cell surface molecules (Fig. 7A, right panels) indicating that these classes of inhibitors do not affect the TCR/CD3 internalization process. Intriguingly, however, efalizumab (alone and cross-linked) impacted on the TCR/CD3 internalization process: in presence of efalizumab cell surface TCR was normally downmodulated after mAb OKT3 stimulation whereas on a significant number of PBMCs cell surface CD3 was still detectable by flow cytometry (Fig. 7A and B, right panels). These results suggest that efalizumab partially inhibits mAb OKT3-induced CD3 cell surface internalization while mAb OKT3-induced TCR internalization is not affected. To determine the selectivity of this efalizumab effect on CD3 internalization, we investigated the downmodulation of engaged TCR/CD3 in the presence of natalizumab. Natalizumab is a therapeutic antibody (approved for the treatment of multiple sclerosis) which targets the α 4 subunit of integrin α 4 β 1 and α 4 β 7. Similar to α L β 2, integrin- α 4 has been reported to be internalized *in vitro* and in patients upon engagement by natalizumab [40,47]. In contrast to α L β 2 however, α 4 β 1 is not involved in IS formation. We found that natalizumab did not impair OKT3-induced CD3/TCR complex internalization despite inducing α 4 β 1 internalization (data not shown). To further elucidate the mechanism of efalizumab-induced decoupling of TCR and CD3 internalization, the effect of efalizumab on ZAP70 expression in T cells was quantified. Previous data indicate that ZAP70 plays a regulatory role in the downregulation of engaged TCR/CD3 complex, i.e. in T cells from patients presenting ZAP70 deficiencies CD3 downmodulation was impaired upon engagement with lower concentrations of anti-CD3 mAb [48]. Consistent with this study we found that efalizumab and efalizumab-x partially reduced ZAP70 expression in resting and OKT3-stimulated lymphocytes (Fig. 8). The α/β I allosteric inhibitor XVA143 decreased ZAP70 protein levels by 22% in resting cells while in OKT3-stimulated cells the XVA143 effect on ZAP70 did not reach significance. The α I allosteric inhibitor LFA878 did not affect ZAP70 expression in lymphocytes under resting and activating conditions (Fig. 8).

Table 4 provides a synoptic overview of the effect profiles of α L β 2 inhibitors of different modes of action, as assessed in this study.

4. Discussion

Several inhibitor classes with different modes of actions have been described for the integrin α L β 2. Although these inhibitors have in common that they potently block α L β 2 function *in vitro*, they exert differential effects on the conformation of α L β 2, its expression, and as described here for the first time to the best of our knowledge, on ZAP70 protein levels and the internalization of engaged TCR/CD3 complex.

A striking feature of the α/β I allosteric α L β 2 inhibitor class – which is not shared by α I allosteric inhibitors or efalizumab – is that they induce activation epitopes in the β 2 chain of α L β 2 characteristic for the extended, intermediate affinity form of α L β 2. In our study the degree of activation epitope exposure was even more prominent than observed for the powerful (yet artificial) integrin

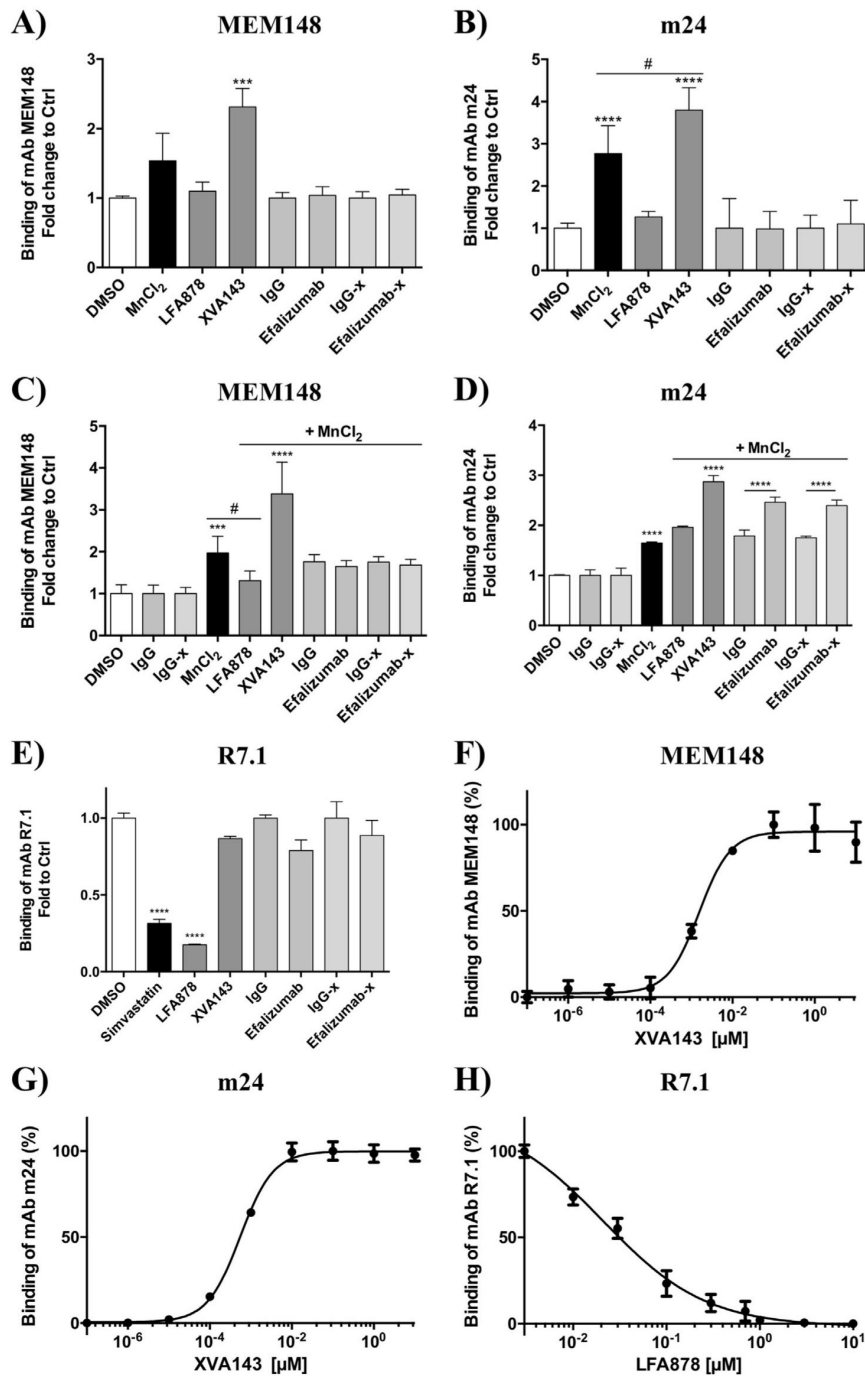


Fig. 4. Effect of α L/ β 2 inhibitors on the conformational status of α L/ β 2 under resting and Mn^{2+} activating conditions. (A) Jurkat cells were exposed to the α L/ β 2 inhibitors LFA878 (10 μ M), XVA143 (10 μ M), efalizumab (10 μ g/ml) or efalizumab-x (10 μ g/ml), the respective controls DMSO (0.1%), IgG (10 μ g/ml), IgG-x (10 μ g/ml) and $MnCl_2$ (2 mM)/DMSO (0.1%) for 40 min. After incubation, the binding of mAb MEM148 (reports α L/ β 2 extension) or (B) mAb m24 (reports β 2 I-like domain activation) was quantified by flow cytometry. Each bar represents the mean values \pm SD of three (A) or four (B) independent experiments with single determinations each. (C) Jurkat cells were exposed to α L/ β 2 inhibitors and controls at concentrations as depicted above for 30 min, then $MnCl_2$ (2 mM) was added as indicated, followed by an incubation of 30 min. The binding of mAb MEM148 and (D) mAb m24 was determined by flow cytometry. Each bar represents the mean value \pm SD of four independent experiments with single determinations each (C) or of triplicates; representative experiment out of two performed (D). (E) Cells were exposed to inhibitors and controls at above indicated concentrations for 40 min. After 40 min the binding of mAb R7.1 (reports α I allosteric inhibitor binding to α L/ β 2) was quantified by flow cytometry. Each bar represents the mean value \pm SD of triplicates. Simvastatin (100 μ M) was included as assay control. (F) MEM148 or (G) m24 epitope exposure was determined by flow cytometry in presence of indicated concentrations of XVA143. Each point represents the mean value \pm SD of three independent experiments with single determinations each. (H) R7.1 epitope loss was quantified by flow cytometry in the presence of indicated concentrations of LFA878. Each point represents the mean value \pm SD of three independent experiments with single determinations each. Fold change to control was calculated as the ratio of the geometric MFI (gMFI) value of the test sample and gMFI value of the respective control. The ratio of controls was set to one. Statistical significance was determined using one-way analysis (ANOVA) (*** $p < 0.001$ and **** $p < 0.0001$ vs DMSO control; # $p < 0.05$ vs second comparison).

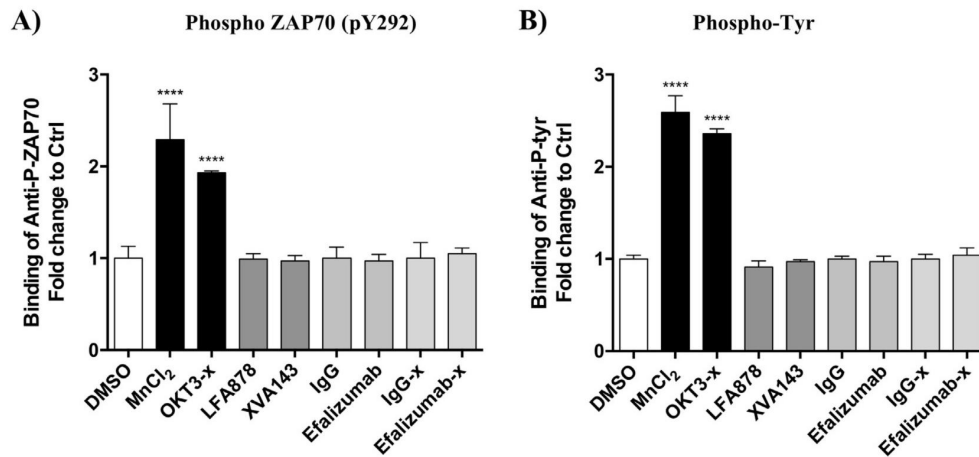


Fig. 5. Effect of α L/ β 2 inhibitors on the phosphorylation state of ZAP70 or protein tyrosine phosphorylation in general. PBMCs were treated with the α L/ β 2 inhibitors LFA878 (10 μ M), XVA143 (10 μ M), efalizumab (10 μ g/ml) or efalizumab-x (10 μ g/ml), respective controls DMSO (0.1%), IgG (10 μ g/ml) and IgG-x (10 μ g/ml) and MnCl₂ (2 mM)/DMSO (0.1%) (Mn²⁺ activates α L/ β 2) or cross-linked anti-CD3 mAb OKT3 (OKT3-x; 5 μ g/ml) (activates the TCR signalling pathway) were pre-incubated on ice and then activated for 1 min at 37 °C. The binding of (A) anti-ZAP70 pY292 (J34-602) mAb and (B) anti-pTyr (PY20) mAb was quantified in CD2+ lymphocytes by flow cytometry. Each bar represents the mean value \pm SD of three independent experiments (different donors, single determinations each). Statistical significance was determined using one-way analysis (ANOVA) (****p < 0.0001 vs DMSO).

activating cation Mn²⁺. Despite this activating effect on the β 2 chain, however, the α / β I allosteric inhibitor investigated did not directly induce outside-in signalling in T cells as assessed by protein tyrosine phosphorylation. On the other hand, the inhibitor-induced extended, intermediate affinity conformation of α L β 2 was found to be associated with mildly reduced α L β 2 surface expression in CD4+ but not CD8+ T cells. A similar partial downregulation of α L β 2 in presence of XVA143 has been recently observed in activated whole blood cultures [34]. However, in this study the effect of XVA143 on T cell subpopulations was not assessed. These results together indicate that the extended semi-active α L β 2 conformation stabilized by XVA143 is able to promote an altered internalization/recycling behaviour of α L β 2. This assumption is supported by a previous study showing that an extended form of α L β 2 of lower affinity is preferentially internalized in T cells [49]. Our findings further indicate for the first time that the degree of α L β 2 internalization/recycling induced by XVA143 is dependent on the cell-type. Interestingly, such differential effect on α L β 2 downmodulation among different cell types has been also noted for efalizumab in the present study (CD4+ versus CD8+ T cells) and by others [42]. Further investigations will be needed to better characterize the biologic implications of this differential downmodulation of α L β 2. Beyond the agonist-like effects described above α / β I allosteric inhibitors are known to induce a phenomenon called ‘rolling adhesion’ by stabilizing the semi-active conformation of α L β 2. Rolling adhesion of leucocytes on vascular surfaces is a first step in recruiting leucocytes to sites of inflammation. Of biologic relevance, α / β I allosteric inhibitors do not only induce rolling adhesion but also support the transition from already pre-existing rolling adhesion to firm adhesion [37,38]. This property was not observed for α I allosteric inhibitors. In consequence one may hypothesize that α I allosteric inhibitors will deliver a stronger anti-adhesive blockade under flow conditions than α / β I allosteric inhibitors.

The most striking effect of the anti- α L β 2 mAb efalizumab is the unscheduled internalization of surface α L β 2 and its subsequent lysosomal translocation in leucocytes [43,44,50]. This effect is not unique to the anti- α L β 2 mAb efalizumab. It has also been noted that binding of the anti-human α L β 2 mAb TS1/22 and the anti-mouse α L β 2 mAb M17 leads to α L β 2 internalization [34,44,51].

These anti- α L β 2 mAb antibodies have in common that they bind close to (anti-human α L β 2 efalizumab, TS1/22) or within the ligand binding site of α L β 2 (anti-mouse α L β 2 mAb M17) [51,52]. Interestingly, our data indicate that efalizumab provoked α L β 2 internalization in resting T cells while at the same time it did not induce an extended conformation of α L β 2 as observed for XVA143. Efalizumab-induced α L β 2 internalization may be caused, therefore, by a different mechanism than the partial internalization mediated by α / β allosteric α L β 2 inhibitors. One may hypothesize that efalizumab induces α L β 2 clustering by its in-built bivalency which in consequence leads to unscheduled internalization of α L β 2 and lysosomal translocation. This hypothesis is supported by our finding that crosslinking of efalizumab via an anti-human IgG antibody amplifies α L β 2 internalization. Moreover, we found that efalizumab affected the downmodulation of engaged TCR/CD3. While the TCR was normally internalized, the downregulation of CD3 was markedly reduced in presence of efalizumab. A similar dissection of TCR/CD3 complex expression has been observed in psoriasis patients treated with efalizumab. In these patients efalizumab treatment was associated with a downmodulation of the TCR to about 64–82% of baseline value in peripheral blood whereas the levels of CD3 were not affected [41,43]. Our research into the mechanism of this phenomenon revealed that efalizumab-induced internalization of α L β 2 was associated with reduced ZAP70 levels. Given that ZAP70 is constitutively associated with α L β 2 [35], the reduced levels of ZAP70 may be explained by enhanced concomitant transport to the lysosome and potential degradation. ZAP70 is also known to regulate engaged TCR/CD3 downmodulation [48]. Thus, it may be possible that enhanced α L β 2 internalization induced by efalizumab impacts the downmodulation of engaged TCR/CD3 via ZAP70 protein levels. Moreover, it is tempting to speculate that α L β 2 internalization leading to reduced ZAP70 levels and disturbed expression of engaged TCR/CD3 may contribute to or may even constitute the basis of the unique state of T cell hyporesponsiveness observed in efalizumab treated patients [43,53,54]. In contrast, de-coupling of TCR and CD3 internalization upon engagement was not detectable in presence of XVA143 although this α / β I allosteric inhibitor slightly reduced α L β 2 surface expression in CD4+ T cells and ZAP70 protein levels in lymphocytes. However, compared to efal-

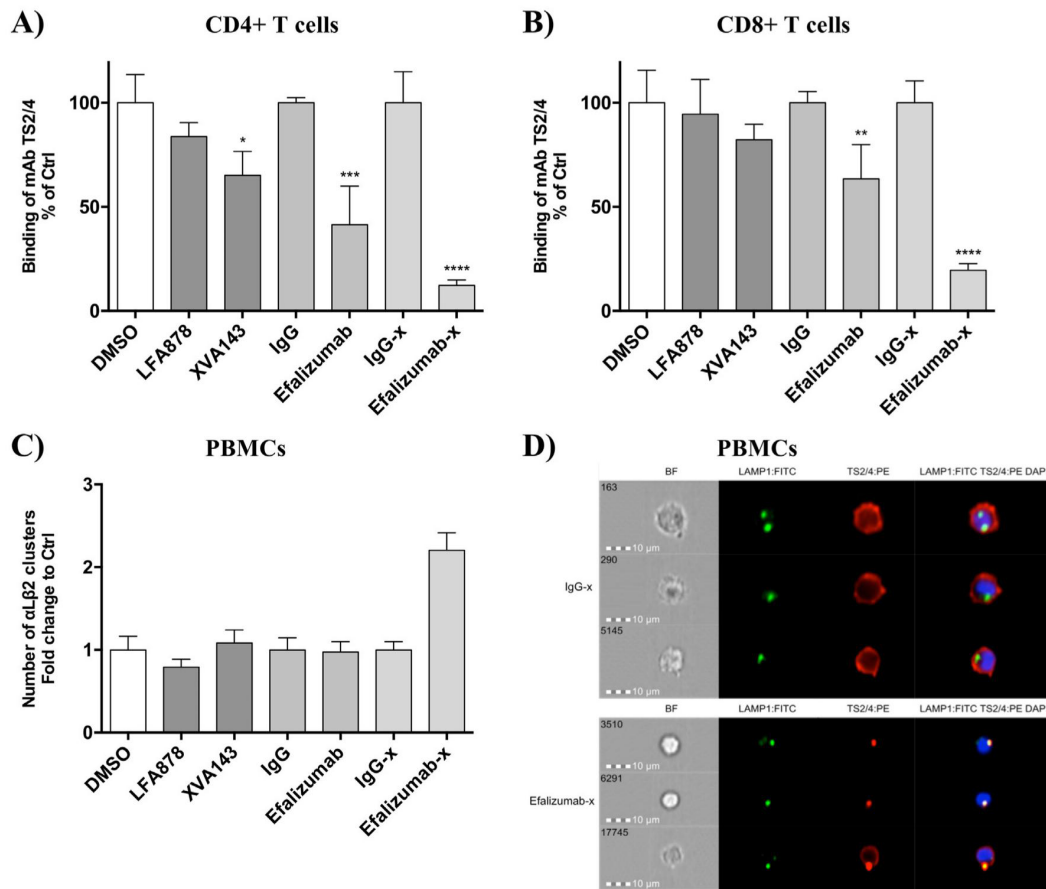


Fig. 6. Effect of α L/ β 2 inhibitors on the localization of α L/ β 2. PBMCs were treated with the α L/ β 2 inhibitors LFA878 (10 μ M), XVA143 (10 μ M), efalizumab (10 μ g/ml) or efalizumab-x (10 μ g/ml) and the respective controls DMSO (0.1%), IgG (10 μ g/ml) and IgG-x (10 μ g/ml) for 24 h. After 24 h α L/ β 2 surface expression on (A) CD4+ and (B) CD8+ T cells was determined by the binding of fluorescently labelled mAb TS2/4 using flow cytometry. Each bar represents the mean value \pm SD of three independent experiments (different donors, single determinations each). Statistical significance was determined using one-way analysis (ANOVA) (* $p < 0.05$, ** $p < 0.01$, *** $p < 0.001$ and **** $p < 0.0001$ vs respective controls). (C) α L/ β 2 clusters (granular stainings) were quantified in inhibitor-treated PBMCs by flow-based imaging and image analysis. Clusters were defined by pixel area size (4–16) plus shape (circularity 0.4–1) and were counted as single events. Each bar represents the mean value \pm SEM of 1000 images analysed. A representative experiment out of two independent experiments is shown. (D) Localization of α L/ β 2 in presence of efalizumab-x or IgG-x was visualized using flow-based imaging. α L/ β 2 was labelled with mAb TS2/4-PE (red), lysosomes with anti-LAMP-1 mAb H4A3-FITC (green) and the nucleus with DAPI (blue). Co-location of α L/ β 2 and LAMP-1 staining is indicated in yellow. Individual cells are displayed by multispectral imaging of brightfield (BF). Representative images are shown. (For interpretation of the references to colour in this figure legend, the reader is referred to the web version of this article.)

izumab these latter effects of XVA143 were moderate and may have been too weak to affect the downmodulation of engaged TCR/CD3. As expected from its mode of action, the α I allosteric α L/ β 2 inhibitor LFA878 did neither internalize α L/ β 2 nor reduce ZAP70 protein levels and, in consequence, allowed for the simultaneous internalization of engaged TCR/CD3. Taken together these results indicate that α L/ β 2 inhibitors – dependent on their mode of action – differentially modulate the internalization of engaged TCR/CD3. Moreover, they support the hypothesis that the observed dissection of TCR/CD3 internalization in OKT3-activated lymphocytes treated with efalizumab is not due to α L/ β 2 inhibition *per se* but due to clustering, internalization and degradation of α L/ β 2 induced by an antibody-based pharmacology. Further our results are in agreement with other studies showing that integrin trafficking pathways can indirectly impact intracellular signalling of other surface receptors and that this needs to be taken into account when developing integrin inhibitors [55,56].

The dissection of the different mechanisms of α L/ β 2 inhibition by their downstream effect profiles, as established by this study, will be of high relevance for future therapeutic translation of these

modes of action. In this context it is intriguing to note that the α L/ β 2 inhibitory mechanism of action which is devoid of unwanted downstream effects, i.e. of paradoxical partial activation of α L/ β 2, of unwanted α L/ β 2 internalization effects as well as of downstream consequences thereof, remains the only mechanism of action not advanced to clinical proof-of-concept, to date. Not suspected initially, the heavy reliance of preclinical research on murine disease models of autoimmunity may have contributed to this lag in translation. While α I allosteric inhibition has been shown to be highly effective in certain murine experimental disease models [26,57,58], mice (for their limited cross-species reactivity) may not be the best suited species to explore the full therapeutic potential. A second reason for the limited progress made with α I allosteric inhibitors in the past, compared to the other pharmacological mechanisms assessed in this study, may be their strict selectivity for α L/ β 2, by itself. The α I allosteric mechanism of action is neither expected to affect β 2 integrins other than α L/ β 2, in contrast to what has been observed with α/β I allosteric inhibitors [16,17], nor to affect the expression of other major immune receptors as observed with the antibody approach [41,43]. Indeed, a strictly α L/ β 2 selec-

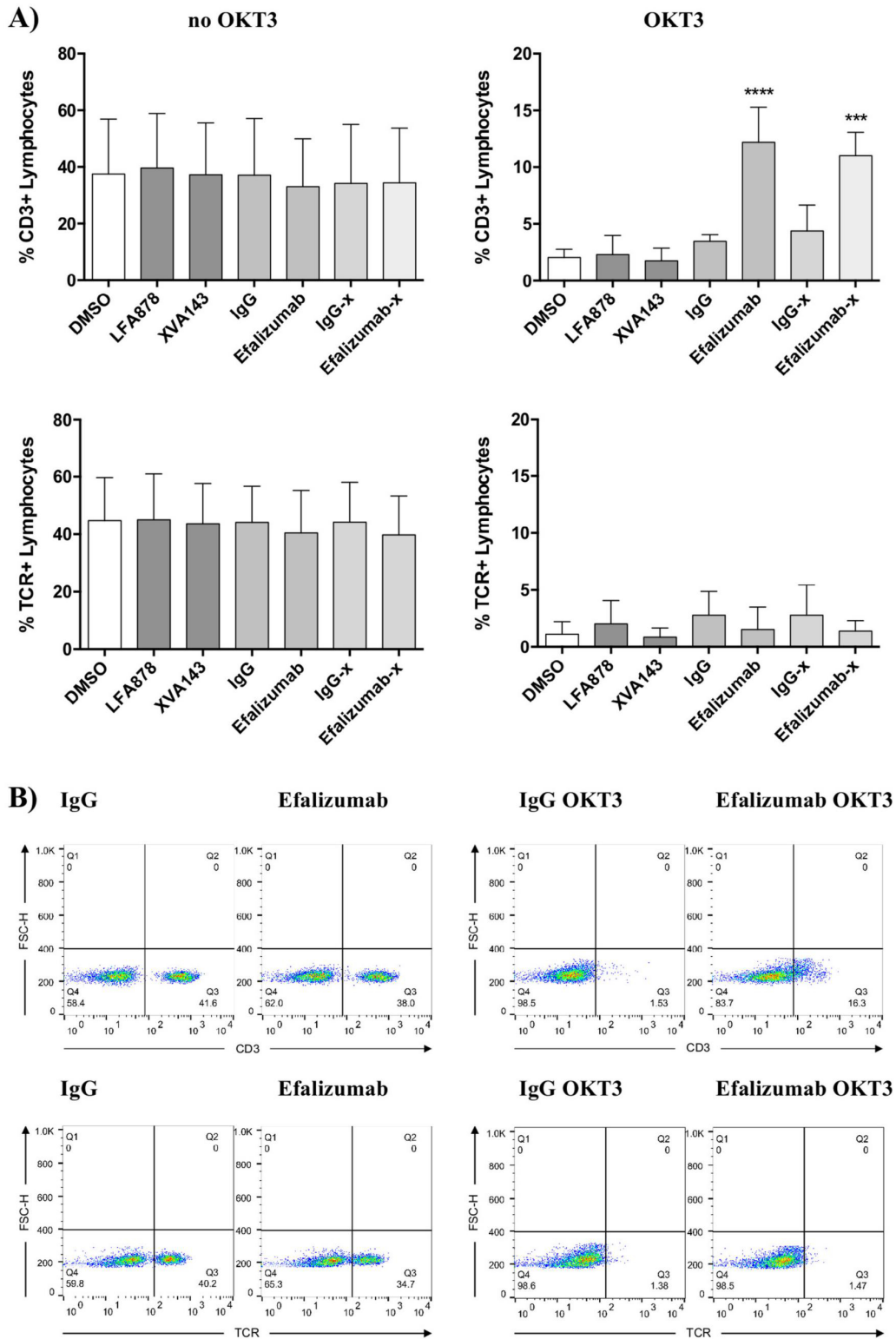


Fig. 7. Effect of α L/ β 2 inhibitors on the internalization of engaged TCR/CD3. (A) PBMCs were incubated with the α L/ β 2 inhibitors LFA878 (10 μ M), XVA143 (10 μ M), efalizumab (10 μ g/ml) or efalizumab-x (10 μ g/ml) and the respective controls DMSO (0.1%), IgG (10 μ g/ml) and IgG-x (10 μ g/ml) with or without mAb OKT3 (50 ng/ml) for 24 h. The binding of fluorescently labelled anti-CD3 mAb UCHT1 or anti-TCR α / β mAb IP26 to lymphocytes was quantified by flow cytometry. Each bar represents the mean value \pm SD of four (CD3) or three (TCR) independent experiments (different donors, single determinations each). Statistical significance was determined using one-way analysis (ANOVA) (*** $p < 0.001$ and **** $p < 0.0001$ vs respective controls). (B) Representative flow cytometry dot plots are shown for efalizumab and IgG control in presence and absence of OKT3. Values in the lower right quadrant represent % of CD3+ cells or % of TCR+ events.

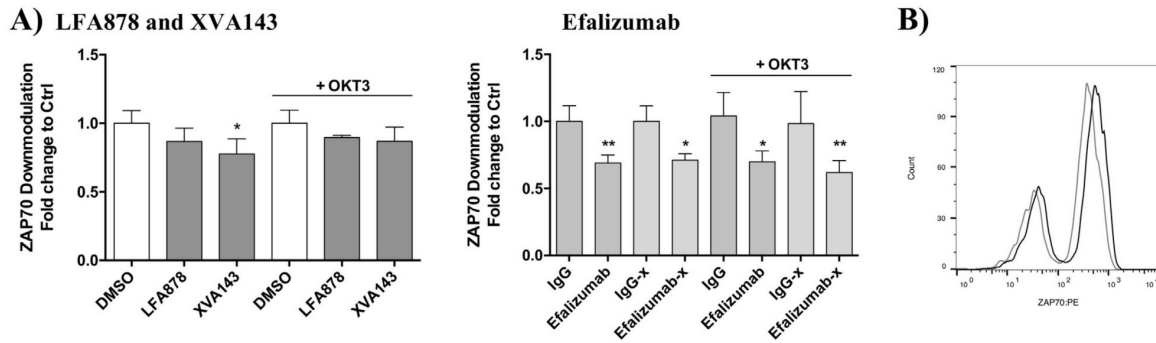


Fig. 8. Effect of α L/ β 2 inhibitors LFA878, XVA143 and efalizumab on ZAP70 expression. (A) PBMCs were treated with the α L/ β 2 inhibitors LFA878 (10 μ M), XVA143 (10 μ M), efalizumab (10 μ g/ml) or efalizumab-x (10 μ g/ml) and the respective controls DMSO (0.1%), IgG (10 μ g/ml) and IgG-x (10 μ g/ml) in presence or absence of mAb OKT3 (50 ng/ml) for 24 h. After 24 h the binding of mAb 1E7.2 to ZAP70 was quantified in lymphocytes by flow cytometry. Each bar represents the mean value \pm SD of three (LFA878, XVA143) or four (Efalizumab) independent experiments (different donors, single determinations each). Statistical significance was determined using one-way analysis (ANOVA) (* $p < 0.05$, ** $p < 0.01$ vs control) (B) Representative histogram illustrating a reduction of ZAP70 expression in presence of efalizumab (grey line) as compared to IgG control (black line).

Table 4

Overview of *in vitro* effect profiles of α L/ β 2 inhibitors with different modes of action.

α L/ β 2 inhibitor	LFA878	XVA143	Efalizumab
Mode of action	α 1 allosteric	α / β 1 allosteric	Competitive
Selectivity of mode of action	α L/ β 2	β 2 integrins	α L/ β 2
Inhibition of α L/ β 2 adhesion	+	+	+
Induction of α L/ β 2 activation epitopes	-	+	-
ZAP70 phosphorylation	-	-	-
α L/ β 2 internalization	-	(+)	+
Disturbance of engaged TCR/CD3 downmodulation	-	-	+
Reduction of ZAP70 protein levels	-	(+)	+

+: effect, -: no effect (+): weak effect.

tive pharmacology may not be best-suited to support conventional therapeutic concepts of suppressive immune modulation. Innovative therapeutic concepts, educated and guided by the exceptionally well-characterized biologic functions of α L/ β 2, may be required to realize the therapeutic potential of an exclusively α L/ β 2 selective pharmacology, eventually.

Conflict of interest

The authors declare that they have no conflict of interest.

Acknowledgements

The authors thank Dr. Berndt Oberhauser, Novartis Pharma AG Basel, for providing compound LFA878, Dr. Paul Gillespie, Hoffmann-La Roche Inc. Nutley, for supplying compound RO0281607-000 (also termed XVA143) and Prof. Dr. Raija Lindberg Gasser, University Hospital Basel for providing natalizumab. The authors are grateful to Dr. Albrecht-Georg Schmidt, AlloCyte Pharmaceuticals AG, Basel, for helpful discussions and critical reading of the manuscript. This research was supported by the Swiss Commission of Technology and Innovation grant 15265.1 PFLS-LS.

References

- [1] B.H.1. Luo, C.V. Carman, T.A. Springer, Structural basis of integrin regulation and signalling, *Annu. Rev. Immunol.* 25 (2007) 619–647.
- [2] N. Hogg, I. Patzak, F. Willenbrock, The insider's guide to leukocyte integrin signalling and function, *Nat. Rev. Immunol.* 11 (6) (2011) 416–426.
- [3] D. Cox, M. Brennan, N. Moran, Integrins as therapeutic targets: lessons and opportunities, *Nat. Rev. Drug Discovery* 9 (10) (2010) 804–820.
- [4] K. Ley, J. Rivera-Nieves, W.J. Sandborn, S.N. Shattil, Integrin-based therapeutics: biological basis, clinical use and new drugs, *Rev. Drug Discovery* 15 (3) (2016) 173–183.
- [5] I. Ahrens, K. Peter, Therapeutic integrin inhibition: allosteric and activation-specific inhibition strategies may surpass the initial ligand-mimetic strategies, *Thromb. Haemost.* 99 (5) (2008) 803–804.
- [6] P.C. Armstrong, K. Peter, GPIIb/IIIa inhibitors: from bench to bedside and back to bench again, *Thromb. Haemost.* 107 (5) (2012) 808–814.
- [7] P.A. Giblin, R.M. Lemieux, LFA-1 as a key regulator of immune function: approaches toward the development of LFA-1-based therapeutics, *Curr. Pharm. Des.* 12 (22) (2006) 2771–2795.
- [8] M.R. Nicolls, R.G. Gill, LFA-1 (CD11a) as a therapeutic target, *Am. J. Transplant.* 6 (1) (2006) 27–36.
- [9] M.L. Dustin, The cellular context of T cell signalling, *Immunity* 30 (4) (2009) 482–492.
- [10] N.K. Verma, E. Dempsey, A. Long, A. Davies, S.P. Barry, P.G. Fallon, Y. Volkov, D. Kelleher, Leukocyte function-associated antigen-1/intercellular adhesion molecule-1 interaction induces a novel genetic signature resulting in T-cells refractory to transforming growth factor- β signalling, *J. Biol. Chem.* 287 (32) (2012) 27204–27216.
- [11] E. Zenaro, E. Pietronigro, V. Della Bianca, G. Piacentino, L. Marongiu, S. Budui, E. Turano, B. Rossi, S. Angiari, S. Dusi, A. Montresor, T. Carlucci, S. Nani, G. Tosadori, L. Calciano, D. Catalucci, G. Berton, B. Bonetti, G. Constantin, Neutrophils promote Alzheimer's disease-like pathology and cognitive decline via LFA-1 integrin, *Nat. Med.* 21 (8) (2015) 880–886.
- [12] S. Li, H. Wang, B. Peng, M. Zhang, D. Zhang, S. Hou, Y. Guo, J. Ding, Efalizumab binding to the LFA-1 α 1L domain blocks ICAM-1 binding via steric hindrance, *Proc. Natl. Acad. Sci. U.S.A.* 106 (11) (2009) 4349–4354.
- [13] N.M. Seminar, J.M. Gelfand, Assessing long-term drug safety: lessons (re) learned from raptiva, *Semin. Cutan. Med. Surg.* 29 (2010) 16–19.
- [14] G. Weitz-Schmidt, K. Welzenbach, V. Brinkmann, T. Kamata, J. Kallen, C. Bruns, S. Cottens, Y. Takada, U. Hommel, Statins selectively inhibit leukocyte function antigen-1 by binding to a novel regulatory integrin site, *Nat. Med.* 7 (6) (2001) 687–692.
- [15] T.R. Gadek, D.J. Burdick, R.S. McDowell, M.S. Stanley, J.C. Marsters Jr., K.J. Paris, D.A. Oare, M.E. Reynolds, C. Ladner, K.A. Zioncheck, W.P. Lee, P. Gribbling, M.S. Dennis, N.J. Skelton, D.B. Tumas, K.R. Clark, S.M. Keating, M.H. Beresini, J.W. Tilley, L.G. Presta, S.C. Bodary, Generation of an LFA-1 antagonist by the transfer of the ICAM-1 immunoregulatory epitope to a small molecule, *Science* 295 (5557) (2002) 1086–1089.
- [16] M. Shimaoka, A. Salas, W. Yang, G. Weitz-Schmidt, T.A. Springer, Small molecule integrin antagonists that bind to the beta2 subunit I-like domain and activate signals in one direction and block them in the other, *Immunity* 19 (3) (2003) 391–402.

- [17] K. Welzenbach, U. Hommel, G. Weitz-Schmidt, Small molecule inhibitors induce conformational changes in the I domain and the I-like domain of lymphocyte function-associated antigen-1. Molecular insights into integrin inhibition, *J. Biol. Chem.* 277 (12) (2002) 10590–10598.
- [18] M. Shimaoka, T.A. Springer, Therapeutic antagonists and conformational regulation of integrin function, *Nat. Rev. Drug Discovery* 2 (9) (2003) 703–716.
- [19] J.D. Sheppard, G.L. Torkildsen, J.D. Lonsdale, F.A. D'Ambrosio Jr., E.B. McLaurin, R.A. Eiferman, K.S. Kennedy, C.P. SembaOPUS-1 Study Group, Lifitegrast ophthalmic solution 5.0% for treatment of dry eye disease: results of the OPUS-1 phase 3 study, *Ophthalmology* 121 (2) (2014) 475–483.
- [20] J. Tauber, P. Karpecki, R. Latkany, J. Luchs, J. Martel, K. Sall, A. Raychaudhuri, V. Smith, C.P. SembaOPUS-2 Investigators, Lifitegrast ophthalmic solution 5.0% versus placebo for treatment of dry eye disease: results of the randomized phase III OPUS-2 study, *Ophthalmology* 122 (12) (2015) 2423–2431.
- [21] M. Weetall, R. Hugo, C. Friedman, S. Maida, S. West, S. Wattanasin, R. Bouhel, G. Weitz-Schmidt, P. Lake, A homogeneous fluorometric assay for measuring cell adhesion to immobilized ligand using V-well microtiter plates, *Anal. Biochem.* 293 (2) (2001) 277–287.
- [22] G. Weitz-Schmidt, S. Chreng, Cell adhesion assays, *Methods Mol. Biol.* 757 (2012) 15–30.
- [23] G. Weitz-Schmidt, K. Welzenbach, J. Dawson, J. Kallen, Improved lymphocyte function-associated antigen-1 (LFA-1) inhibition by statin derivatives: molecular basis determined by X-ray analysis and monitoring of LFA-1 conformational changes in vitro and ex vivo, *J. Biol. Chem.* 279 (45) (2004) 46764–46771. Epub 2004 Aug 10.
- [24] M. Lebwohl, S.K. Tyring, T.K. Hamilton, D. Toth, S. Glazer, N.H. Tawfik, P. Walicke, W. Dummer, X. Wang, M.R. Garovoy, D. PariserEfalizumab Study Group, A novel targeted T-cell modulator, efalizumab, for plaque psoriasis, *N. Engl. J. Med.* 349 (21) (2003) 2004–2013.
- [25] R.J. Winqvist, S. Desai, S. Fogal, N.A. Haynes, G.H. Nabozny, P.L. Reilly, D. Souza, M. Panzenbeck, The role of leukocyte function-associated antigen-1 in animal models of inflammation, *Eur. J. Pharmacol.* 429 (1–3) (2001) 297–302.
- [26] D. Potin, M. Launay, F. Monatlik, P. Malabre, M. Fabreguettes, A. Fouquet, M. Maillat, E. Nicolai, L. Dorgeret, F. Chevallier, D. Besse, M. Dufort, F. Caussade, S. Z. Ahmad, D.K. Stetsko, S. Skala, P.M. Davis, P. Balimane, K. Patel, Z. Yang, P. Marathe, J. Postelneck, R.M. Townsend, V. Goldfarb, S. Sheriff, H. Einspahr, K. Kish, M.F. Malley, J.D. DiMarco, J.Z. Gougoutas, P. Kadiyala, D.L. Cheney, R.W. Tejwani, D.K. Murphy, K.W. McIntyre, X. Yang, S. Chao, L. Leith, Z. Xiao, A. Mathur, B.C. Chen, D.R. Wu, S.C. Traeger, M. McKinnon, J.C. Barrish, J.A. Robl, E. J. Iwanowicz, S.J. Suchard, T.G. Dhar, Discovery and development of 5-[(5S,9R)-9-(4-cyanophenyl)-3-(3,5-dichlorophenyl)-1-methyl-2,4-dioxo-1,3,7-triazaspiro[4.4]non-7-yl-methyl]-3-thiophenecarboxylic acid (BMS-587101) – a small molecule antagonist of leukocyte function associated antigen-1, *J. Med. Chem.* 49 (24) (2006) 6946–6949.
- [27] P.G. Vanden Bergh, T. Fett, L.L. Zecchinon, A.V. Thomas, D.J. Desmecht, The CD11a partner in *Sus scrofa* lymphocyte function-associated antigen-1 (LFA-1): mRNA cloning, structure analysis and comparison with mammalian homologues, *BMC Vet. Res.* 1 (2005) 5.
- [28] M. Champe, B.W. McIntyre, P.W. Berman, Monoclonal antibodies that block the activity of leukocyte function-associated antigen 1 recognize three discrete epitopes in the inserted domain of CD11a, *J. Biol. Chem.* 270 (3) (1995) 1388–1394.
- [29] A. Felser, K. Blum, P.W. Lindinger, J. Bouitbir, S. Krähenbühl, Mechanisms of hepatocellular toxicity associated with dronedarone—a comparison to amiodarone, *Toxicol. Sci.* 131 (2) (2013) 480–490.
- [30] R.H. Tang, E. Tng, S.K. Law, S.M. Tan, Epitope mapping of monoclonal antibody to integrin alphaL beta2 hybrid domain suggests different requirements of affinity states for intercellular adhesion molecules (ICAM)-1 and ICAM-3 binding, *J. Biol. Chem.* 280 (32) (2005) 29208–29216.
- [31] X. Chen, C. Xie, N. Nishida, Z. Li, T. Walz, T.A. Springer, Requirement of open headpiece conformation for activation of leukocyte integrin alphaXbeta2, *Proc. Natl. Acad. Sci. U.S.A.* 107 (33) (2010) 14727–14732.
- [32] G. Weitz-Schmidt, T. Schürpf, T.A. Springer, The C-terminal α I domain linker as a critical structural element in the conformational activation of α I integrins, *J. Biol. Chem.* 286 (49) (2011) 42115–42122.
- [33] M. Sen, K. Yuki, T.A. Springer, An internal ligand-bound, metastable state of a leukocyte integrin, α X β 2, *J. Cell Biol.* 203 (4) (2013) 629–642.
- [34] K. Welzenbach, R.V. Mancuso, S. Krähenbühl, G. Weitz-Schmidt, A novel multi-parameter assay to dissect the pharmacological effects of different modes of integrin α L β 2 inhibition in whole blood, *Br. J. Pharmacol.* 172 (20) (2015) 4875–4887.
- [35] R. Evans, A.C. Lellouch, L. Svensson, A. McDowall, N. Hogg, The integrin LFA-1 signals through ZAP-70 to regulate expression of high-affinity LFA-1 on T lymphocytes, *Blood* 117 (12) (2011) 3331–3342.
- [36] J.C. Houtman, R.A. Houghtling, M. Barda-Saad, Y. Toda, L.E. Samelson, Early phosphorylation kinetics of proteins involved in proximal TCR-mediated signalling pathways, *J. Immunol.* 175 (4) (2005) 2449–2458.
- [37] A. Salas, M. Shimaoka, A.N. Kogan, C. Harwood, U.H. von Andrian, T.A. Springer, Rolling adhesion through an extended conformation of integrin alphaBeta2 and relation to alpha I and beta I-like domain interaction, *Immunity* 20 (4) (2004) 393–406.
- [38] A. Salas, M. Shimaoka, U. Phan, M. Kim, T.A. Springer, Transition from rolling to firm adhesion can be mimicked by extension of integrin alphaBeta2 in an intermediate affinity state, *J. Biol. Chem.* 281 (16) (2006) 10876–10882.
- [39] R.D. Soede, M.H. Driessens, L. Ruuls-Van Stalle, P.E. Van Hulsten, A. Brink, E. Roos, LFA-1 to LFA-1 signals involve zeta-associated protein-70 (ZAP-70) tyrosine kinase: relevance for invasion and migration of a T cell hybridoma, *J. Immunol.* 163 (8) (1999) 4253–4261.
- [40] T.F. Benkert, L. Dietz, E.M. Hartmann, E. Leich, A. Rosenwald, E. Serfling, M. Buttman, F. Berberich-Siebelt, Natalizumab exerts direct signalling capacity and supports a pro-inflammatory phenotype in some patients with multiple sclerosis, *PLoS ONE* 7 (12) (2012) e52208.
- [41] Y. Vugmeyster, T. Kikuchi, M.A. Lowes, F. Chamian, M. Kagen, P. Gilleaudeau, E. Lee, K. Howell, S. Bodary, W. Dummer, J.G. Krueger, Efalizumab (anti-CD11a)-induced increase in peripheral blood leukocytes in psoriasis patients is preferentially mediated by altered trafficking of memory CD8+ T cells into lesional skin, *Clin. Immunol.* 113 (1) (2004) 38–46.
- [42] D.L. Mortensen, P.A. Walicke, X. Wang, P. Kwon, P. Kuebler, A.B. Gottlieb, J.G. Krueger, C. Leonardi, B. Miller, A. Joshi, Pharmacokinetics and pharmacodynamics of multiple weekly subcutaneous efalizumab doses in patients with plaque psoriasis, *J. Clin. Pharmacol.* 45 (3) (2005) 286–298.
- [43] E. Guttman-Yassky, Y. Vugmeyster, M.A. Lowes, F. Chamian, T. Kikuchi, M. Kagen, P. Gilleaudeau, E. Lee, B. Hunte, K. Howell, W. Dummer, S.C. Bodary, J.G. Krueger, Blockade of CD11a by efalizumab in psoriasis patients induces a unique state of T-cell hyporesponsiveness, *J. Invest. Dermatol.* 128 (5) (2008) 1182–1191.
- [44] G.P. Coffey, E. Stefanich, S. Palmieri, R. Eckert, J. Padilla-Eagar, P.J. Fielder, S. Pippig, In vitro internalization, intracellular transport, and clearance of an anti-CD11a antibody (Raptiva) by human T-cells, *J. Pharmacol. Exp. Ther.* 310 (3) (2004) 896–904.
- [45] N. Martínez-Martín, E. Fernández-Arenas, S. Cemerski, P. Delgado, M. Turner, J. Heuser, D.J. Irvine, B. Huang, X.R. Bustelo, A. Shaw, B. Alarcón, T cell receptor internalization from the immunological synapse is mediated by TC21 and Rho GTPase-dependent phagocytosis, *Immunity* 35 (2) (2011) 208–222.
- [46] D.G. Osborne, J.T. Piotrowski, C.J. Dick, J.S. Zhang, D.D. Billadeau, SNX17 affects T cell activation by regulating TCR and integrin recycling, *J. Immunol.* 194 (9) (2015) 4555–4566.
- [47] A. Harrer, P. Wipfler, M. Einhaeupl, G. Pilz, K. Oppermann, W. Hitzl, S. Afazel, E. Haschke-Becher, P. Strasser, E. Trinkka, J. Kraus, Natalizumab therapy decreases surface expression of both VLA-heterodimer subunits on peripheral blood mononuclear cells, *J. Neuroimmunol.* 234 (1–2) (2011) 148–154.
- [48] C.I. Dumont, N. Blanchard, V. Di Bartolo, N. Lezot, E. Dufour, S. Jauliac, C. HIVroz, TCR/CD3 downmodulation and zeta degradation are regulated by ZAP-70, *J. Immunol.* 169 (4) (2002) 1705–1712.
- [49] P. Stanley, S. Tooze, N. Hogg, A role for Rap2 in recycling the extended conformation of LFA-1 during T cell migration, *Biol. Open* 1 (11) (2012) 1161–1168.
- [50] A.B. Gottlieb, J.G. Krueger, K. Wittkowski, R. Dedrick, P.A. Walicke, M. Garovoy, Psoriasis as a model for T-cell-mediated disease: immunobiologic and clinical effects of treatment with multiple doses of efalizumab, an anti-CD11a antibody, *Arch. Dermatol.* 138 (5) (2002) 591–600.
- [51] J. Clarke, W. Leach, S. Pippig, A. Joshi, B. Wu, R. House, J. Beyer, Evaluation of a surrogate antibody for preclinical safety testing of an anti-CD11a monoclonal antibody, *Regul. Toxicol. Pharmacol.* 40 (3) (2004) 219–226.
- [52] C. Lu, M. Shimaoka, A. Salas, T.A. Springer, The binding sites for competitive antagonistic, allosteric antagonistic, and agonistic antibodies to the I domain of integrin LFA-1, *J. Immunol.* 173 (6) (2004) 3972–3978.
- [53] F. Koszik, G. Stary, N. Selenko-Gebauer, G. Stingl, Efalizumab modulates T cell function both in vivo and in vitro, *J. Dermatol. Sci.* 60 (3) (2010) 159–166.
- [54] W.M. Kuschei, J. Leitner, O. Majdic, W.F. Pickl, G.J. Zlabinger, K. Grabmeier-Pfistershammer, P. Steinberger, Costimulatory signals potentially modulate the T cell inhibitory capacity of the therapeutic CD11a antibody Efalizumab, *Clin. Immunol.* 139 (2) (2011) 199–207.
- [55] A.R. Reynolds, I.R. Hart, A.R. Watson, J.C. Welti, R.G. Silva, S.D. Robinson, G. Da Violante, M. Gourlaouen, M. Salih, M.C. Jones, D.T. Jones, G. Saunders, V. Kostourou, F. Perron-Sierra, J.C. Norman, G.C. Tucker, K.M. Hodivala-Dilke, Stimulation of tumor growth and angiogenesis by low concentrations of RGD-mimetic integrin inhibitors, *Nat. Med.* 15 (4) (2009) 392–400.
- [56] R.E. Bridgewater, J.C. Norman, P.T. Caswell, Integrin trafficking at a glance, *J. Cell Sci.* 125 (Pt 16) (2012) 3695–3701.
- [57] M.X. Wan, R. Schramm, D. Klintman, K. Welzenbach, G. Weitz-Schmidt, H. Thorlacius, A statin-based inhibitor of lymphocyte function antigen-1 protects against ischemia/reperfusion-induced leukocyte adhesion in the colon, *Br. J. Pharmacol.* 140 (2) (2003) 395–401.
- [58] S.J. Suchard, D.K. Stetsko, P.M. Davis, S. Skala, D. Potin, M. Launay, T.G. Dhar, J.C. Barrish, V. Susulic, D.J. Shuster, K.W. McIntyre, M. McKinnon, L. Salter-Cid, An LFA-1 (alphaBeta2) small-molecule antagonist reduces inflammation and joint destruction in murine models of arthritis, *J. Immunol.* 184 (7) (2010) 3917–3926.

Paper 3

RESEARCH PAPER

A novel multi-parameter assay to dissect the pharmacological effects of different modes of integrin α L β 2 inhibition in whole blood

Karl Welzenbach¹, Riccardo V Mancuso², Stephan Krähenbühl² and Gabriele Weitz-Schmidt^{1,3*}

¹Novartis Pharma AG, Novartis Institutes of Biomedical Research, Basel, Switzerland ²Division of Clinical Pharmacology and Toxicology, University Hospital, Basel, Switzerland

Correspondence

Dr Gabriele Weitz-Schmidt, AlloCyte Pharmaceuticals AG, Hochbergerstrasse 60C, CH-4057 Basel, Switzerland.
E-mail: gabriele.weitz@alloyte-pharma.com
* AlloCyte Pharmaceuticals AG, Basel, Switzerland

Received

12 February 2015

Revised

13 June 2015

Accepted

11 July 2015

BACKGROUND AND PURPOSE

The integrin α L β 2 plays central roles in leukocyte adhesion and T cell activation, rendering α L β 2 an attractive therapeutic target. Compounds with different modes of α L β 2 inhibition are in development, currently. Consequently, there is a foreseeable need for bedside assays, which allow assessment of the different effects of diverse types of α L β 2 inhibitors in the peripheral blood of treated patients.

EXPERIMENTAL APPROACH

Here, we describe a flow cytometry-based technology that simultaneously quantitates α L β 2 conformational change upon inhibitor binding, α L β 2 expression and T cell activation at the single-cell level in human blood. Two classes of allosteric low MW inhibitors, designated α I and α/β I allosteric α L β 2 inhibitors, were investigated. The first application revealed intriguing inhibitor class-specific profiles.

KEY RESULTS

Half-maximal inhibition of T cell activation was associated with 80% epitope loss induced by α I allosteric inhibitors and with 40% epitope gain induced by α/β I allosteric inhibitors. This differential establishes that inhibitor-induced α L β 2 epitope changes do not directly predict the effect on T cell activation. Moreover, we show here for the first time that α/β I allosteric inhibitors, in contrast to α I allosteric inhibitors, provoked partial downmodulation of α L β 2, revealing a novel property of this inhibitor class.

CONCLUSIONS AND IMPLICATIONS

The multi-parameter whole blood α L β 2 assay described here may enable therapeutic monitoring of α L β 2 inhibitors in patients' blood. The assay dissects differential effect profiles of different classes of α L β 2 inhibitors.

Abbreviations

CsA, cyclosporin A; ICAM-1, intercellular adhesion molecule-1; I domain, inserted domain; LFA-1, lymphocyte function-associated antigen-1; mAbs, monoclonal antibodies; PE, phycoerythrin; PerCp, peridinin-chlorophyll-protein complex; TCR, T cell receptor



Tables of Links

TARGETS
CD28
Catalytic receptors
Integrin α L β 2 (LFA-1)

LIGANDS
CsA, cyclosporin A
ICAM-1, intercellular adhesion molecule-1
Pravastatin

These Tables list key protein targets and ligands in this article which are hyperlinked to corresponding entries in <http://www.guidetopharmacology.org>, the common portal for data from the IUPHAR/BPS Guide to PHARMACOLOGY (Pawson *et al.*, 2014) and are permanently archived in the Concise Guide to PHARMACOLOGY 2013/14 (Alexander *et al.*, 2013).

Introduction

The integrin α L β 2 [also known as lymphocyte function-associated antigen-1 (LFA-1) or CD11a/CD18] is an α/β heterodimeric receptor belonging to the integrin superfamily of cell surface adhesion molecules and is expressed exclusively on leukocytes. The main ligand of α L β 2 is intercellular adhesion molecule-1 (ICAM-1) (CD54), which is up-regulated on both leukocytes and endothelial cells by different pro-inflammatory stimuli (Tan, 2012).

The integrin α L β 2 has at least two major functions: firstly, as an adhesion molecule, α L β 2 mediates leukocyte extravasation out of the blood stream into inflamed tissue, and secondly, as a costimulatory receptor, α L β 2 is involved in lymphocyte activation and proliferation during immune responses (Tan, 2012). Moreover, there is recent evidence that α L β 2 engagement may play an important role in directing the differentiation of naive T cells (Verma *et al.*, 2012; Verhagen and Wraith, 2014).

These central roles of α L β 2 in the immune system require tight control. Normally, α L β 2 resides on the cell surface in an inactive state. Intracellular inside-out signalling, typically induced by chemokine receptor or T cell receptor (TCR) engagement, is required to convert α L β 2 from its inactive state to an active, ligand binding state (Hogg *et al.*, 2011). The activity of α L β 2 can also be modulated extracellularly by divalent cations such as Mg²⁺ or Mn²⁺ (Li *et al.*, 2013). During the activation process, α L β 2 and its ligand binding domain [the so-called inserted (I) domain] undergo remarkable conformational changes, which can be detected via conformation-sensitive monoclonal antibodies (mAbs) (Weitz-Schmidt *et al.*, 2011). Upon ligand binding, α L β 2 transduces signals back into the cell (outside-in signalling), triggering subsequent cellular responses depending on the cell type involved (Hogg *et al.*, 2011).

α L β 2 has been recognized as an important therapeutic target in autoimmune diseases and transplant rejection (Ford and Larsen, 2009; Suchard *et al.*, 2010; Reisman *et al.*, 2011; Kitchens *et al.*, 2012; Sheppard *et al.*, 2014). To date, several classes of low MW α L β 2 inhibitors have been identified and characterized (Giblin and Lemieux, 2006; Zhong *et al.*, 2012; Kollmann *et al.*, 2014). Currently, the most advanced small molecule α L β 2 inhibitor is in phase III clinical trials as a topical treatment for dry eye syndrome (Sheppard *et al.*, 2014).

According to their mode of action, low MW α L β 2 inhibitors can be grouped into two major classes. The first class

has been designated α I allosteric inhibitors. These inhibitors act via the α I chain of α L β 2 by binding to an allosteric site within the α I domain, thereby stabilizing the bent, low-affinity conformation of α L β 2. α I allosteric inhibitors are known to be highly selective for α L β 2 (Shimaoka and Springer, 2003a). In contrast, the second group of inhibitors, designated α/β I allosteric inhibitors, act via the β 2 chain of α L β 2, thereby perturbing an important interface between the β 2 subunit and the α subunit of α L β 2 (Shimaoka and Springer, 2003a). Intriguingly, upon binding of α/β I allosteric inhibitors, the α I domain (ligand binding domain) of the α chain of α L β 2 remains in an inactive state, while the rest of α L β 2 adapts an extended pseudo-liganded conformational state, as shown by the exposure of several activation epitopes. This conformation of α L β 2 has been shown to be 'semi-active' by mediating α L β 2/ICAM-1-dependent rolling adhesion but not firm adhesion of leukocytes (Salas *et al.*, 2004). α/β I allosteric inhibitors have been demonstrated to also target other β 2 integrins such as α M β 2 and α X β 2 (Shimaoka and Springer, 2003a).

Given these fundamental differences in the modes of action of α L β 2 inhibitors, it is highly desirable to establish a methodology that allows the assessment, in patients' whole blood, of the effects of these inhibitors in terms of receptor interactions and immune cell functions. Here, we established a multi-parameter flow cytometry assay that simultaneously measures inhibitor interaction with α L β 2 by epitope change, α L β 2 surface expression and T cell activation at the single-cell level in human whole blood. The assay was validated using α L β 2 inhibitors of both the α I allosteric and α/β I allosteric classes.

Methods

Preparation of test compounds

The α I allosteric inhibitor LFA878 and the α/β I allosteric inhibitor XVA143 (also referred to as Roche compound #5) (Shimaoka *et al.*, 2003b) were dissolved in DMSO at 10 mM and serially pre-diluted in DMSO to avoid precipitation, before they were added to human whole blood from healthy volunteers or before performing final dilution steps in buffer. All samples contained identical DMSO concentrations. The final DMSO concentration in the samples was kept at $\leq 1\%$ and did not alter the cell viability as indicated by light scattering properties of the samples.



Human blood $\alpha\beta 2$ epitope gain or epitope loss assays

The interaction of α I allosteric and α/β I allosteric $\alpha\beta 2$ inhibitors with $\alpha\beta 2$ were detected by measuring the binding of the conformation-sensitive anti- α L (CD11a) mAb R7.1 and anti- $\beta 2$ (CD18) mAb MEM48 respectively. Blood samples from healthy volunteers were obtained from the Blood Donation Center at the University Hospital of Basel and the Novartis Medical Center, Basel. Blood was drawn according to the institutional regulations accepted by the local Ethics Committee, which includes informed consent by all volunteers that the blood or blood constituents can be used for scientific purposes after anonymization. All blood samples were destroyed upon completion of analysis. Blood samples were heparinized with sodium heparin (B. Braun Medical AG, Switzerland; 100 U·mL⁻¹). Blood aliquots (198 μ L) were mixed with the compound solution or DMSO (2 μ L) and incubated for 30–60 min at room temperature (RT). The compound-containing blood samples (90 μ L) were transferred to 96-deep-well plates (2 mL, polypropylene, conical bottom, BD Biosciences, Switzerland). The FITC-conjugated mAb R7.1 or mAb MEM48 were added at final concentrations of 1–3 μ g·mL⁻¹. After 25 min staining at RT, erythrocytes were lysed with FACS lysing solution (BD Biosciences). Samples were centrifuged at 200 \times g for 5 min, and pellets were washed twice in PBS, pH 7.4 containing 0.5% BSA (Sigma-Aldrich, Switzerland) and resuspended in 150 μ L of the same buffer. Bound antibodies were detected by flow cytometry (FACSCalibur, Becton & Dickinson, BD) gating the major leukocyte populations according to their light scatter properties. In each sample, 10 000 lymphocytes were counted. Mean fluorescence intensities were calculated using the CellQuest software (BD). In some experiments, mAb MEM48 binding to human CD3⁺ lymphocytes was quantified by using FITC-conjugated mAb MEM48 and peridinin–chlorophyll–protein complex-conjugated (PerCp) anti-CD3. IC₅₀ and EC₅₀ values were determined by using the dose response curve fitting tool of ORIGIN V 7.0 (OriginLab Corporation).

Mg²⁺ effect on T cell activation in human blood

The anti-CD3 mAb OKT3 (purified in-house from hybridoma supernatants, if not otherwise indicated) or an isotype antibody control (IgG2a) in PBS, pH 8, was adsorbed onto 96-well microtiter plates (Maxisorb, Nunc, USA) (0.01–30 μ g·mL⁻¹, 100 μ L per well) at 4°C, overnight. The plates were washed twice and blocked with PBS, pH 8, containing 0.5% BSA for 1 h at 37°C. After this incubation and washing steps, PBS, pH 7.4, with or without 4 mM MgCl₂ (if not otherwise indicated) was added to each well (50 μ L per well) followed by the transfer of heparinized human blood (50 μ L per well). After 22 h incubation in a cell culture incubator (37°C and 5% CO₂), CD69 expression on human CD2⁺CD4⁺ lymphocytes was analysed in three individually activated blood samples (referred to as technical replicates) by flow cytometry using phycoerythrin-conjugated (PE) anti-CD69 mAb, FITC-conjugated anti-CD2 mAb and PerCp-conjugated anti-CD4 mAb. CD69 expression on CD3⁺ lymphocytes was analysed using PE-conjugated anti-CD69 mAb and PerCp-conjugated anti-CD3 mAb.

Simultaneous assessment of $\alpha\beta 2$ expression, $\alpha\beta 2$ inhibitor-induced epitope changes and T cell activation in human blood

The anti-CD3 mAb OKT3 (purified in-house from hybridoma supernatants) in PBS, pH 8 (1 μ g·mL⁻¹) – or alternatively a combination of anti-CD3 mAb OKT3 (0.1 μ g·mL⁻¹) and anti-CD28 mAb (clone 15E8, 1 μ g·mL⁻¹) in PBS, pH 8 – were immobilized on 96-well microtiter plates at 4°C, overnight. The plates were washed and blocked as described above. Heparinized human blood (1 mL) was added to wells of 2 mL 96-deep-well plates (polypropylene, conical bottom, BD Biosciences) and supplemented with test compounds (2 μ L) or DMSO (2 μ L). After an incubation step of 1 h at room temperature, the blood samples were transferred to the anti-CD3 or anti-CD3/anti-CD28 coated microtiter plates (50 μ L per well) containing 4 mM MgCl₂ in PBS, pH 7.4 (50 μ L per well) or PBS alone (50 μ L per well) respectively. The plates were incubated for 22 h at 37°C. Following this incubation step, four individually activated blood samples were combined and 200 μ L of the pooled blood samples transferred to 2 mL 96-deep-well plates. Leukocytes in the blood cultures were stained simultaneously with FITC-conjugated mAb R7.1 (1.5 μ L) or FITC-conjugated mAb MEM48 (1 μ g·mL⁻¹), PE-conjugated anti-CD69 (2.5 μ L), PerCp-conjugated anti-CD3 mAb (1.3 μ L) and ALEXA Fluor 647-conjugated anti- α L (CD11a) mAb TS2/4 (1 μ L) for 20 min at RT. Erythrocytes were lysed with FACS lysing solution (1.4 mL). After 10 min lysis, the plates were centrifuged (250 \times g) at RT for 6–7 min. Samples were washed once with PBS containing 0.5% BSA, and bound mAbs were analysed by flow cytometry. For all calculations, the compound concentration added to undiluted whole blood samples was used. Six to seven different concentrations per compound were tested to generate concentration response curves.

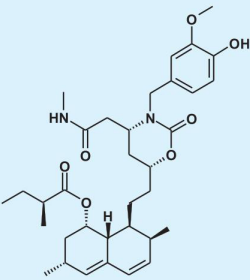
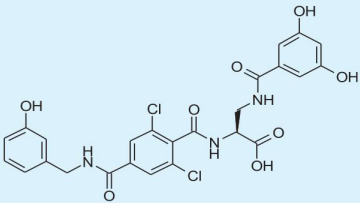
Data analysis

All values are expressed as the mean \pm SD of three determinations, unless otherwise stated. For statistical analysis the Mann-Whitney test algorithm (GraphPad Prism V6.04), paired t-test (GraphPad Prism V6.04) and one-way ANOVA and Tukey-Kramer multiple comparison test were used as indicated. P < 0.05 was considered statistically significant. Data analyses were conducted using ORIGIN V7.0 (OriginLab Corporation).

Materials

FITC-conjugated anti-human α L (CD11a) mAb R7.1 was obtained from Biosource, Camarillo, CA, USA. FITC-conjugated anti-human $\beta 2$ (CD18) mAb IB4 was purchased from Ancell Corp., USA. FITC-conjugated anti-human $\beta 2$ (CD18) mAb MEM48 or FITC-conjugated anti-human CD2 mAb (clone MEM65) and all isotype controls (IgG1 and IgG2a) were obtained from Immunotools, Germany. PE-labelled anti-human CD69 mAb (clone L78) and PerCp-conjugated anti-human CD3 mAb (clone UCHT1) were purchased from BD Biosciences. Anti-human CD28 mAb (clone 15E8) was a kind gift of Prof. L. Aarden, Sanguin Inc., Netherlands. Hybridoma cell lines producing anti-human α L (CD11a) mAb TS2/4.1.1 (TS2/4) or anti-human CD3 mAb OKT3 were obtained from the American Type Culture Collection (USA).

**Table 1**Chemical structure of α L β inhibitors LFA878 and XVA143, mode of action and activity in α L β 2-dependent binding assays

Parameter	LFA878	XVA143
Chemical structure		
Mode of action	α I allosteric	α/β I allosteric
α L β 2/ICAM-1: IC ₅₀ (μ M)	0.050 \pm 0.01*	0.020 \pm 0.008*
HUT78/ICAM-1: IC ₅₀ (μ M)	0.280 \pm 0.15*	0.005 \pm 0.004*

*Values were taken from Welzenbach *et al.*, 2002 and Weitz-Schmidt *et al.*, 2004. Results were generated in a cell-free ELISA-type binding assay measuring the interaction of immobilized α L β 2 with recombinant ICAM-1 (α L β 2/ICAM-1) and in a cell-based assay quantifying the adhesion of HUT78 cells to immobilized ICAM-1 (HUT78/ICAM-1).

Production and purification of mAbs were conducted by standard protocols. TS2/4 was conjugated with ALEXA Fluor 647 using an antibody labelling kit (Life Technologies, Switzerland) and following manufacturer's instructions. LEAFTM purified anti-human CD3 mAb OKT3 was purchased from Biologend, San Diego, CA. Anti-human IgG was purchased from Sigma-Aldrich. The α I allosteric inhibitor LFA878 and the α/β I allosteric inhibitor XVA143 were synthesized and supplied by Novartis, Switzerland. Pravastatin was purchased from Sigma-Aldrich. Cyclosporin A (CsA) was supplied by Novartis.

Results

α L β 2 inhibitors investigated

The well-established allosteric α L β 2 inhibitors LFA878 and XVA143 were selected for the present study as representatives for the α I allosteric and α/β I allosteric inhibitor classes respectively. LFA878 is a statin-derived and XVA143 a peptidomimetic α L β 2 inhibitor (Welzenbach *et al.*, 2002; Weitz-Schmidt *et al.*, 2004). The chemical structures of these α L β 2 inhibitors and their biological activity in cell-free and cell-based α L β 2-dependent binding assays are shown in Table 1.

Conformational change is a sensitive marker of inhibitor binding to α L β 2 in whole blood

The development of the whole blood flow cytometry assay described here required the stepwise optimization of several read-outs. Firstly, we developed a method to measure the interaction of α I or α/β I allosteric inhibitors with α L β 2. This method was based on the prior observation that binding of

allosteric inhibitors to α L β 2 induces epitope changes, detectable by conformation-sensitive mAbs (Welzenbach *et al.*, 2002; Woska *et al.*, 2003; Weitz-Schmidt *et al.*, 2004).

For the measurement of α I allosteric inhibitor binding to α L β 2, the anti- α L chain mAb R7.1 was selected. mAb R7.1 binds to a region involving the C-terminal linker of the α L β 2 I domain located on the α L chain and the β propeller located on the β 2 chain of α L β 2 (Weitz-Schmidt *et al.*, 2011). All α I allosteric inhibitors (of diverse chemical scaffolds) investigated to date with this antibody, that is, BIRT377, lovastatin, LFA703, LFA451 and LFA878, consistently induced R7.1 epitope loss (Welzenbach *et al.*, 2002; Shimaoka *et al.*, 2003b; Weitz-Schmidt *et al.*, 2004). The sensitivity of the R7.1 epitope to α I allosteric inhibition can be considered to be established for the entire class of inhibitors. In agreement with the earlier studies we found that LFA878 reduced the binding of mAb R7.1 to α L β 2 in a concentration-dependent manner in whole blood cultures (Figure 1A). In comparison, XVA143 did not affect the R7.1 epitope, indicating the specificity of the read-out for the compound's mode of action (Figure 1A).

For the quantification of α/β I allosteric inhibitor interactions with α L β 2 we identified the anti- β 2 chain mAbs MEM48 and MEM148 as the best suited antibodies (see Supporting Information Table S1 for all mAbs investigated). mAb MEM48 binds equally well to resting and activated α L β 2 (Lu *et al.*, 2001) whereas MEM148 is known to bind to activated but not resting α L β 2 (Tang *et al.*, 2005). To validate the MEM48 epitope as a 'reporter' epitope for the α/β I allosteric class of α L β 2 inhibitors, we investigated the effect of three different α/β I allosteric inhibitors. We were able to demonstrate that all three inhibitors assessed induced a MEM48 epitope gain by > 2 fold in whole blood. The results obtained for the α/β I allosteric inhibitor XVA143 are shown here. XVA143 increased the binding of mAb

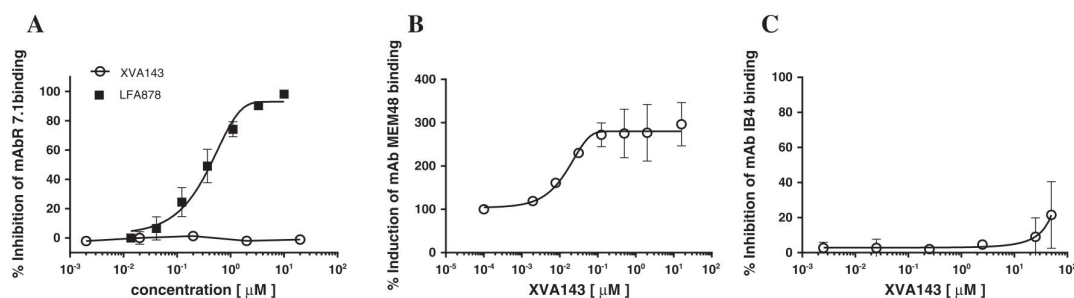


Figure 1

Effect of $\alpha\text{L}\beta 2$ inhibitors LFA878 and XVA143 on mAbs R7.1, MEM48 and IB4 binding to leukocytes in human whole blood. The binding of mAb R7.1 (A) or mAb MEM48 (B) and mAb IB4 (C) to blood lymphocyte, monocyte and granulocyte subsets in presence of indicated inhibitor concentrations was individually quantified by flow cytometry as described. Each point represents the mean value \pm SD of these measurements. Representative experiments out of three independent experiments are shown.

MEM48 to $\alpha\text{L}\beta 2$ by ≥ 2.5 fold (Figure 1B) whereas the α I allosteric inhibitor LFA878 did not modulate the $\beta 2$ chain specific antibody (data not shown). We also attempted to measure the α/β I allosteric inhibitor interaction by monitoring the epitope of the anti- $\beta 2$ chain mAb IB4. In the presence of cations, that is, Mg^{2+} and Mn^{2+} , the expression of the IB4 epitope had been shown to be attenuated by α/β I allosteric inhibitors (Welzenbach *et al.*, 2002). However, in blood cultures the binding of mAb IB4 to $\alpha\text{L}\beta 2$ was not altered by XVA143 (Figure 1C), even if the blood was supplemented with Mn^{2+} (data not shown). This result indicated that mAb IB4 was not suitable to assess the interaction of α/β I allosteric inhibitors with $\alpha\text{L}\beta 2$ in human whole blood. Taken together, these results establish that conformational changes reported by R7.1 and MEM48 reliably detect interactions of α I allosteric or α/β allosteric inhibitors with $\alpha\text{L}\beta 2$ respectively. As the respective epitope changes were observed consistently with different inhibitors of either class, it can be assumed that these changes are inhibitor class-specific rather than compound-specific.

Detection of $\alpha\text{L}\beta 2$ -dependent T cell activation in human blood cultures

In a second step, we developed a procedure permitting the detection of $\alpha\text{L}\beta 2$ -dependent T cell activation by flow cytometry in whole blood. Regarding the selection of stimuli, we focused on activating principles known to trigger $\alpha\text{L}\beta 2$ -dependent T cell activation (Weitz-Schmidt *et al.*, 2001; Kuschei *et al.*, 2011). T cells in human whole blood were exposed to immobilized anti-CD3 mAb OKT3 (aCD3), triggering signal 1 via the TCR. TCR engagement also activates $\alpha\text{L}\beta 2$ (via the inside-out pathway), which upon binding to its ligand ICAM-1 (expressed by neighbouring leukocytes) provide costimulatory signal 2 to the T cells (Leitner *et al.*, 2010). T cell activation was quantified in the present study by the up-regulation of the CD69 receptor on $\text{CD}3^+$ T cells. CD69 is an established T cell activation marker and has been used as a surrogate for T cell activation and proliferation in several previous studies (e.g. González-Amaro *et al.*, 2013). However, under the initially used conditions, the blood samples tended to coagulate; immobilized aCD3 induced the internalization of the CD3 antigen (preventing accurate

measurement of the $\text{CD}3^+$ T cell population), and CD69 up-regulation was only marginal and barely reproducible (data not shown). In consequence, we optimized assay conditions by diluting the blood samples 1:1 in PBS and investigating CD69 expression of $\text{CD}2^+\text{CD}4^+$ T helper cells (a subpopulation of T cells) instead of $\text{CD}3^+$ T cells. Furthermore, to enhance the CD69 signal, aCD3-stimulated blood was supplemented with MgCl_2 . We hypothesized that Mg^{2+} would strengthen $\alpha\text{L}\beta 2$ /ICAM-1-mediated cell-cell interactions, thereby boosting $\alpha\text{L}\beta 2$ -mediated costimulatory signalling. Indeed, we found that the addition of Mg^{2+} significantly augmented CD69 expression on $\text{CD}2^+\text{CD}4^+$ T cells. Further, the degree of CD69 expression was dependent on both the concentration of immobilized aCD3 and the concentration of Mg^{2+} (Figure 2A and B). In contrast, an immobilized non-related antibody control failed to activate T cells in the presence and absence of MgCl_2 (Figure 2A). The combination of $1 \mu\text{g}\cdot\text{mL}^{-1}$ immobilized aCD3 OKT3 and 2mM MgCl_2 was found to be optimal for T cell activation in 1:1 diluted blood cultures as assessed by CD69 expression. Under these conditions, the CD3 antigen was still detectable and suitable to reliably quantify the $\text{CD}3^+$ T cell subpopulation. On average, $9.9 \pm 3.9\%$ of the $\text{CD}3^+$ cells expressed CD69 upon aCD3/ Mg^{2+} stimulation as compared with $1.2 \pm 0.7\%$ in the absence of stimulus (Figure 3C). The relatively low proportion of $\text{CD}3^+$ cells that can be activated in whole blood, as compared with isolated peripheral blood mononuclear cells in medium, is in line with earlier observations (Hoffmeister *et al.*, 2003). Both LFA878 and XVA143 at $10 \mu\text{M}$ potently inhibited aCD3/ MgCl_2 -induced CD69 up-regulation on $\text{CD}3^+$ T cells (Figure 3). This finding provided the first evidence that CD69 up-regulation is sensitive to $\alpha\text{L}\beta 2$ inhibition under the conditions applied.

Combined assessment of $\alpha\text{L}\beta 2$ conformational change, $\alpha\text{L}\beta 2$ expression and $\alpha\text{L}\beta 2$ -mediated T cell activation in human blood cultures in the presence or absence of inhibitors

The methods established for the measurement of compound interactions with $\alpha\text{L}\beta 2$ were combined with the method for the detection of $\alpha\text{L}\beta 2$ -dependent CD69 up-regulation. Moreover, as a third read-out, the quantification

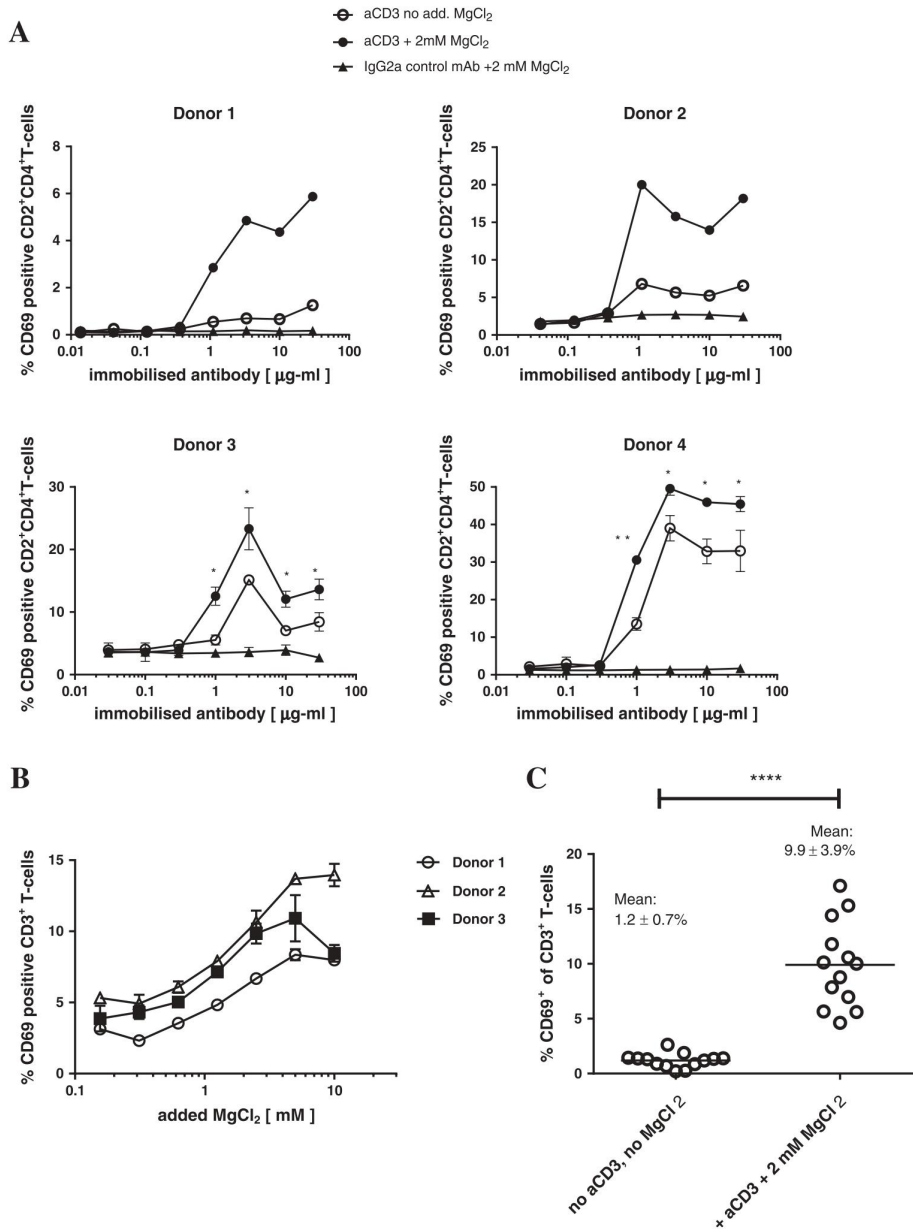
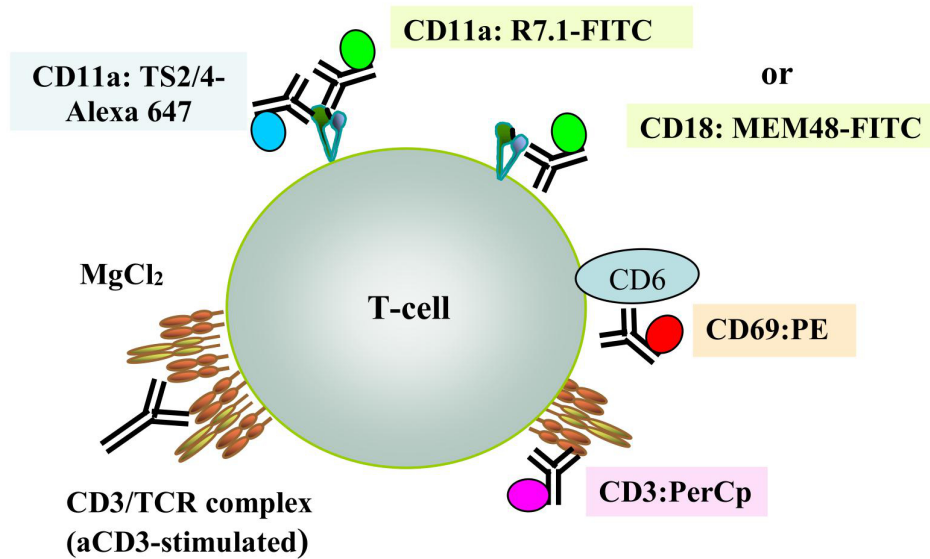


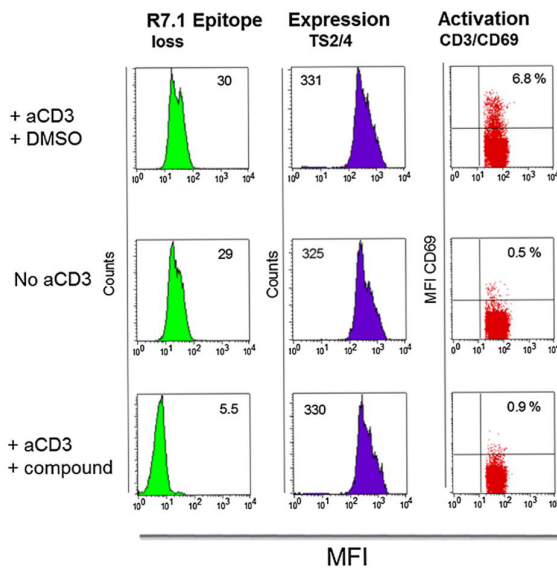
Figure 2

Mg²⁺ augments aCD3-induced CD69 up-regulation on T cells in human blood cultures. (A) Blood cultures with or without added MgCl₂ were stimulated with increasing concentrations of immobilized anti-CD3 mAb OKT3 (aCD3) (a commercially available mAb was used in case of donors 3 and 4) or a non-related antibody control (IgG2a) for 22 h. CD69 up-regulation on blood CD2⁺CD4⁺ T cells was quantified by flow cytometry as described. Single values generated from pooled technical triplicates are shown for donors 1 and 2 while mean values ± SD of three technical triplicates are shown for donors 3 and 4. * *P* < 0.05, ** *P* < 0.01; significant difference between groups aCD3 and aCD3 with added MgCl₂ from donors 3 and 4; paired *t*-test. (B) Blood cultures supplemented with MgCl₂ at indicated concentrations were stimulated with immobilized aCD3 (OKT3, 1 µg·mL⁻¹; a commercially available mAb was used in case of donor 3) for 22 h. CD69 up-regulation on CD3⁺ T cells was quantified by flow cytometry as described. Mean values ± SD of three individually activated samples of three donors are shown. (C) Frequency of CD69⁺CD3⁺ T cells in blood cultures after overnight incubation in presence or absence of immobilized aCD3 (OKT3, 1 µg·mL⁻¹) and 2 mM MgCl₂. Each circle represents the mean percentage of CD69⁺CD3⁺ T cells of three technical replicates. Data shown are means ± SD from seven independent experiments using a total of 14 healthy blood donors. **P* < 0.05, significant difference between groups aCD3 and aCD3 with added MgCl₂; Mann-Whitney test.

A Multi-parameter flow cytometry $\alpha\text{L}\beta\text{2}$ assay: Schematic representation



B Effect of LFA878



C Effect of XVA143

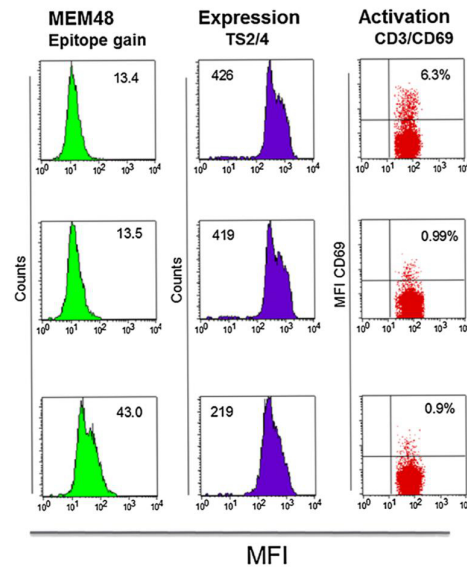


Figure 3

Multi-parameter human whole blood flow cytometry assay. (A) Schematic drawing of assay concept: the assay quantifies simultaneously $\alpha\text{L}\beta\text{2}$ epitope loss (detected by FITC-labelled mAb R7.1) and epitope gain (detected by FITC-labelled mAb MEM48) induced by small molecule αI or $\alpha/\beta\text{I}$ allosteric inhibitors, respectively, $\alpha\text{L}\beta\text{2}$ surface expression (detected by Alexa 647-labelled mAb TS2/4) and CD69 expression (detected by PE-labelled anti-CD69 mAb) on T cells (detected by PerCp-labelled anti-CD3 mAb) in blood cultures activated via immobilized anti-CD3 mAb OKT3 (aCD3) plus MgCl_2 by flow cytometry. (B) Simultaneous assessment of $\alpha\text{L}\beta\text{2}$ epitope change, $\alpha\text{L}\beta\text{2}$ expression and T cell activation in presence of LFA878 (10 μM) and (C) XVA143 (2 μM) and solvent control DMSO (0.2%) in blood cultures as described. Numbers inserted into the histograms indicate either median fluorescence intensities (MFIs) or percentage of $\text{CD69}^+\text{CD3}^+$ T cells. Results from one experiment out of more than three independent experiments are shown.

of $\alpha\text{L}\beta\text{2}$ expression was introduced. $\alpha\text{L}\beta\text{2}$ surface expression was investigated by quantifying the binding of mAb TS2/4 to $\alpha\text{L}\beta\text{2}$ expressed on CD3^+ T cells. This mAb detects the

intact α/β heterodimer of $\alpha\text{L}\beta\text{2}$ and has been previously shown to bind to a region of $\alpha\text{L}\beta\text{2}$ unaffected by the presence of αI and $\alpha/\beta\text{I}$ allosteric inhibitors (Welzenbach

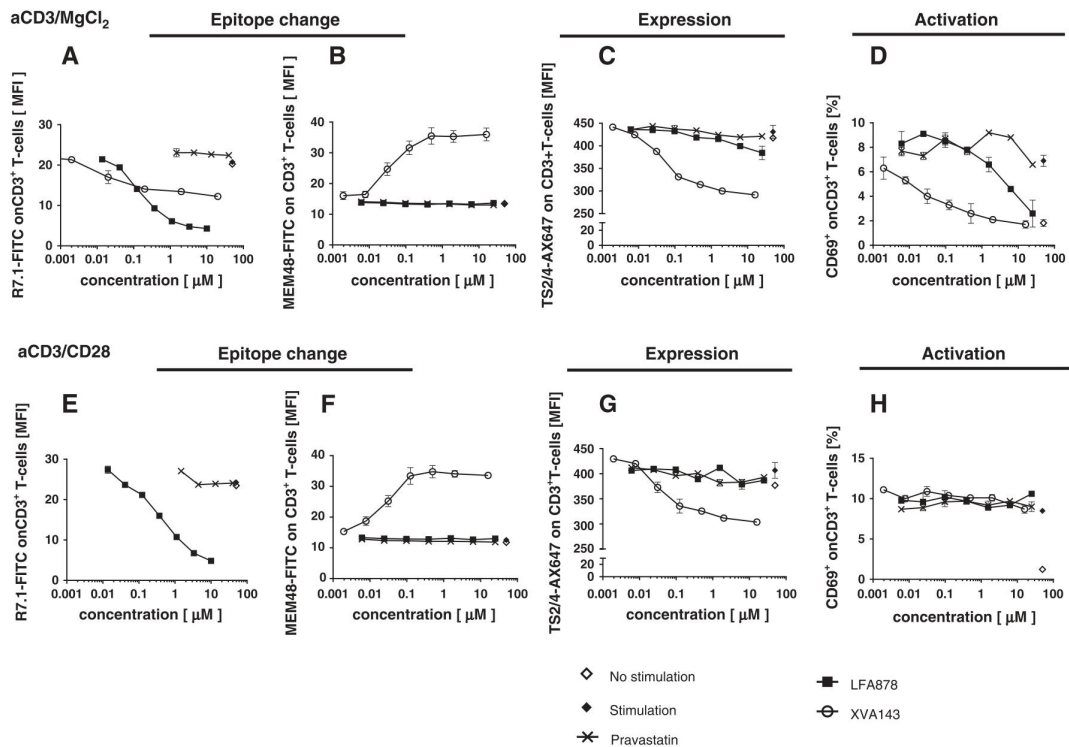


Figure 4

Simultaneous assessment of compound-induced α L β 2 epitope, α L β 2 expression and CD69 up-regulation in presence of LFA878, XVA143 or pravastatin in activated human blood. Human whole blood was pre-incubated for 1 h with the compounds at indicated concentrations. After incubation, the blood samples were diluted 1:1 with PBS and activated with aCD3/MgCl₂ (A–D) or aCD3/aCD28 (without MgCl₂) (E–H), respectively, for 22 h. The binding of anti- α L β 2 mAbs R7.1 or MEM48 (epitope change) and TS2/4 (expression) as well as the binding of anti-CD69 mAb (activation) to CD3⁺ T cells was quantified by flow cytometry as described under the Methods section. Four individually activated blood samples per donor were pooled. From this pool, two samples were independently stained and measured. Data shown are mean values \pm SD of these two samples. SD is shown to indicate range of data. Stimulation: activated blood in presence of solvent control (0.2% DMSO); no stimulation: resting blood in presence of solvent control (0.2% DMSO). One representative experiment out of more than three independent experiments is shown.

et al., 2002). The principle of the final α L β 2 multi-parameter flow cytometry blood test used in this study is illustrated in Figure 3A.

The assay was utilized to simultaneously assess the effect of LFA878 and XVA143 on α L β 2 conformation, α L β 2 expression and aCD3/MgCl₂-induced CD69 expression. For the first time, we demonstrated at the single-cell level that LFA878 affects the R7.1 but not the MEM48 epitope, marginally reduced α L β 2 expression at high concentrations, and inhibited CD69 expression on T cells with an IC₅₀ value of $2.6 \pm 1.7 \mu\text{M}$ (Figure 4A–D, Table 2). In contrast, the 3-hydroxy-3-methylglutaryl-coenzyme-A reductase inhibitor pravastatin did not modify any of the parameters assessed (Figure 4A–D, Table 2). This cholesterol-lowering drug is structurally related to the statin-derived α L β 2 inhibitor LFA878 but does not inhibit α L β 2 (Weitz-Schmidt *et al.*, 2001).

On the other hand, binding of XVA143 to α L β 2 led to an increased exposure of the MEM48 epitope and surprisingly at the same time partially reduced the binding of both, mAb TS2/4 and mAb R7.1, indicating an effect of the compound on α L β 2 surface expression (Figure 4A and C). Moreover, XVA143 potently inhibited CD69 expression

with an IC₅₀ value of $0.049 \pm 0.016 \mu\text{M}$ (Figure 4D, Table 2).

The XVA143-induced downmodulation of α L β 2 measured in the multi-parameter assay after 22 h of exposure was highly reproducible (Figure 5) and was confirmed with two other inhibitors of the α/β I allosteric class (data not shown). However, the effect did not become evident in experiments involving XVA143 exposure times of less than 1 h, for example, as it was the case in the α L β 2 MEM48 epitope alteration assay shown in Figure 1A. This indicates that the reduction of α L β 2 surface expression by XVA143 is dependent on mechanisms requiring exposure times longer than 1 h. The exact nature of these mechanisms remains to be elucidated.

Next, we investigated the effect of the compounds on CD3⁺ T cells in blood cultures activated with aCD3/aCD28. CD28 is a co-receptor on T cells providing costimulatory signalling independent from the α L β 2 pathway (Leitner *et al.*, 2010; Kuschei *et al.*, 2011). As expected, XVA143 and LFA878 failed to block aCD3/aCD28-induced CD69 up-regulation (Figure 4H, Table 2). The effects of the α L β 2 inhibitors on R7.1 and MEM48 epitope expression as well as the effect on α L β 2 surface expression were similar in



Table 2

Activity profile of LFA878, XVA143, pravastatin and CsA in activated human blood

Compounds	Epitope change		$\alpha\text{L}\beta 2$ expression	Suppression of CD69 up-regulation	
	aCD3/Mg ²⁺ or aCD3/aC28		mAbTS2/4 IC ₅₀ (μM)	aCD3/Mg ²⁺	aCD3/aC28
	mAb R7.1 IC ₅₀ (μM)	mAb MEM48 EC ₅₀ (μM)		aCD69 mAb IC ₅₀ (μM)	aCD69 mAb IC ₅₀ (μM)
LFA878	0.5 \pm 0.2*	>10 [#]	>10 [#]	2.6 \pm 1.7*	>10 [#]
XVA143	>50 [#]	0.031 \pm 0.007*	30 \pm 4% \downarrow at 10 μM [#]	0.049 \pm 0.016*	>10 [#]
Pravastatin	>40 [#]	>40 [#]	>10 [#]	>40 [#]	>40 [#]
CsA	>10 [#]	>10 [#]	>10 [#]	0.8 \pm 0.26*	35% \downarrow at 10 μM [#]

All data were generated in aCD3/Mg²⁺ or aCD3/aC28 activated human blood using the multi-parameter flow cytometry assay as described.

*Mean value \pm SD of more than three independent experiments.

[#]Value represents the highest concentration tested, representative result of more than three independent experiments shown.

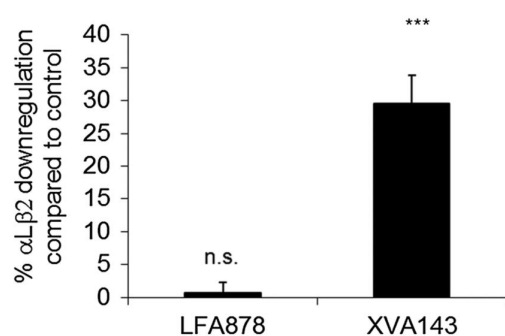


Figure 5

Effect of inhibitors on $\alpha\text{L}\beta 2$ surface expression. Human whole blood was supplemented with LFA878 (10 μM) or XVA143 (10 μM), pre-incubated for 1 h, diluted 1:1 with PBS and then stimulated for 22 h with aCD3/MgCl₂. Integrin $\alpha\text{L}\beta 2$ expression on CD3⁺ T cells was quantified by assessing the binding of mAb TS2/4. Data shown are mean values \pm SD from six (LFA878) and eight (XVA143) independent experiments, that is, six and eight blood donors respectively. *** $P < 0.001$, significantly different from control; one-way ANOVA with the Tukey–Kramer multiple comparison test; n.s., not significantly different from control.

aCD3/aC28 and aCD3/Mg²⁺ stimulated blood (Figure 4). This demonstrates that the level of epitope alteration and the effect on $\alpha\text{L}\beta 2$ surface expression are independent of the stimulus utilized to activate the blood samples. It needs to be noted here that under conditions of aCD3/aC28 activation, levels of R7.1 epitope change was measured using α I allosteric inhibitors only (Figure 4E).

Correlation of inhibitor-induced $\alpha\text{L}\beta 2$ epitope changes with CD69 up-regulation in blood cultures

When correlating compound-induced epitope changes with aCD3/MgCl₂-induced CD69 up-regulation at the single-cell level, another interesting differential feature of α I allosteric and α/β I allosteric inhibitors became evident. More than 80% epitope loss was associated with half-maximal inhibition of

CD69 expression in presence of LFA878 (Figure 6). In contrast, less than 40% epitope gain induced by XVA143 was associated with half-maximal inhibition of CD69 expression (Figure 6). The ratio of half-maximal inhibition of CD69 expression to half-maximal epitope change was calculated to be 5.1 for LFA878 and 1.1 for XVA143 respectively (Table 2). These differential epitope change / T cell response relationships were also observed when inhibitor-induced $\alpha\text{L}\beta 2$ epitope changes were directly correlated to aCD3-induced T cell proliferation (rather than MgCl₂-induced CD69 up-regulation) in whole blood (Supporting Information Fig. S6).

Effect of CsA in the multi-parameter assay

Although the development of the present multi-parameter assay was tailored to characterize $\alpha\text{L}\beta 2$ inhibitors, we were interested to assess in the test system, therapeutically used immunosuppressive drugs with targets different from $\alpha\text{L}\beta 2$. Thus, we compared the profile of the $\alpha\text{L}\beta 2$ inhibitors with the profile of the immunosuppressant cyclosporin A (CsA). CsA is a calcineurin inhibitor modulating TCR-mediated activation of T cells (signal 1), as reviewed recently (Azzi *et al.*, 2013). CsA did not affect $\alpha\text{L}\beta 2$ conformation as monitored by mAb R7.1 and mAb MEM48 binding and did not impede $\alpha\text{L}\beta 2$ surface expression as assessed by mAb TS2/4 binding (Table 2). As expected from its mechanism of action, CsA inhibited aCD3/MgCl₂-stimulated T cell activation with an IC₅₀ value of 0.8 \pm 0.26 μM (Table 2). Moreover, as observed for $\alpha\text{L}\beta 2$ inhibitors, T cell activation was largely unaffected by CsA in blood cultures stimulated by aCD3/aC28 (Table 2). These data establish that the assay methodology can be extended to immunomodulatory modalities of different mechanisms of action, such as CsA.

Discussion

With several classes of $\alpha\text{L}\beta 2$ inhibitors in development, there is a clear need for methodologies that allow the correlation of compound/ $\alpha\text{L}\beta 2$ interactions with therapeutically relevant, downstream biological effects. Preferably, this assessment should be performed in blood taken from treated patients, enabling *ex vivo* bedside monitoring.

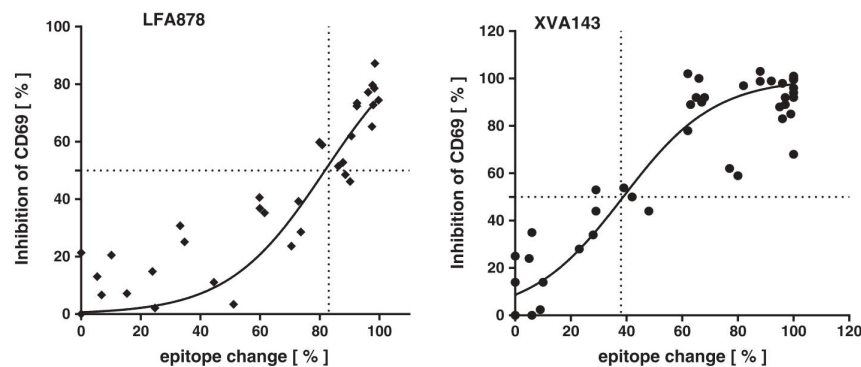


Figure 6

Correlation of α L β 2 receptor occupancy with T cell activation. Following treatment with LFA878 or XVA143, α L β 2 occupancy (as measured by mAb R7.1 or MEM48 epitope alteration) was correlated with aCD3/MgCl₂-induced CD69 up-regulation on T cells in human blood. Raw data from three independent experiments (three donors) are shown.

At the core of the methodology described here lies the realization that inhibitor-induced epitope changes can be used to indirectly detect integrin/inhibitor interactions in whole blood, with the nature of epitope alteration depending on the molecular mode of action. Epitope monitoring has been applied in the past to analyse the binding of low MW antagonists to the integrin receptor α IIb/ β 3 (GPIIb/IIIa) *in vitro* and *ex vivo* in blood samples from treated patients (Quinn *et al.*, 2000). Furthermore, it has been applied to α I allosteric α L β 2 inhibitors (but not α/β I allosteric inhibitors) *in vitro* and in preclinical animal studies (Woska *et al.*, 2003; Weitz-Schmidt *et al.*, 2004). These epitope alteration assays have in common that they quantify epitopes, which are shielded upon compound binding to the integrin, that is, which are lost.

We used the experimental knowledge gained from the earlier studies to establish *in vitro* assays of human whole blood which allowed the detection of the interactions of different inhibitor classes with the integrin α L β 2 and, at the same time, to visualize their mode of action by monitoring inhibitor-specific α L β 2 conformational changes. For the first time, we introduced compound-induced epitope *gain*, rather than epitope *loss*, as a method to assess inhibitor interaction. Moreover, the methodology is the first to apply the principle of epitope monitoring to inhibitors, which block the same integrin by different modes of action. Our study establishes the correlation between α I allosteric and α/β I allosteric inhibitor concentrations and R7.1 and MEM48 epitope changes respectively. However, the study does not measure inhibitor binding to integrin α L β 2, that is, receptor occupancy, directly and does not correlate this direct binding with respective epitope changes. This will be addressed by future investigations.

Unexpectedly, the extension of the whole blood epitope monitoring assays to the assessment of the effect of α L β 2 inhibition on immune cell function at the single-cell level posed significant methodological hurdles. These difficulties were resolved by increasing the Mg²⁺ concentration of the blood cultures beyond the normal physiological levels of 0.5 to 1 mM. The addition of Mg²⁺ finally enabled us to reproducibly quantify α L β 2-dependent T cell activation (as assessed by CD69 up-regulation) on T cells in blood. It also allowed

to complete the α L β 2 multi-parameter flow cytometry assay by combining the epitope change measurements with T cell activation and α L β 2 surface expression measurements. Our observations in blood cultures further substantiate the physiological and clinical relevance of the regulatory function of Mg²⁺ within the immune system. Mg²⁺ is not only crucial for the maintenance of active conformations of immune receptors such as the integrin α L β 2 but it is also essential in the regulation of lipid-derived and phosphoinositide-derived second messengers as well as various transporters and ion channels involved in the immune response (Brandao *et al.*, 2013). Interestingly, tissue injury has been reported to result in a local increase in extracellular Mg²⁺ most likely due to leakage from damaged tissue (intracellular Mg²⁺ concentrations vary from 15 to 25 mM) (Grzesiak and Pierschbacher, 1995). Based on this finding, it has been postulated that increased Mg²⁺ levels serve to stimulate leukocyte migration into wounds (Stewart *et al.*, 1996). Here, we provide evidence in a physiological relevant environment that increased Mg²⁺ may also facilitate T cell activation driven by α L β 2-mediated co-stimulation at sites of inflammation.

The first application of the newly established whole blood flow cytometry methodology yielded interesting and surprising results. One such finding related to the differential effect of the inhibitors on the surface expression of α L β 2 itself. α L β 2 inhibitors with an α/β I allosteric mode of action reduced α L β 2 surface expression, in contrast to α I allosteric inhibitors. Reduced expression of α L β 2 has not been reported before in the presence of low MW inhibitors. In contrast, down-regulation of α L β 2 is a well-known phenomenon with anti- α L β 2 antibodies (Gottlieb *et al.*, 2002; Clarke *et al.*, 2004; Coffey *et al.*, 2004). For instance, the anti-human α L β 2 mAb efalizumab (originally approved for the indication of plaque psoriasis but withdrawn from markets in 2009 following four cases of progressive multifocal leukoencephalopathy; Seminara and Gelfand, 2010) has been shown to induce almost complete internalization of α L β 2 in treated patients, thought to be due to α L β 2 cross-linking by the antibody (Gottlieb *et al.*, 2002; Coffey *et al.*, 2004). The α/β I allosteric inhibitor-induced downmodulation of α L β 2 was partial only and may be caused by other mechanisms. It is intriguing to



speculate that the extended, semi-active conformation stabilized by α/β I allosteric inhibitors (but not by α I allosteric $\alpha\text{L}\beta\text{2}$ inhibitors) may influence the dynamics of $\alpha\text{L}\beta\text{2}$ receptor recycling to the cell surface. This hypothesis is supported by the recent finding that an extended conformation of $\alpha\text{L}\beta\text{2}$, sharing several properties with the α/β I allosteric inhibitor-induced conformation of the integrin, is internalized and that the conformational state of LFA-1 directly affects LFA-1 recycling and turnover (Stanley *et al.*, 2012). Further investigations are required to elucidate the mechanisms of α/β I allosteric inhibitor-induced downmodulation of $\alpha\text{L}\beta\text{2}$ surface expression.

Additional interesting differences between α I allosteric and α/β I allosteric inhibitors became evident when levels of epitope changes were correlated with effects on T cell activation at the single-cell level. We found that more than 80% R7.1 epitope loss induced by α I allosteric inhibitors was associated with half-maximal inhibition of T cell activation. In contrast, an almost linear correlation between MEM48 epitope gain and blockade of T cell activation was observed for α/β I allosteric inhibitors. This remarkable difference may be explained by the fact that α I and α/β I allosteric inhibitors act via different $\alpha\text{L}\beta\text{2}$ subunits. α/β I allosteric inhibitors bind to the β2 chain of $\alpha\text{L}\beta\text{2}$. As this subunit is responsible for signal transduction into the cell, a direct relationship between compound-induced MEM48 epitope alteration and inhibitory function is not surprising (Hogg *et al.*, 2011). The absence of such relationship in the case of α I allosteric inhibitors may reflect the fact that signals from the α chain need to be conveyed to the β2 chain before they translate into functional effects. Another explanation could be that the α I and α/β I allosteric inhibitors stabilize $\alpha\text{L}\beta\text{2}$ in different conformational and activity states (bent vs. extended and inactive vs. semi-active). These different states could translate into different thresholds for downstream effects. The detailed molecular mechanisms at receptor and intracellular pathway levels leading to these differential effect profiles remain to be elucidated.

Intriguingly in this context, treatment of psoriasis patients with efalizumab indicated a similar relationship between the degree of efalizumab binding and clinical efficacy as has been observed for low MW α I allosteric inhibitors between the degree of R7.1 epitope change and T cell activation *in vitro* in whole blood. Doses of efalizumab resulting in partial saturation of the receptor did not result in significant decreases in T cell infiltration, nor significant improvement of skin conditions as assessed by the Psoriasis Area and Severity Index score (Gottlieb *et al.*, 2000; Gottlieb *et al.*, 2002). In contrast, doses that resulted in high (>75%) levels of $\alpha\text{L}\beta\text{2}$ saturation led to a significant decrease in T cell infiltration and a decrease of the Psoriasis Area and Severity Index score by approximately 45% (Gottlieb *et al.*, 2000; Gottlieb *et al.*, 2002). The fact that efalizumab binds to the α chain of $\alpha\text{L}\beta\text{2}$ (as α I allosteric inhibitors do) may explain the similarity of the correlations observed with these two modalities.

Taken together, these data demonstrate that the degree of R7.1 and MEM48 epitope change induced by α I allosteric and α/β I allosteric inhibitors does not directly predict the magnitude of effect on immune cell function. In consequence, there is a need to establish the relationship between epitope change and biological response for each inhibitor class and for each epitope monitored individually. The assay methodology described here allowed us to achieve that.

Conclusion

The flow cytometry-based technology described here allows, for the first time, to simultaneously assess and correlate, at the single-cell level, inhibitor-specific $\alpha\text{L}\beta\text{2}$ conformational change, $\alpha\text{L}\beta\text{2}$ expression and T cell activation in human whole blood. The format, robustness and sensitivity of the assay indicate that it may be suitable for bedside monitoring of newly developed $\alpha\text{L}\beta\text{2}$ inhibitors. Further, the assay allowed us to identify unexpected effects of one inhibitor class not exhibited by the other class of inhibitor. This indicates that the assay may also be used as an investigational methodology to assess molecular pathways differentially affected by $\alpha\text{L}\beta\text{2}$ inhibitors with different modes of action. Initial data using CsA indicate that the methodology may be extended to immunomodulatory modalities of mechanisms not related to $\alpha\text{L}\beta\text{2}$, thus widening the context of therapeutic guidance.

Acknowledgements

The authors thank A.-G. Schmidt for critical review of the manuscript. This work was in part supported by the Swiss Commission of Technology and Innovation (15265.1 PFLS-LS).

Author contributions

K. W. and R.V.M. performed the research work. K. W., G. W.-S. and S. K. contributed to the conception of the work. All authors contributed to the analysis of the data. G. W.-S. and K. W. prepared the manuscript.

Conflict of interest

The authors declare no conflicts of interest.

References

- Alexander SPH, Benson HE, Faccenda E, Pawson AJ, Sharman JL, Spedding M *et al.* (2013). The Concise Guide to PHARMACOLOGY 2013/14: Catalytic Receptors. *Br J Pharmacol* 170: 1676–1705.
- Azzi JR, Sayegh MH, Mallat SG (2013). Calcineurin inhibitors: 40 years later, can't live without. *J Immunol* 12: 5785–5791.
- Brandao K, Deason-Towne F, Perraud AL, Schmitz C (2013). The role of Mg²⁺ in immune cells. *Immunol Res* 55: 261–269.
- Clarke J, Leach W, Pippig S, Joshi A, Wu B, House R *et al.* (2004). Evaluation of a surrogate antibody for preclinical safety testing of an anti-CD11a monoclonal antibody. *Regul Toxicol Pharmacol* 40: 219–226.
- Coffey GJ, Stefanich E, Palmieri S, Eckert R, Padilla-Eagar J, Fielder PJ *et al.* (2004). *In vitro* internalization, intracellular transport, and clearance of an anti-CD11a antibody (Raptiva) by human T-cells. *Pharmacol Exp Ther* 310: 896–904.
- Ford ML, Larsen CP (2009). Translating costimulation blockade to the clinic: lessons learned from three pathways. *Immunol Rev* 229: 294–306.



- Giblin PA, Lemieux RM (2006). LFA-1 as a key regulator of immune function: approaches toward the development of LFA-1-based therapeutics. *Curr Pharm Des* 12: 2771–2795.
- Grzesiak JJ, Pierschbacher MD (1995). Shifts in the concentrations of magnesium and calcium in early porcine and rat wound fluids activate the cell migratory response. *J Clin Invest* 95: 227–233.
- González-Amaro R, Cortés JR, Sánchez-Madrid F, Martín P (2013). Is CD69 an effective brake to control inflammatory diseases? *Trends Mol Med* 19: 625–632.
- Gottlieb A, Krueger JG, Bright R, Ling M, Lebwohl M, Kang S *et al.* (2000). Effects of administration of a single dose of a humanized monoclonal antibody to CD11a on the immunobiology and clinical activity of psoriasis. *J Am Acad Dermatol* 42: 428–435.
- Gottlieb AB, Krueger JG, Wittkowski K, Dedrick R, Walicke PA, Garovoy M (2002). Psoriasis as a model for T-cell-mediated disease: immunobiologic and clinical effects of treatment with multiple doses of efalizumab, an anti-CD11a antibody. *Arch Dermatol* 138: 591–600.
- Hoffmeister B, Bunde T, Rudawsky IM, Volk HD, Kern F (2003). Detection of antigen-specific T cells by cytokine flow cytometry: the use of whole blood may underestimate frequencies. *Eur J Immunol* 33: 3484–3492.
- Hogg N, Patzak I, Willenbrock F (2011). The insider's guide to leukocyte integrin signaling and function. *Nat Rev Immunol* 11: 416–426.
- Kitchens WH, Haridas D, Wagener ME, Song M, Ford ML (2012). Combined costimulatory and leukocyte functional antigen-1 blockade prevents transplant rejection mediated by heterologous immune memory alloresponses. *Transplantation* 93: 997–1005.
- Kollmann CS, Bai X, Tsai CH, Yang H, Lind KE, Skinner SR *et al.* (2014). Application of encoded library technology (ELT) to a protein-protein interaction target: discovery of a potent class of integrin lymphocyte function-associated antigen 1 (LFA-1) antagonists. *Bioorg Med Chem* 22: 2353–2365.
- Kuschei WM, Leitner J, Majdic O, Pickl WF, Zlabinger GJ, Grabmeier-Pfistershammer K *et al.* (2011). Costimulatory signals potently modulate the T cell inhibitory capacity of the therapeutic CD11a antibody efalizumab. *Clin Immunol* 139: 199–207.
- Leitner J, Grabmeier-Pfistershammer K, Steinberger P (2010). Receptors and ligands implicated in human T cell costimulatory processes. *Immunol Lett* 128: 89–97.
- Li N, Mao D, Lü S, Tong C, Zhang Y, Long M (2013). Distinct binding affinities of Mac-1 and LFA-1 in neutrophil activation. *J Immunol* 190: 4371–4381.
- Lu C, Ferzly M, Takagi J, Springer TA (2001). Epitope mapping of antibodies to the C-terminal region of the integrin beta 2 subunit reveals regions that become exposed upon receptor activation. *J Immunol* 166: 5629–5637.
- Pawson AJ, Sharman JL, Benson HE, Faccenda E, Alexander SP, Buneman OP *et al.* (2014). The IUPHAR/BPS Guide to PHARMACOLOGY: an expert-driven knowledge base of drug targets and their ligands. *Nucl Acids Res* 42 Database Issue: D1098–1106.
- Quinn MJ, Cox D, Foley JB, Fitzgerald DJ (2000). Glycoprotein IIb/IIIa receptor number and occupancy during chronic administration of an oral antagonist. *J Pharmacol Exp Ther* 295: 670–676.
- Reisman NM, Floyd TL, Wagener ME, Kirk AD, Larsen CP, Ford ML (2011). LFA-1 blockade induces effector and regulatory T-cell enrichment in lymph nodes and synergizes with CTLA-4Ig to inhibit effector function. *Blood* 118: 5851–5861.
- Salas A, Shimaoka M, Kogan AN, Harwood C, von Andrian UH, Springer TA (2004). Rolling adhesion through an extended conformation of integrin alphaLbeta2 and relation to alpha I and beta I-like domain interaction. *Immunity* 20: 393–406.
- Sheppard JD, Torkildsen GL, Lonsdale JD, D'Ambrosio FA Jr, McLaurin EB, Eiferman RA *et al.* (2014). Lifitegrast ophthalmic solution 5.0% for treatment of dry eye disease: results of the OPUS-1 phase 3 study. *Ophthalmology* 121: 475–483.
- Seminara NM, Gelfand JM (2010). Assessing long-term drug safety: lessons (re)learned from Raptiva. *Semin Cutan Med Surg* 29: 16–19.
- Shimaoka M, Springer TA (2003a). Therapeutic antagonists and conformational regulation of integrin function. *Nat Rev Drug Discov* 2: 703–716.
- Shimaoka M, Salas A, Yang W, Weitz-Schmidt G, Springer TA (2003b). Small molecule integrin antagonists that bind to the beta2 subunit I-like domain and activate signals in one direction and block them in the other. *Immunity* 19: 391–402.
- Stanley P, Tooze S, Hogg N (2012). A role for Rap2 in recycling the extended conformation of LFA-1 during T cell migration. *Biol Open* 1: 1161–1168.
- Stewart MP, Cabanas C, Hogg N (1996). T cell adhesion to intercellular adhesion molecule-1 (ICAM-1) is controlled by cell spreading and the activation of integrin LFA-1. *J Immunol* 156: 1810–1817.
- Suchard SJ, Stetsko DK, Davis PM, Skala S, Potin D, Launay M *et al.* (2010). An LFA-1 (alphaLbeta2) small-molecule antagonist reduces inflammation and joint destruction in murine models of arthritis. *J Immunol* 184: 3917–3926.
- Tan SM (2012). The leucocyte beta2 (CD18) integrins: the structure, functional regulation and signaling properties. *Biosci Rep* 32: 241–269.
- Tang RH, Tng E, Law SK, Tan SM (2005). Epitope mapping of monoclonal antibody to integrin alphaL beta2 hybrid domain suggests different requirements of affinity states for intercellular adhesion molecules (ICAM)-1 and ICAM-3 binding. *J Biol Chem* 280: 29208–29216.
- Vérhagen J, Wraith DC (2014). Blockade of LFA-1 augments *in vitro* differentiation of antigen-induced Foxp3+ Treg cells. *J Immunol Methods* pii S0022-1759(14)00244-0. doi:10.1016/j.jim.2014.07.012[Epub ahead of print].
- Verma NK, Dempsey E, Long A, Davies A, Barry SP, Fallon PG *et al.* (2012). Leukocyte function-associated antigen-1/intercellular adhesion molecule-1 interaction induces a novel genetic signature resulting in T-cells refractory to transforming growth factor-beta signaling. *J Biol Chem* 287: 27204–27216.
- Weitz-Schmidt G, Welzenbach K, Brinkmann V, Kamata T, Kallen J, Bruns C *et al.* (2001). Statins selectively inhibit leukocyte function antigen-1 by binding to a novel regulatory integrin site. *Nat Med* 7: 687–692.
- Weitz-Schmidt G, Welzenbach K, Dawson J, Kallen J (2004). Improved lymphocyte function-associated antigen-1 (LFA-1) inhibition by statin derivatives: molecular basis determined by X-ray analysis and monitoring of LFA-1 conformational changes *in vitro* and *ex vivo*. *J Biol Chem* 279: 46764–46771.
- Weitz-Schmidt G, Schürpf T, Springer TA (2011). The C-terminal alpha domain linker as a critical structural element in the conformational activation of alphaL integrins. *J Biol Chem* 286: 42115–42122.
- Welzenbach K, Hommel U, Weitz-Schmidt G (2002). Small molecule inhibitors induce conformational changes in the I domain and the I-like domain of lymphocyte function-associated antigen-1. Molecular insights into integrin inhibition. *J Biol Chem* 277: 10590–10598.



Woska JR Jr, Last-Barney K, Rothlein R, Kroe RR, Reilly PL, Jeanfavre DD *et al.* (2003). Small molecule LFA-1 antagonists compete with an anti-LFA-1 monoclonal antibody for binding to the CD11a I domain: development of a flow-cytometry-based receptor occupancy assay. *J Immunol Methods* 277: 101–115.

Zhong M, Gadek TR, Bui M, Shen W, Burnier J, Barr KJ *et al.* (2012). Discovery and development of potent LFA-1/ICAM-1 antagonist SAR 1118 as an ophthalmic solution for treating dry eye. *ACS Med Chem Lett* 3: 203–206.

Supporting Information

Additional supporting information may be found in the online version of this article at the publisher's web-site.

<http://dx.doi.org/10.1111/bph.13256>

Table S1 List of commercially available anti- β2 (CD18) mAbs tested for the establishment of the $\alpha/\beta\text{I}$ allosteric $\alpha\text{L}\beta\text{2}$ inhibitor occupancy assay. MEM48 and MEM148 were found to be the best suited antibodies to quantify the interaction of this inhibitor class with $\alpha\text{L}\beta\text{2}$.

Figure S6 Correlation of inhibitor-induced $\alpha\text{L}\beta\text{2}$ epitope change with *T* cell proliferation in whole blood. Following treatment with the LFA878 (αI allosteric inhibitor) or XVA143 ($\alpha/\beta\text{I}$ allosteric inhibitor), $\alpha\text{L}\beta\text{2}$ epitope alteration (as measured by mAb R7.1 or MEM48 binding, see method section of manuscript) was correlated with aCD3-induced *T* cell proliferation in human blood (see method described below). Raw values of three independent experiments (three donors) are shown.

2. Discussion

“A drug is a substance which, if injected into a rabbit, produces a paper.”

Otto Loewi

3 Jun 1873 - 25 Dec 1961

German-American physician, physiologist and pharmacologist

2.1. Back to the future

Crude extracts from wild plants, herbs, roots, vines and fungi constituted the first medicines that were used mainly for the relief of pain and suffering, to heal wounds, and to treat maladies. The first “painkiller” used was the juice obtained from the opium poppy plant (*Papaver somniferum*) and it can be dated to the ~3,000 BC (Jones 2011).

For the first synthetic drug, we need to wait until the 1832 when chloral hydrate was discovered by Justus von Liebig. Its sedative properties were first published in 1869; it is still available today in some countries (Liebig 1831) (Liebig 1832).

In ancient times, drug discovery was mainly based on the accumulation of experience from generation to generation, the *Ebers Papyrus* can be considered the first written record of medical therapeutics. It is a 20 meters long papyrus of 110 pages dating to ~1500 BC. It was purchased at Luxor in 1872 by the German Egyptologist and novelist Georg Ebers and it was named after him.

In the *Ebers Papyrus* it is possible to find the description of hundreds of treatments for the diseases inflicting ancient Egyptians. These treatments were prepared by mixing together herbs, leaves, minerals, and animal excreta (Jones 2011).

The early history of drug discovery is therefore all about natural products and herbal remedies, the use of which dates back thousands of years. The driving force in their discovery was mainly serendipity.

Nowadays there is a shift from serendipity to rationality in drug discovery that is more and more based on the knowledge of the biological system and on the development of modern chemistry. This allowed the discovery of highly specific and selective new drugs (Chen and Du 2007).

2.2. Drug discovery

In pharmacology, biotechnology and medicine, drug discovery is the process of identification, creation, or design of a compound or a complex that could become a therapeutic (Wyatt, et al. 2011).

This process requires a big investment in time and money, a single new drug can cost up to 1 billion euros and take 10-14 years to develop and there is no guarantee about the end result (Chen and Du 2007).

A drug target is a broad term which can be applied to a range of biological entities which may include for example proteins, genes and RNA and the specific binding site for a drug through which the drug exerts its action (Overington, et al. 2006).

A good target needs to be druggable. Druggability defines a biological target that is known to or is predicted to bind with high affinity to a drug, be it a small molecule or larger biologicals. Further, upon binding, the drug must elicit via the target a therapeutic benefit to the patient, this effect may be measured both *in vitro* and *in vivo*. A good target needs to be efficacious, safe and meet clinical and commercial needs (Hughes, et al. 2011).

2.3. Target identification



Our drug target is the integrin $\alpha\text{L}\beta\text{2}$. This integrin is expressed on the cell surface of leukocytes and it mediates the adhesion of leukocytes to each other and to other cells, thereby regulating leukocyte trafficking, T cell costimulation and immunological synapse (IS) formation (Hogg, et al. 2011).

$\alpha\text{L}\beta\text{2}$ is also centrally involved in immune-mediated diseases of high medical need, including chronic plaque psoriasis, multiple sclerosis, rheumatoid arthritis, small vessel vasculitis, dry eye disease and transplantation indications, among other diseases (Zecchinon, et al. 2006). In several of these diseases, $\alpha\text{L}\beta\text{2}$ has been validated by biologic therapies as a target of high therapeutic potential (Nicolls and Gill 2006).

2.4. Target validation



Target validation is defined as a pharmacologic, physiologic and pathologic process that evaluates a biomolecule during the development of pharmaceuticals for therapeutic application.

This process can be performed at the molecular, cellular, or whole animal level (Chen and Du 2007).

This validation could be for instance chemical/biological or genetic. In the chemical/biological validation the use of drugs or proteins provides evidence that the inhibition of a target results in inhibition of its activity.

In the genetic validation, using knockdown methodologies it is possible to suppress the target (i.e. gene knockout) with a dominant-negative approach (Wyatt, et al. 2011).

In case of α L β 2, mAbs validated the integrin as a promising therapeutic target. The anti- α L β 2 mAb efalizumab was efficacious in patients with psoriasis. Moreover, preclinically anti- α L β 2 mAbs were efficacious in transplant and autoimmune disease models (Nicolls and Gill 2006).

Another validation of α L β 2 comes from subjects affected by leukocyte adhesion deficiency (LAD). Mutations in β 2 chain can lead to LAD. LAD-I has been identified in patients having a deficiency in β 2 (CD18) integrins. LAD-I is characterized by recurring bacterial and fungal infections, impaired wound healing and severe gingivitis, patients also exhibit impaired leukocyte adhesion, and reduced trafficking to inflammatory sites (Becker and Lowe 1999) (Hogg and Bates 2000). LAD provides a genetic validation of our target.

2.5. Assay development



Once a target has been identified and validated the following step is the development of screening assays that allows the identification of hits.

Cell-based assays are usually used to target classes such as membrane receptors, nuclear receptors and ion channels. These assays provide a functional read-out as consequence of the activity of the compound (Michelini, et al. 2010).

The primary cell-based *in vitro* screening assay optimised to identify novel α L β 2 inhibitors was the V well assay.

Compared with standard adhesion assays, the V well adhesion assay avoids washing steps and involves precisely controlled centrifugal forces to separate adherent from non-adherent cells. In this way the variations are reduced, the assay is more reliable and reproducible. This method has been validated with different classes of adhesion molecule families (selectins and integrins) and is adaptable to several other adhesive interactions. The time necessary to perform the assay is also reduced compared with standard adhesion assay and it can be readily utilized for high throughput applications. Moreover, it may be applied to diagnose disease associated with cell adhesion defects

such as LAD (Weitz-Schmidt and Chreng 2012). Potential hits active in the V well adhesion assay, able to inhibit the interaction between α L β 2 and ICAM-1, were then planned to be screened in another assay to identify their inhibition mode. The *in vitro* assay used to determine the allosteric mode of action of the compounds was the reporter epitope assay. For the measurement of α I allosteric inhibitor binding to α L β 2, the anti- α L chain mAb R7.1 was selected. mAb R7.1 binds to a region involving the C-terminal linker of the α L β 2 I domain located on the α L chain and the β propeller located on the β 2 chain of α L β 2 (Weitz-Schmidt, et al. 2011). All α I allosteric inhibitors (of diverse chemical scaffolds) investigated to date with this antibody consistently induced R7.1 epitope loss (Welzenbach, et al. 2002) (Shimaoka, et al. 2003) (Weitz-Schmidt, et al. 2004). The sensitivity of the R7.1 epitope to α I allosteric inhibition can be considered to be established for the entire class of inhibitors.

Furthermore, we developed a whole blood assay that allows the correlation of compound/ α L β 2 interactions with therapeutically relevant, downstream biological effects.

This methodology based on flow cytometry technology allow to simultaneously assess and correlate, at the single-cell level, inhibitor-specific α L β 2 conformational change, α L β 2 expression and T cell activation in human whole blood (Welzenbach, et al. 2015).

2.6. Hit identification



Computer aided drug design (CADD) offers valuable tools for the *in silico* identification of compounds, minimizing the risk of later rejection and saving time, money and resources.

“Fail fast, fail early”, this is the new philosophy beyond the systems which could immediately reports and indicate a possible failure (Katsila, et al. 2016), and it was the driving force since the beginning of the project.

In this project, CADD has been used to identify novel allosteric inhibitors that modulate α L β 2 function via binding to the I allosteric site.

The availability of crystal structure information and different chemical lead compounds facilitates computer-assisted drug design. The CADD approach pursued addressed the task of finding novel hits and leads from two conceptually complementary angles: (1) ligand-based and (2) structure-based similarity. A collection of several million commercially available compounds with drug-like properties has been compiled. These virtual screens yielded in ranked lists of compounds tested *in*

in vitro in the adhesion assay. The first hit emerged from the V well adhesion assay approach fulfilled the selected criteria: inhibition of α L β 2-dependent adhesion with an IC₅₀ in the low mM range, lack of *in vitro* cytotoxicity, allosteric mode of action, molecular weight < 500 Da, selectivity over the integrin VLA-4, druggability and patentability.

Moreover, our first hit bound the target in a reversible manner, this kind of compounds are favoured because their effects can be more easily ‘washed-out’ following drug withdrawal, an important consideration for a drug supposed to be used in patients (Hughes, et al. 2011).

2.7. Hit to lead



The output of the hit identification in a drug discovery process should be usually a molecule, typically with potency in the range of 0.100 to 5 mM against the drug target. Our first hit, in line with this statement, shows an IC₅₀ of ~ 1.9 mM in inhibiting the adhesion of Jurkat cells to immobilized ICAM-1. Next step in the project was a chemistry programme to improve the potency of the hit (Hughes, et al. 2011).

We proceeded with intensive SAR investigations around the core compound structure (Hughes, et al. 2011), also paying attention to the physicochemical properties. Solubility and permeability assessments are crucial for a compound to be a drug, to access to the circulation if injected or to be adsorbed in the digestive system (Hogg and Bates 2000).

2.8. Lead optimization



Lead optimization is a stage of the drug discovery process in which the chemical structures of compounds or biologics are modified to improve target specificity and selectivity, pharmacodynamic and pharmacokinetic, and toxicological properties to produce a preclinical drug candidate.

Our lead, Compound 1, blocked α L β 2 mediated Jurkat cell adhesion to immobilized ICAM-1 with an IC₅₀ of 16 nM.

In the selectivity Jurkat/VCAM-1 adhesion assay, Compound 1 did not impair the adhesion, indicating selectivity for α L β 2 over VLA-4. Moreover, profiling Compound 1 activity in a mouse specific α L β 2 adhesion assay, our lead compound exhibited greater potency toward inhibition of human versus murine α L β 2, (IC₅₀: 630 nM). Such limited cross-species reactivity can be explained by the fact that the identity between the amino acid sequence of the human I domain and the murine I domain is 74.7%.

Concerning the toxicological properties, Compound 1 did not induce *in vitro* cytotoxicity in the human lymphoblastoid cell line Jurkat and in the human liver cell line HepG2 and apoptosis and/or necrosis in Jurkat cells. Compound 1 also showed *in vitro* stability in human and rat plasma.

To differentiate our lead compound from other existing α L β 2 pharmacologies, we compared Compound 1 to the α I allosteric inhibitors LFA878, the α/β I allosteric inhibitor XVA143 and the monoclonal antibody anti- α L β 2 efalizumab. These are different inhibitor classes with different mode of actions. Although these inhibitors have in common that they potently block α L β 2 function *in vitro*, they exert differential effects on the conformation of α L β 2, its expression, on ZAP70 protein levels and the internalization of engaged TCR/CD3 complex.

Compound 1, in contrast to XVA143, did not induce activation epitopes in the β 2 chain of α L β 2, a striking feature of the α/β I allosteric α L β 2 inhibitor class characteristic for the extended, intermediate affinity form of α L β 2. This induced extended, intermediate affinity form is associated with a phenomenon called ‘rolling adhesion’.

Furthermore, Compound 1, in contrast to anti- α L β 2 mAb, did not induce the unscheduled internalization of surface α L β 2 and its subsequent lysosomal translocation in leukocytes. This effect is not unique to the anti- α L β 2 mAb efalizumab. It has also been noted in other anti- α L β 2 mAb antibodies that bind close to or within the ligand binding site of α L β 2.

Moreover, we found that efalizumab affected the downmodulation of engaged TCR/CD3. While the TCR was normally internalized, the downregulation of CD3 was markedly reduced in presence of efalizumab. A similar dissection of TCR/CD3 complex expression has been observed in psoriasis patients treated with efalizumab (Vugmeyster, et al. 2004) (Guttman-Yassky, et al. 2008).

Our research into the mechanism of this phenomenon revealed that efalizumab-induced internalization of α L β 2 was associated with reduced ZAP70 levels. As ZAP70 is constitutively bound to α L β 2 (Evans, et al. 2011), these reduced ZAP70 levels may be explained by enhanced concomitant transport of ZAP70 and α L β 2 to the lysosome and potential degradation.

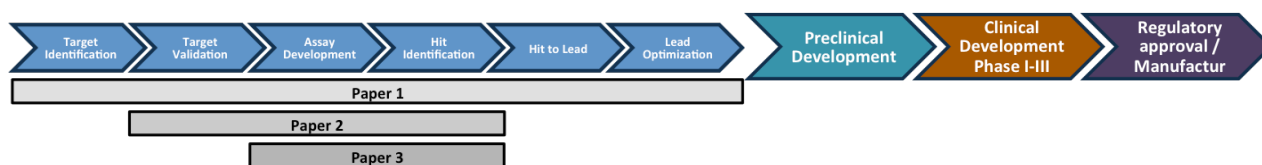
Moreover, it is tempting to speculate that α L β 2 internalization leading to reduced ZAP70 levels and disturbed expression of engaged TCR/CD3 may contribute to or may even constitute the basis of the unique state of T cell hyporesponsiveness observed in efalizumab treated patients (Guttman-Yassky, et al. 2008) (Koszik, et al. 2010) (Kuschei, et al. 2011).

In contrast to efalizumab and α/β I allosteric inhibitors, α I allosteric α L β 2 inhibitors did neither internalize α L β 2 nor reduce ZAP70 protein levels and, as a consequence, allowed for the simultaneous internalization of engaged TCR/CD3.

In the light of these favourable results, Compound 1 was assessed for oral bioavailability *in vivo* in rats where it showed to be absorbed and detectable in plasma.

It is possible to further optimize compound characteristics by knowing how fast a drug is metabolized and cleared from the body, the fraction of the drug administered that enters systemic circulation upon dosing, the volume of plasma the dose dissolved in, and the estimate of the dose required in humans using animal models (Hughes, et al. 2011).

3. Outlook



The next major step in our project will be to assess the efficacy of the selected lead compounds in an animal disease model (Whiteside and Kennedy 2010). Animal disease models are designed to simulate some pathological conditions of the human. Animal models are essential for translation of drug findings from bench to bedside (Denayer, et al. 2014).

The presence of lymphocytes strongly expressing α L β 2 adjacent to the ICAM-1 expressing cells suggests that the interaction of ICAM-1 with α L β 2 is important in the development of ocular inflammation in uveitis in humans (Uchio, et al. 1994). mAbs directed against α L β 2 or ICAM-1 can be used to protect against experimental uveitis (Uchio, et al. 1994). For those reasons, animal models of autoimmune uveitis can be suitable for POC.

To date no animal model can reproduce the full complexity of the human disease, it is necessary to develop and use a variety of models to represent the different aspects and diverse clinical/immunological manifestations of uveitis. Experimental autoimmune uveitis (EAU) is induced by immunization of animals with the retinal antigens known to elicit responses in lymphocytes isolated from patients with uveitis (Caspi 2010).

There are mouse models of experimental autoimmune uveitis well characterized and validated. These models already helped in elucidating the genetic influences, dissecting the basic mechanisms of pathogenesis and testing novel immunotherapeutic paradigms (Caspi, et al. 2008).

Rabbit models of experimental uveitis are promising to test the efficacy of compounds that target the α I domain because of the high homology score between human α L β 2 and rabbit α L β 2.

The dissection of the different mechanisms of α L β 2 inhibition by their downstream effect profiles, as established by this study, the proof of concept in animal models will be of high relevance for future therapeutic translation of these modes of action.

In this context, it is intriguing to note that our α L β 2 inhibitory mechanism of action, which is devoid of unwanted downstream effects, remains the only mechanism of action not advanced to clinical proof-of-concept, to date.

Not suspected initially, the heavy reliance of preclinical research on murine disease models of autoimmunity may have contributed to this lag in translation. While α I allosteric inhibition have been shown to be highly effective in certain murine experimental disease models (Zhong, et al. 2012) (Wan, et al. 2003) (Suchard, et al. 2010), mice (for their limited cross-species reactivity) may

not be the best suited species to explore the full therapeutic potential. A second reason for the limited progress made with α I allosteric inhibitors in the past, compared to the other pharmacological mechanisms assessed in this study, may be their strict selectivity for α L β 2, by itself. The α I allosteric mechanism of action is neither expected to affect β 2 integrins other than α L β 2, in contrast to what has been observed with α/β I allosteric inhibitors (Shimaoka, et al. 2003) (Welzenbach, et al. 2002), nor to affect the expression of other major immune receptors as observed with the antibody approach (Vugmeyster, et al. 2004) (Guttman-Yassky, et al. 2008). Indeed, a strictly α L β 2 selective pharmacology may not be best-suited to support conventional therapeutic concepts of suppressive immune modulation. Innovative therapeutic concepts, educated and guided by the exceptionally well-characterized biologic functions of α L β 2, may be required to realize the therapeutic potential of an exclusively α L β 2 selective pharmacology, eventually.

“The whole is more than the sum of its parts”

Aristotle

384–322 BC

Greek philosopher and scientist

Drug discovery is a multidisciplinary process where different fields of knowledge come across, and where people with different background need to work together aiming for a common result.

The success of a project, the medical and scientific advances, are often built on the back of a synergic work.

References

- Ahrens, I., and K. Peter
2008 Therapeutic integrin inhibition: allosteric and activation-specific inhibition strategies may surpass the initial ligand-mimetic strategies. *Thromb Haemost* 99(5):803-4.
- Almokadem, S., and C. P. Belani
2012 Volociximab in cancer. *Expert Opin Biol Ther* 12(2):251-7.
- Arefanian, H., et al.
2010 Short-term administrations of a combination of anti-LFA-1 and anti-CD154 monoclonal antibodies induce tolerance to neonatal porcine islet xenografts in mice. *Diabetes* 59(4):958-66.
- Bailly, P., et al.
1994 The LW blood group glycoprotein is homologous to intercellular adhesion molecules. *Proc Natl Acad Sci U S A* 91(12):5306-10.
- Becker, Daniel J., and John B. Lowe
1999 Leukocyte adhesion deficiency type II. *Biochimica et Biophysica Acta (BBA) - Molecular Basis of Disease* 1455(2-3):193-204.
- Benkert, T. F., et al.
2012 Natalizumab exerts direct signaling capacity and supports a pro-inflammatory phenotype in some patients with multiple sclerosis. *PLoS One* 7(12):e52208.
- Bloy, C., et al.
1989 Properties of the blood group LW glycoprotein and preliminary comparison with Rh proteins. *Mol Immunol* 26(11):1013-9.
- Boehncke, W. H.
2007a Efalizumab in the treatment of psoriasis. *Biologics* 1(3):301-9.
- Boehncke, Wolf-Henning
2007b Efalizumab in the treatment of psoriasis. *Biologics : Targets & Therapy* 1(3):301-309.
- Brennan, F. R., et al.
2010 Safety and immunotoxicity assessment of immunomodulatory monoclonal antibodies. *MAbs* 2(3):233-55.
- Burke, P. A., et al.
2002 Cilengitide targeting of alpha(v)beta(3) integrin receptor synergizes with radioimmunotherapy to increase efficacy and apoptosis in breast cancer xenografts. *Cancer Res* 62(15):4263-72.
- Burke, R. D.
1999 Invertebrate integrins: structure, function, and evolution. *Int Rev Cytol* 191:257-84.
- Campbell, I. D., and M. J. Humphries
2011 Integrin structure, activation, and interactions. *Cold Spring Harb Perspect Biol* 3(3).
- Carson, K. R., et al.
2009 Monoclonal antibody-associated progressive multifocal leucoencephalopathy in patients treated with rituximab, natalizumab, and efalizumab: a Review from the Research on Adverse Drug Events and Reports (RADAR) Project. *Lancet Oncol* 10(8):816-24.
- Caspi, R. R.
2010 A look at autoimmunity and inflammation in the eye. *J Clin Invest* 120(9):3073-83.
- Caspi, Rachel R., et al.
2008 Mouse Models of Experimental Autoimmune Uveitis. *Ophthalmic research* 40(3-4):169-174.
- Champe, M., B. W. McIntyre, and P. W. Berman

- 1995 Monoclonal antibodies that block the activity of leukocyte function-associated antigen 1 recognize three discrete epitopes in the inserted domain of CD11a. *J Biol Chem* 270(3):1388-94.
- Chan, J. R., S. J. Hyduk, and M. I. Cybulsky
2000 Alpha 4 beta 1 integrin/VCAM-1 interaction activates alpha L beta 2 integrin-mediated adhesion to ICAM-1 in human T cells. *J Immunol* 164(2):746-53.
- Chen, W., J. Lou, and C. Zhu
2010 Forcing switch from short- to intermediate- and long-lived states of the alphaA domain generates LFA-1/ICAM-1 catch bonds. *J Biol Chem* 285(46):35967-78.
- Chen, X. P., and G. H. Du
2007 Target validation: A door to drug discovery. *Drug Discov Ther* 1(1):23-9.
- Chetty, Manoranjenni, et al.
2014 Prediction of the Pharmacokinetics, Pharmacodynamics, and Efficacy of a Monoclonal Antibody, Using a Physiologically Based Pharmacokinetic FcRn Model. *Frontiers in Immunology* 5:670.
- Chigaev, A., and L. A. Sklar
2012 Aspects of VLA-4 and LFA-1 regulation that may contribute to rolling and firm adhesion. *Front Immunol* 3:242.
- Chigaev, A., et al.
2015 FRET detection of lymphocyte function-associated antigen-1 conformational extension. *Mol Biol Cell* 26(1):43-54.
- Chigaev, A., et al.
2011 Discovery of very late antigen-4 (VLA-4, alpha4beta1 integrin) allosteric antagonists. *J Biol Chem* 286(7):5455-63.
- Chiricozzi, A., et al.
2016 Small molecules and antibodies for the treatment of psoriasis: a patent review (2010-2015). *Expert Opin Ther Pat*:1-10.
- Chittasupho, C., et al.
2010 cIBR effectively targets nanoparticles to LFA-1 on acute lymphoblastic T cells. *Mol Pharm* 7(1):146-55.
- Clarke, J., et al.
2004 Evaluation of a surrogate antibody for preclinical safety testing of an anti-CD11a monoclonal antibody. *Regul Toxicol Pharmacol* 40(3):219-26.
- Coffey, G. P., et al.
2005 Tissue distribution and receptor-mediated clearance of anti-CD11a antibody in mice. *Drug Metab Dispos* 33(5):623-9.
- Coller, B. S.
2014 The platelet: life on the razor's edge between hemorrhage and thrombosis. *Transfusion* 54(9):2137-46.
- Conrad, C., et al.
2007 Alpha1beta1 integrin is crucial for accumulation of epidermal T cells and the development of psoriasis. *Nat Med* 13(7):836-42.
- Cook-Mills, J. M., M. E. Marchese, and H. Abdala-Valencia
2011 Vascular cell adhesion molecule-1 expression and signaling during disease: regulation by reactive oxygen species and antioxidants. *Antioxid Redox Signal* 15(6):1607-38.
- Corbi, A. L., et al.
1987 cDNA cloning and complete primary structure of the alpha subunit of a leukocyte adhesion glycoprotein, p150,95. *Embo j* 6(13):4023-8.
- Davignon, D., et al.

- 1981 Lymphocyte function-associated antigen 1 (LFA-1): a surface antigen distinct from Lyt-2,3 that participates in T lymphocyte-mediated killing. *Proc Natl Acad Sci U S A* 78(7):4535-9.
- de Fougerolles, A. R., X. Qin, and T. A. Springer
1994 Characterization of the function of intercellular adhesion molecule (ICAM)-3 and comparison with ICAM-1 and ICAM-2 in immune responses. *J Exp Med* 179(2):619-29.
- de Fougerolles, A. R., and T. A. Springer
1992 Intercellular adhesion molecule 3, a third adhesion counter-receptor for lymphocyte function-associated molecule 1 on resting lymphocytes. *J Exp Med* 175(1):185-90.
- de Fougerolles, A. R., et al.
1991 Characterization of ICAM-2 and evidence for a third counter-receptor for LFA-1. *J Exp Med* 174(1):253-67.
- Denayer, Tinneke, Thomas Stöhr, and Maarten Van Roy
2014 Animal models in translational medicine: Validation and prediction. *New Horizons in Translational Medicine* 2(1):5-11.
- Dustin, M. L., et al.
1986 Induction by IL 1 and interferon-gamma: tissue distribution, biochemistry, and function of a natural adherence molecule (ICAM-1). *J Immunol* 137(1):245-54.
- Elices, M. J., et al.
1990 VCAM-1 on activated endothelium interacts with the leukocyte integrin VLA-4 at a site distinct from the VLA-4/fibronectin binding site. *Cell* 60(4):577-84.
- Estevez, B., B. Shen, and X. Du
2015 Targeting integrin and integrin signaling in treating thrombosis. *Arterioscler Thromb Vasc Biol* 35(1):24-9.
- Evans, R., et al.
2011 The integrin LFA-1 signals through ZAP-70 to regulate expression of high-affinity LFA-1 on T lymphocytes. *Blood* 117(12):3331-42.
- Faia, L. J., et al.
2011a Treatment of inflammatory macular edema with humanized anti-CD11a antibody therapy. *Invest Ophthalmol Vis Sci* 52(9):6919-24.
- Faia, Lisa J., et al.
2011b Treatment of Inflammatory Macular Edema with Humanized Anti-CD11a Antibody Therapy. *Investigative Ophthalmology & Visual Science* 52(9):6919-6924.
- Feigelson, S. W., et al.
2010 Occupancy of lymphocyte LFA-1 by surface-immobilized ICAM-1 is critical for TCR- but not for chemokine-triggered LFA-1 conversion to an open headpiece high-affinity state. *J Immunol* 185(12):7394-404.
- Fritzsche, J., D. Simonis, and G. Bendas
2008 Melanoma cell adhesion can be blocked by heparin in vitro: suggestion of VLA-4 as a novel target for antimetastatic approaches. *Thromb Haemost* 100(6):1166-75.
- Gao, J., et al.
2004 ICAM-1 expression predisposes ocular tissues to immune-based inflammation in dry eye patients and Sjogrens syndrome-like MRL/lpr mice. *Exp Eye Res* 78(4):823-35.
- Giblin, P. A., and R. M. Lemieux
2006 LFA-1 as a key regulator of immune function: approaches toward the development of LFA-1-based therapeutics. *Curr Pharm Des* 12(22):2771-95.
- Glawe, J. D., et al.
2009 Genetic deficiency of Itgb2 or ItgaL prevents autoimmune diabetes through distinctly different mechanisms in NOD/LtJ mice. *Diabetes* 58(6):1292-301.
- Graf, B., T. Bushnell, and J. Miller

- 2007 LFA-1-mediated T cell costimulation through increased localization of TCR/class II complexes to the central supramolecular activation cluster and exclusion of CD45 from the immunological synapse. *J Immunol* 179(3):1616-24.
- Greve, J. M., et al.
1989 The major human rhinovirus receptor is ICAM-1. *Cell* 56(5):839-47.
- Guttman-Yassky, E., et al.
2008 Blockade of CD11a by efalizumab in psoriasis patients induces a unique state of T-cell hyporesponsiveness. *J Invest Dermatol* 128(5):1182-91.
- Hafezi-Moghadam, A., et al.
2007 VLA-4 blockade suppresses endotoxin-induced uveitis: in vivo evidence for functional integrin up-regulation. *FASEB J* 21(2):464-74.
- Hemler, M. E., et al.
1990 Structure of the integrin VLA-4 and its cell-cell and cell-matrix adhesion functions. *Immunol Rev* 114:45-65.
- Hemler, M. E., C. Huang, and L. Schwarz
1987 The VLA protein family. Characterization of five distinct cell surface heterodimers each with a common 130,000 molecular weight beta subunit. *J Biol Chem* 262(7):3300-9.
- Hildreth, J. E., and J. T. August
1985 The human lymphocyte function-associated (HLFA) antigen and a related macrophage differentiation antigen (HMac-1): functional effects of subunit-specific monoclonal antibodies. *J Immunol* 134(5):3272-80.
- Hogg, N., and P. A. Bates
2000 Genetic analysis of integrin function in man: LAD-1 and other syndromes. *Matrix Biol* 19(3):211-22.
- Hogg, Nancy, Irene Patzak, and Frances Willenbrock
2011 The insider's guide to leukocyte integrin signalling and function. *Nat Rev Immunol* 11(6):416-426.
- Holland, E. J., et al.
2016 Lifitegrast clinical efficacy for treatment of signs and symptoms of dry eye disease across three randomized controlled trials. *Curr Med Res Opin*:1-7.
- Hughes, J. P., et al.
2011 Principles of early drug discovery. *Br J Pharmacol* 162(6):1239-49.
- Humphries, J. D., A. Byron, and M. J. Humphries
2006 Integrin ligands at a glance. *J Cell Sci* 119(Pt 19):3901-3.
- Hynes, R. O.
2002 Integrins: bidirectional, allosteric signaling machines. *Cell* 110(6):673-87.
- Johnson, M. S., and B. S. Chouhan
2014 Evolution of integrin I domains. *Adv Exp Med Biol* 819:1-19.
- Jones, A. W.
2011 Early drug discovery and the rise of pharmaceutical chemistry. *Drug Test Anal* 3(6):337-44.
- Kapp, T. G., et al.
2013 Integrin modulators: a patent review. *Expert Opin Ther Pat* 23(10):1273-95.
- Karsan, A., et al.
1998 Leukocyte Adhesion Deficiency Type II is a generalized defect of de novo GDP-fucose biosynthesis. Endothelial cell fucosylation is not required for neutrophil rolling on human nonlymphoid endothelium. *J Clin Invest* 101(11):2438-45.
- Katsila, Theodora, et al.
2016 Computational approaches in target identification and drug discovery. *Computational and Structural Biotechnology Journal* 14:177-184.
- Ke, Y., et al.

- 2007 Suppression of established experimental autoimmune uveitis by anti-LFA-1alpha Ab. *Invest Ophthalmol Vis Sci* 48(6):2667-75.
- Keene, D. L., et al.
2011 Monoclonal antibodies and progressive multifocal leukoencephalopathy. *Can J Neurol Sci* 38(4):565-71.
- Kern, A., and E. E. Marcantonio
1998 Role of the I-domain in collagen binding specificity and activation of the integrins alpha1beta1 and alpha2beta1. *J Cell Physiol* 176(3):634-41.
- Kishimoto, T. K., et al.
1987 Heterogeneous mutations in the beta subunit common to the LFA-1, Mac-1, and p150,95 glycoproteins cause leukocyte adhesion deficiency. *Cell* 50(2):193-202.
- Koszik, F., et al.
2010 Efalizumab modulates T cell function both in vivo and in vitro. *J Dermatol Sci* 60(3):159-66.
- Kuschei, W. M., et al.
2011 Costimulatory signals potently modulate the T cell inhibitory capacity of the therapeutic CD11a antibody Efalizumab. *Clin Immunol* 139(2):199-207.
- Laberge, S., et al.
1995 Role of VLA-4 and LFA-1 in allergen-induced airway hyperresponsiveness and lung inflammation in the rat. *Am J Respir Crit Care Med* 151(3 Pt 1):822-9.
- Landen, C. N., et al.
2008 Tumor-selective response to antibody-mediated targeting of alphavbeta3 integrin in ovarian cancer. *Neoplasia* 10(11):1259-67.
- Lau, T. L., et al.
2009 The structure of the integrin alphaIIb beta3 transmembrane complex explains integrin transmembrane signalling. *Embo j* 28(9):1351-61.
- Lebwohl, M., et al.
2003 A novel targeted T-cell modulator, efalizumab, for plaque psoriasis. *N Engl J Med* 349(21):2004-13.
- Lee, J. O., et al.
1995 Two conformations of the integrin A-domain (I-domain): a pathway for activation? *Structure* 3(12):1333-40.
- Lee, S. H., et al.
2008 Developmental control of integrin expression regulates Th2 effector homing. *J Immunol* 180(7):4656-67.
- Ley, K., et al.
2016 Integrin-based therapeutics: biological basis, clinical use and new drugs. *Nat Rev Drug Discov* 15(3):173-83.
- Li, S., et al.
2009 Efalizumab binding to the LFA-1 alphaL I domain blocks ICAM-1 binding via steric hindrance. *Proc Natl Acad Sci U S A* 106(11):4349-54.
- Liebig, J.
1831 Ueber die Zersetzung des Alkohols durch Chlor. *Annalen der Physik* 99(11):444-444.
- Liebig, Justus
1832 Ueber die Verbindungen, welche durch die Einwirkung des Chlors auf Alkohol, Aether, ölbildendes Gas und Essiggeist entstehen. *Annalen der Pharmacie* 1(2):182-230.
- Lin, K. C., and A. C. Castro
1998 Very late antigen 4 (VLA4) antagonists as anti-inflammatory agents. *Curr Opin Chem Biol* 2(4):453-7.
- Littler, A. J., et al.

- 1997 A distinct profile of six soluble adhesion molecules (ICAM-1, ICAM-3, VCAM-1, E-selectin, L-selectin and P-selectin) in rheumatoid arthritis. *Br J Rheumatol* 36(2):164-9.
- Lutterotti, A., and R. Martin
2008 Getting specific: monoclonal antibodies in multiple sclerosis. *Lancet Neurol* 7(6):538-47.
- Major, E. O.
2010 Progressive multifocal leukoencephalopathy in patients on immunomodulatory therapies. *Annu Rev Med* 61:35-47.
- Marlin, S. D., and T. A. Springer
1987 Purified intercellular adhesion molecule-1 (ICAM-1) is a ligand for lymphocyte function-associated antigen 1 (LFA-1). *Cell* 51(5):813-9.
- Martin, A. P., et al.
2005 Administration of a peptide inhibitor of alpha4-integrin inhibits the development of experimental autoimmune uveitis. *Invest Ophthalmol Vis Sci* 46(6):2056-63.
- Meira, M., et al.
2016 Natalizumab-induced POU2AF1/Spi-B upregulation: A possible route for PML development. *Neurol Neuroimmunol Neuroinflamm* 3(3):e223.
- Michelini, E., et al.
2010 Cell-based assays: fuelling drug discovery. *Anal Bioanal Chem* 398(1):227-38.
- Millard, M., S. Odde, and N. Neamati
2011 Integrin targeted therapeutics. *Theranostics* 1:154-88.
- Minoux, H., et al.
2000 Structural analysis of the KGD sequence loop of barbourin, an alphaIIb beta3-specific disintegrin. *J Comput Aided Mol Des* 14(4):317-27.
- Mittelbrunn, M., et al.
2004 VLA-4 integrin concentrates at the peripheral supramolecular activation complex of the immune synapse and drives T helper 1 responses. *Proc Natl Acad Sci U S A* 101(30):11058-63.
- Naik, U. P., et al.
2001 Characterization and chromosomal localization of JAM-1, a platelet receptor for a stimulatory monoclonal antibody. *J Cell Sci* 114(Pt 3):539-47.
- Nakakura, E. K., et al.
1993 Potent and effective prolongation by anti-LFA-1 monoclonal antibody monotherapy of non-primarily vascularized heart allograft survival in mice without T cell depletion. *Transplantation* 55(2):412-7.
- Navarini, A. A., et al.
2010 Control of widespread hypertrophic lupus erythematosus with T-cell-directed biologic efalizumab. *Dermatology* 220(3):249-53.
- Ng, C. M., et al.
2010 Mechanism-based receptor-binding model to describe the pharmacokinetic and pharmacodynamic of an anti-alpha5beta1 integrin monoclonal antibody (volociximab) in cancer patients. *Cancer Chemother Pharmacol* 65(2):207-17.
- Nicolls, M. R., and R. G. Gill
2006 LFA-1 (CD11a) as a therapeutic target. *Am J Transplant* 6(1):27-36.
- Nijsten, T., et al.
2009 The misperception that clinical trial data reflect long-term drug safety: lessons learned from Efalizumab's withdrawal. *Arch Dermatol* 145(9):1037-9.
- Nishida, N., et al.
2006 Activation of leukocyte beta2 integrins by conversion from bent to extended conformations. *Immunity* 25(4):583-94.
- Overington, J. P., B. Al-Lazikani, and A. L. Hopkins

- 2006 How many drug targets are there? *Nat Rev Drug Discov* 5(12):993-6.
- Paczesny, Sophie, Sung W. Choi, and James L. M. Ferrara
2009 Acute Graft versus Host Disease: New Treatment Strategies. *Current opinion in hematology* 16(6):427-436.
- Pankov, R., and K. M. Yamada
2002 Fibronectin at a glance. *J Cell Sci* 115(Pt 20):3861-3.
- Philipsen, L., et al.
2013 Multimolecular analysis of stable immunological synapses reveals sustained recruitment and sequential assembly of signaling clusters. *Mol Cell Proteomics* 12(9):2551-67.
- Plow, E. F., et al.
2000 Ligand binding to integrins. *J Biol Chem* 275(29):21785-8.
- Poria, R. B., et al.
2006 Characterization of a radiolabeled small molecule targeting leukocyte function-associated antigen-1 expression in lymphoma and leukemia. *Cancer Biother Radiopharm* 21(5):418-26.
- Porter, J. C., and N. Hogg
1997 Integrin cross talk: activation of lymphocyte function-associated antigen-1 on human T cells alters alpha4beta1- and alpha5beta1-mediated function. *J Cell Biol* 138(6):1437-47.
- Posselt, A. M., et al.
2010 Islet transplantation in type 1 diabetics using an immunosuppressive protocol based on the anti-LFA-1 antibody efalizumab. *Am J Transplant* 10(8):1870-80.
- Rahman, A., and F. Fazal
2009 Hug tightly and say goodbye: role of endothelial ICAM-1 in leukocyte transmigration. *Antioxid Redox Signal* 11(4):823-39.
- Reimann, K. A., et al.
1994 Use of human leukocyte-specific monoclonal antibodies for clinically immunophenotyping lymphocytes of rhesus monkeys. *Cytometry* 17(1):102-8.
- Reisman, N. M., et al.
2011 LFA-1 blockade induces effector and regulatory T-cell enrichment in lymph nodes and synergizes with CTLA-4Ig to inhibit effector function. *Blood* 118(22):5851-61.
- Rispens, T., et al.
2011 Measurement of serum levels of natalizumab, an immunoglobulin G4 therapeutic monoclonal antibody. *Anal Biochem* 411(2):271-6.
- Robert, P., et al.
2011 A novel leukocyte adhesion deficiency III variant: kindlin-3 deficiency results in integrin- and nonintegrin-related defects in different steps of leukocyte adhesion. *J Immunol* 186(9):5273-83.
- Ronald, J. A., et al.
2001 Differential regulation of transendothelial migration of THP-1 cells by ICAM-1/LFA-1 and VCAM-1/VLA-4. *J Leukoc Biol* 70(4):601-9.
- Rothlein, R., et al.
1986 A human intercellular adhesion molecule (ICAM-1) distinct from LFA-1. *J Immunol* 137(4):1270-4.
- Rothlein, R., and T. A. Springer
1986 The requirement for lymphocyte function-associated antigen 1 in homotypic leukocyte adhesion stimulated by phorbol ester. *J Exp Med* 163(5):1132-49.
- Ruoslahti, E., and M. D. Pierschbacher
1986 Arg-Gly-Asp: a versatile cell recognition signal. *Cell* 44(4):517-8.
- Salas, A., et al.

References

- 2004 Rolling adhesion through an extended conformation of integrin alphaLbeta2 and relation to alpha I and beta I-like domain interaction. *Immunity* 20(4):393-406.
- Sanchez-Madrid, F., et al.
1982 Three distinct antigens associated with human T-lymphocyte-mediated cytotoxicity: LFA-1, LFA-2, and LFA-3. *Proc Natl Acad Sci U S A* 79(23):7489-93.
- Sawada, K., et al.
2012 Integrin inhibitors as a therapeutic agent for ovarian cancer. *J Oncol* 2012:915140.
- Schlesinger, M., et al.
2009 Binding between heparin and the integrin VLA-4. *Thromb Haemost* 102(5):816-22.
- Schmidmaier, R., et al.
2007 Inhibition of lymphocyte function associated antigen 1 by LFA878 induces apoptosis in multiple myeloma cells and is associated with downregulation of the focal adhesion kinase/phosphatidylinositol 3 kinase/Akt pathway. *Int J Oncol* 31(4):969-76.
- Schmidmaier, R., et al.
2006 Synergistic antimyeloma effects of zoledronate and simvastatin. *Anticancer Drugs* 17(6):621-9.
- Schurpf, T., and T. A. Springer
2011 Regulation of integrin affinity on cell surfaces. *EMBO J* 30(23):4712-27.
- Semba, C. P., et al.
2012 A phase 2 randomized, double-masked, placebo-controlled study of a novel integrin antagonist (SAR 1118) for the treatment of dry eye. *Am J Ophthalmol* 153(6):1050-60 e1.
- Seminara, N. M., and J. M. Gelfand
2010 Assessing long-term drug safety: lessons (re) learned from raptiva. *Semin Cutan Med Surg* 29(1):16-9.
- Shaw, J. M., et al.
2001 Characterization of four CD18 mutants in leucocyte adhesion deficient (LAD) patients with differential capacities to support expression and function of the CD11/CD18 integrins LFA-1, Mac-1 and p150,95. *Clin Exp Immunol* 126(2):311-8.
- Sheppard, J. D., et al.
2014 Lifitegrast ophthalmic solution 5.0% for treatment of dry eye disease: results of the OPUS-1 phase 3 study. *Ophthalmology* 121(2):475-83.
- Shimaoka, M., et al.
2003 Small molecule integrin antagonists that bind to the beta2 subunit I-like domain and activate signals in one direction and block them in the other. *Immunity* 19(3):391-402.
- Stewart, P. L., and G. R. Nemerow
2007 Cell integrins: commonly used receptors for diverse viral pathogens. *Trends Microbiol* 15(11):500-7.
- Suchard, S. J., et al.
2010 An LFA-1 (alphaLbeta2) small-molecule antagonist reduces inflammation and joint destruction in murine models of arthritis. *J Immunol* 184(7):3917-26.
- Suzuki, J., et al.
2007 The actin cloud induced by LFA-1-mediated outside-in signals lowers the threshold for T-cell activation. *Blood* 109(1):168-75.
- Tamkun, J. W., et al.
1986 Structure of integrin, a glycoprotein involved in the transmembrane linkage between fibronectin and actin. *Cell* 46(2):271-82.
- Tan, S. M.
2012 The leucocyte beta2 (CD18) integrins: the structure, functional regulation and signalling properties. *Biosci Rep* 32(3):241-69.
- Tardif, M. R., et al.

- 2009 LFA-1 antagonists as agents limiting human immunodeficiency virus type 1 infection and transmission and potentiating the effect of the fusion inhibitor T-20. *Antimicrob Agents Chemother* 53(11):4656-66.
- Tauber, J., et al.
2015 Lifitegrast Ophthalmic Solution 5.0% versus Placebo for Treatment of Dry Eye Disease: Results of the Randomized Phase III OPUS-2 Study. *Ophthalmology* 122(12):2423-31.
- Tofteng, C. L., et al.
2007 Integrin beta3 Leu33Pro polymorphism and risk of hip fracture: 25 years follow-up of 9233 adults from the general population. *Pharmacogenet Genomics* 17(1):85-91.
- Toivanen, A., et al.
2008 Importance of molecular studies on major blood groups--intercellular adhesion molecule-4, a blood group antigen involved in multiple cellular interactions. *Biochim Biophys Acta* 1780(3):456-66.
- Tyler, K. L.
2010 Progressive multifocal leukoencephalopathy: can we reduce risk in patients receiving biological immunomodulatory therapies? *Ann Neurol* 68(3):271-4.
- Uchio, E., et al.
1994 Suppression of experimental uveitis with monoclonal antibodies to ICAM-1 and LFA-1. *Invest Ophthalmol Vis Sci* 35(5):2626-31.
- Usmani, N., and M. Goodfield
2007 Efalizumab in the treatment of discoid lupus erythematosus. *Arch Dermatol* 143(7):873-7.
- Verma, N. K., et al.
2012 Leukocyte function-associated antigen-1/intercellular adhesion molecule-1 interaction induces a novel genetic signature resulting in T-cells refractory to transforming growth factor-beta signaling. *J Biol Chem* 287(32):27204-16.
- Vicente-Manzanares, M., and F. Sanchez-Madrid
2004 Role of the cytoskeleton during leukocyte responses. *Nat Rev Immunol* 4(2):110-22.
- Vugmeyster, Y., et al.
2004 Efalizumab (anti-CD11a)-induced increase in peripheral blood leukocytes in psoriasis patients is preferentially mediated by altered trafficking of memory CD8+ T cells into lesional skin. *Clin Immunol* 113(1):38-46.
- Wan, M. X., et al.
2003 A statin-based inhibitor of lymphocyte function antigen-1 protects against ischemia/reperfusion-induced leukocyte adhesion in the colon. *Br J Pharmacol* 140(2):395-401.
- Wayner, E. A., et al.
1989 Identification and characterization of the T lymphocyte adhesion receptor for an alternative cell attachment domain (CS-1) in plasma fibronectin. *J Cell Biol* 109(3):1321-30.
- Weitz-Schmidt, G., and S. Chreng
2012 Cell adhesion assays. *Methods Mol Biol* 757:15-30.
- Weitz-Schmidt, G., S. Chreng, and S. Riek
2009 Allosteric LFA-1 inhibitors modulate natural killer cell function. *Mol Pharmacol* 75(2):355-62.
- Weitz-Schmidt, G., T. Schurpf, and T. A. Springer
2011 The C-terminal alphaI domain linker as a critical structural element in the conformational activation of alphaI integrins. *J Biol Chem* 286(49):42115-22.
- Weitz-Schmidt, G., et al.
2001 Statins selectively inhibit leukocyte function antigen-1 by binding to a novel regulatory integrin site. *Nat Med* 7(6):687-92.

- Weitz-Schmidt, G., et al.
 2004 Improved lymphocyte function-associated antigen-1 (LFA-1) inhibition by statin derivatives: molecular basis determined by x-ray analysis and monitoring of LFA-1 conformational changes in vitro and ex vivo. *J Biol Chem* 279(45):46764-71.
- Welzenbach, K., U. Hommel, and G. Weitz-Schmidt
 2002 Small molecule inhibitors induce conformational changes in the I domain and the I-like domain of lymphocyte function-associated antigen-1. Molecular insights into integrin inhibition. *J Biol Chem* 277(12):10590-8.
- Welzenbach, K., et al.
 2015 A novel multi-parameter assay to dissect the pharmacological effects of different modes of integrin alphaLbeta2 inhibition in whole blood. *Br J Pharmacol* 172(20):4875-87.
- Whitcup, S. M., et al.
 1993 Monoclonal antibodies against ICAM-1 (CD54) and LFA-1 (CD11a/CD18) inhibit experimental autoimmune uveitis. *Clin Immunol Immunopathol* 67(2):143-50.
- Whitcup, S. M., et al.
 1995 Monoclonal antibodies against CD54 (ICAM-1) and CD11a (LFA-1) prevent and inhibit endotoxin-induced uveitis. *Exp Eye Res* 60(6):597-601.
- Whiteside, G. T., and J. D. Kennedy
 2010 *Frontiers in Neuroscience*
 Consideration of Pharmacokinetic Pharmacodynamic Relationships in the Discovery of New Pain Drugs. *In Translational Pain Research: From Mouse to Man*. L. Kruger and A.R. Light, eds. Boca Raton, FL: CRC Press/Taylor & Francis
- Llc.
- Witkowska, A. M.
 2005 Soluble ICAM-1: a marker of vascular inflammation and lifestyle. *Cytokine* 31(2):127-34.
- Witkowska, A. M., and M. H. Borawska
 2004 Soluble intercellular adhesion molecule-1 (sICAM-1): an overview. *Eur Cytokine Netw* 15(2):91-8.
- Wojcikiewicz, E. P., et al.
 2009 LFA-1 binding destabilizes the JAM-A homophilic interaction during leukocyte transmigration. *Biophys J* 96(1):285-93.
- Wyatt, P. G., et al.
 2011 Target validation: linking target and chemical properties to desired product profile. *Curr Top Med Chem* 11(10):1275-83.
- Xiao, X., D. D. Mruk, and C. Y. Cheng
 2013 Intercellular adhesion molecules (ICAMs) and spermatogenesis. *Hum Reprod Update* 19(2):167-86.
- Xing, L., J. M. Casasnovas, and R. H. Cheng
 2003 Structural analysis of human rhinovirus complexed with ICAM-1 reveals the dynamics of receptor-mediated virus uncoating. *J Virol* 77(11):6101-7.
- Yang, W., et al.
 2006 A small molecule agonist of an integrin, alphaLbeta2. *J Biol Chem* 281(49):37904-12.
- Yang, W., et al.
 2004 Activation of integrin beta-subunit I-like domains by one-turn C-terminal alpha-helix deletions. *Proc Natl Acad Sci U S A* 101(8):2333-8.
- Yednock, T. A., et al.
 1992 Prevention of experimental autoimmune encephalomyelitis by antibodies against alpha 4 beta 1 integrin. *Nature* 356(6364):63-6.
- Yoshihara, Y., et al.

References

- 1994 An ICAM-related neuronal glycoprotein, telencephalin, with brain segment-specific expression. *Neuron* 12(3):541-53.
- Yousry, T. A., et al.
2006 Evaluation of patients treated with natalizumab for progressive multifocal leukoencephalopathy. *N Engl J Med* 354(9):924-33.
- Yousry, Tarek A., et al.
2006 Evaluation of Patients Treated with Natalizumab for Progressive Multifocal Leukoencephalopathy. *New England Journal of Medicine* 354(9):924-933.
- Zaidel-Bar, R., et al.
2007 Functional atlas of the integrin adhesome. *Nat Cell Biol* 9(8):858-67.
- Zecchinon, L., et al.
2006 LFA-1 and associated diseases: The dark side of a receptor. *Clinical and Applied Immunology Reviews* 6(3-4):201-216.
- Zhong, M., et al.
2012 Discovery and Development of Potent LFA-1/ICAM-1 Antagonist SAR 1118 as an Ophthalmic Solution for Treating Dry Eye. *ACS Med Chem Lett* 3(3):203-6.
- Zohren, F., et al.
2008 The monoclonal anti-VLA-4 antibody natalizumab mobilizes CD34+ hematopoietic progenitor cells in humans. *Blood* 111(7):3893-5.
- Zonneveld, R., et al.
2014 Soluble adhesion molecules as markers for sepsis and the potential pathophysiological discrepancy in neonates, children and adults. *Crit Care* 18(2):204.

Riccardo Mancuso

Mobile: +41 078 96 32 095
Email: riccardo.mancuso@unibas.ch
mancuso.riccardo.bio@gmail.com
Birth: 3, June 1986 Alcamo (I)
Citizenship: Italian

Professional Experiences

12.2016 – Current **Postdoc Researcher**, University Hospital Basel.
Subject: Identification and characterization of novel α L β 2 inhibitors and their differentiation from known inhibitors

01.2013 – 11.2016 **PhD Student**, University Hospital Basel.
Subject: Identification and characterization of novel α L β 2 inhibitors and their differentiation from known inhibitors

03.2012 - 12.2014 **Scientific Assistant**, Alloocyte Pharmaceuticals AG, Basel.
Subject: Identification of Novel Integrin Modulators

10.2009 - 07.2010 **Master Thesis**, Institute for Chemistry and Bioanalytics, FHNW Basel.
Subject: Transient Gene Expression (TGE): New Fully-Deacetylated Polyethylenimines

04.2008 - 06.2008 **Bachelor Thesis**, Department of Cellular and Development Biology, University of Studies of Palermo, Italy.
Subject: Analysis on K1b clone derived from cell line HT-29

Academic Degrees

11.2016 **PhD in Pharmaceutical Sciences**, University of Basel (CH) Overall Mark "Magna cum Laude"

11.2016 **PhD Educational Program "Predeictive Toxicology / Bioactive Compounds", ProDoc/SUK**, University of Zurich (CH)

04.2011 **Master of Science Diploma in Biotechnology**, University of Studies of Palermo (I)
Overall Mark 110 / 110 "Summa cum Laude"

07.2008 **Bachelor of Science Diploma in Biotechnology**, University of Studies of Palermo (I)
Overall Mark 110 / 110 "Summa cum Laude"

Academic Education

- 02.2015 **Safety Pharmacology** - DGPT German Society for Experimental and Clinical Pharmacology and Toxicology, Basel – CH
- 07.2014 **Immunotoxicology** - Postgraduate Education in Toxicology (P.E.T.) Course, Utrecht – NL
- 04.2014 **LTK Module 1** - Introductory Course in Laboratory Animal Science, accredited as FELASA, Basel – CH
- 09.2013 **Xenobiotic metabolism/toxicokinetics** - DGPT German Society for Experimental and Clinical Pharmacology and Toxicology, Zurich – CH
- 09.2012 **Basic Flow Cytometry Training Course (Basel – CH)**, under supervision of Natasha Barteneva MD, PhD at the Immune Disease Institute, Harvard University - USA

Scientific Experiences and Awards

- 02.2017 Annual Research Meeting (Basel – CH) **12th World Congress on Inflammation (Boston – USA)**. Oral presentation: “Identification and characterization of novel α L β 2 inhibitors and their differentiation from known inhibitors” - *Riccardo Mancuso, Marianne Hürzeler, Martin Gut, Gisbert Schneider, Stephan Krähenbühl and Gabriele Weitz-Schmidt*
- 08.2015 **12th World Congress on Inflammation (Boston – USA)**. Poster: “Different mechanism of LFA-1 inhibition trigger different downstream effect *in vitro*” - *Riccardo Mancuso, Stephan Krähenbühl and Gabriele Weitz-Schmidt*
- 05.2015 **SSPT Travel Grant** Swiss Society of Pharmacology and Toxicology
- 04.2015 **SSPT Spring Meeting 2015 of the Swiss Society of Pharmacology and Toxicology (Bern – CH)**. Oral presentation and poster: “Identification of novel LFA-1 “silencers” and their differentiation from known LFA-1 inhibitors” - *Riccardo Mancuso, Marianne Hürzeler, Martin Gut, Gisbert Schneider, Stephan Krähenbühl and Gabriele Weitz-Schmidt*
- 09-2014 **1 week research visit at ATI, Novartis (Basel – CH)**. Medium-throughput technologies for single cell analysis (96-well flow cytometry) and for cytokine detection (homogenous time-resolved readout, HTRF) under the supervision of Karl Welzenbach
- 04.2014 **SSPT Spring Meeting 2014 of the Swiss Society of Pharmacology and Toxicology (Bern – CH)**. Poster: “Different mechanisms of LFA-1 inhibition trigger different downstream effects *in vitro*” - *Riccardo Mancuso, Stephan Krähenbühl and Gabriele Weitz-Schmidt*

Curriculum

- 02.2014 **LS2 Annual Meeting (Lausanne – CH).** Poster: “Different mechanisms of LFA-1 inhibition trigger different downstream effects *in vitro*” - Riccardo Mancuso, *Stephan Krähenbühl and Gabriele Weitz-Schmidt*
- 09.2012 **7th International Summer School on Advanced Biotechnology (Santa Margherita di Belice – I).** Oral presentation: “Identification of Novel Integrin Modulators” - Riccardo Mancuso and *Gabriele Weitz-Schmidt*
- 10.2010 **10 months Erasmus Project, Master Thesis position at FHNW (Basel – CH):** EuRopean Community Action Scheme for the Mobility of University Students

Languages

Italian (mother tongue)
English (fluent)
German (basic)
Spanish (basic)

Publication and Patent

- 11.2016 **Downstream effect profiles discern different mechanisms of integrin α L β 2 inhibition.** Riccardo V Mancuso, *Karl Welzenbach, Peter Steinberger, Stephan Krähenbühl and Gabriele Weitz-Schmidt*
- 10.2015 **A novel multi-parameter assay to dissect the pharmacological effects of different modes of integrin α L β 2 inhibition in whole blood.** *Karl Welzenbach, Riccardo V Mancuso, Stephan Krähenbühl and Gabriele Weitz-Schmidt*
- 08.2014 **Patent No. 14172200.9 – 1462: Small molecule LFA-1 inhibitors.** *Werner Breitenstein, Marianne Huerzeler, Terence Kelly, Riccardo Mancuso, Gisbert Schneider and Gabriele Weitz-Schmidt*

References

PD Dr. Gabriele Weitz-Schmidt, AlloCyte Pharmaceuticals AG, Basel, Switzerland
email: gabriele.weitz@allocyte-pharma.com

Prof. Dr. med. Dr. pharm. Stephan Krähenbühl, Clinical Pharmacy and Head Clinical Pharmacology & Toxicology, University Hospital Basel, Switzerland.
email: stephan.kraehenbuehl@usb.ch

Prof. Dr. Daniel Gygax, Institute of Chemistry and Bioanalytics, FHNW Basel, Switzerland.
email: daniel.gygax@fhnw.ch

